

REMOTE SENSING: APPLICATION TO GEOLOGICAL MAPPING
WITH REFLECTANCE IMPLICATION OF ROCKS
OF THE WEBUYE - BUNGOMA AREA "

UNIVERSITY OF NAIROBI
LIBRARY
P. O. Box 30197
NAIROBI

BY

TITUS ZAKAYO INGANA

THIS THESIS HAS BEEN ACCEPTED FOR
THE DEGREE OF...MSc... 1993.
AND A COPY MAY BE PLACED IN THE
UNIVERSITY LIBRARY.

A thesis submitted to the Department of Geology in
partial fulfillment of the requirements for
the degree of Master of Science (MSc.),
Geology

[UNIVERSITY OF NAIROBI]

1993

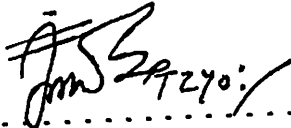
UNIVERSITY OF NAIROBI LIBRARY



0133593 4

DECLARATION

This thesis is my original work and has not been presented for a degree in any other University.



.....

T. Z. Ingana

This thesis has been submitted for examination with our approval as University Supervisors.

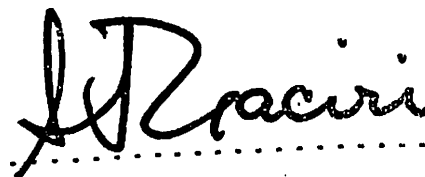


.....

Dr. P. L. Legge

Department of Geology

University of Nairobi



.....

Prof. S. J. Gaciri

Department of Geology

University of Nairobi

DEDICATION

For so much work the satellites
Machines that by nature
Soar high into the unknown
With schooning endeavour
Do they delf into mystery of discovery
Now the mystery unravelled to us
For so much do we cherish this
The Science of today and tomorrow
- And so be it till umpteenth days
Of Science and Technology

Ingana T. Z. (1993)

_____ Unto my son, Irvine _____

ABSTRACT

This research is based on the application of conventional, photogeological and remote sensing techniques in geological mapping of the Webuye-Bungoma area, Kenya.

Conventional techniques focused on field traverses involving sampling of rocks and their subsequent macroscopic and microscopic examination as well as dip and strike data analysis. Fusion, accommodation and convergence methods were used in photogeology. In remote sensing, geological mapping was based on MSS, TM and SPOT imageries plus radiometric data. Their spatial and spectral information in relation to the present terrain, climate, geomorphology, environment, instrument response, spectral region and data display were used to establish geology, geological structures, natural resources and land-use.

It was established that rocks have two main plunges; 40° and 42° in the $N60^\circ E$ and $N5^\circ W$ directions respectively. The general strike of foliations of rocks is $N60^\circ W$. Spectroradiometry of rocks reveals that molecules in their minerals occupy unordered or several equivalent sites and that their vibrations are directly related to overtones and combinations involving high fundamental frequencies. The area east of Nandi escarpment has suffered eastward progressive metamorphism (manifested in gneisses, schists, metamorphosed granodiorites and granites), complex faulting, folding and shear. Episodes of plastic deformation, metasomatism and deformation have severally

rejuvenated Nandi escarpment. West of the Nandi escarpment, there are outcrops of granodiorites, medium-grained greywacke, phyllites, grits and mudstone; granodiorites and related rocks being unmoved rigid masses.

Although, aerial photographs derived from low sun-angle were versatile and useful in enhancing subtle topographical features, the precision of locating boundaries and identifying small or isolated features is inhibited by the small scale and low resolution of imageries.

ACKNOWLEDGEMENTS

I thank DAAD most sincerely for awarding me a scholarship without which this work would otherwise be a story verbally narrated. My unrelenting appreciation goes to the Kenya government for allowing me to carry out my Master of science (MSc.) studies at the University of Nairobi.

I received unequivocal support from lecturers and subordinate staff of Geology Department. My supervisors: Prof. Gaciri, S. J. and Dr. Legge, L. P. worked tirelessly in this academic tenure in their quest to execute supervision. I definitely owe them credit since their effort is well manifested in this work. Many thanks are extended to Mr. Mutonyi for his well done cartography and so to Mr. Wewa for assisting in preparing for microscopic examinations.

I thank the Regional Centre for Services in Surveying, Mapping and Remote Sensing (RCSSMRS) for allowing me to use their facilities. Thanks are also extended to Survey of Kenya (SK) and the Kenya Resourceful Mapping Unit (KREMU) for assisting in procuring aerial photographs and satellite imageries.

More appreciation goes to my colleagues in the Geology Department for they provided unmatched academic stimuli plus resounding and ambitious heartfelt crescendo. They will be remembered for a long time to come. Mrs. Kahuthia, the department secretary deserves a pat on the back for her wonderful typing services which she provided when most needed.

Lastly, I thank my wife, Treza Atemo for her perseverance and unprecedented moral support in the course of my studies.

CONTENTS

	Page
ABSTRACT	iv
ACKNOWLEDGEMENTS	vi
CHAPTER ONE	
1. OBJECTIVES OF STUDY -----	1
1.1. Introduction to the study area -----	3
1.1.1. Location -----	3
1.1.2. Climate and Vegetation -----	3
1.1.3. Communication -----	5
1.1.4. Physiography -----	5
1.1.5. Drainage -----	6
CHAPTER TWO	
2. LITERATURE REVIEW -----	7
2.1. A review of the geology -----	7
2.2. Previous geological studies in remote sensing -	10
CHAPTER THREE	
3. METHODOLOGY OF STUDY -----	12
3.1. Rock sampling and analysis -----	12
3.2. Photogeology -----	12
3.3. Multispectral Scanner (MSS), Thematic Mapper (TM) and SPOT images -----	13
3.4. Lithological interpretation -----	14
3.5. Structural geology interpretation -----	14
3.6. Spectroradiometry -----	17
3.6.1. Reflectance data -----	20

CHAPTER FOUR

4.	GEOLOGICAL INTERPRETATION	40
4.1.	Introduction	40
4.2.	Detailed Photogeology	43
4.3.	Geology	49
4.3.1.	Summary of geology	49
4.3.2.	Detailed geology	52
4.3.3.	Nyanzian Group	53
4.3.3.1.	Schists	53
4.3.3.2.	Banded ironstone	54
4.3.4.	Kavirondian Group	55
4.3.4.1.	Mudstone	55
4.3.4.2.	Grit	56
4.3.4.3.	Phyllite	57
4.3.5.	Mount Elgon Series	58
4.3.5.1.	Nephelinite	58
4.3.6.	Turoka group	59
4.3.6.1.	Schists	59
4.3.6.2.	Gneisses	63
4.3.6.3.	Plutonics and related rocks	64
4.3.7.	Intrusives	67
4.3.7.1.	Granodiorites	67
4.3.7.2.	Dolerites	68
4.3.7.3.	Quartz-monzonite	70
4.3.8.	Ironstone	71
4.3.9.	Vegetation	72
4.4.	Structural geology	73

4.4.1.	Introduction	73
4.4.2.	Detailed structural geology	74
4.5.	Economic minerals and water resources	82
4.5.1.	Economic minerals	82
4.5.2.	Water resources	83
4.5.2.1.	Introduction	83
4.5.2.2.	Subsurface water	83
4.6.	Discussion	86
4.7	Conclusion and Recommendations	88
	Reference	90
	Appendix	95

LIST OF PLATES

Plate 1:	Nephelinite rock along Mount Elgon slopes at Kapkateny market
Plate 2:	Nandi escarpment
Plate 3:	Broderick Falls along river Nzoia
Plate 4:	Granodiorite with xenoliths and dioritic mixing
Plate 5:	Dolerite (Tholeiitic intrusion)
Plate 6:	Nzoia peneplain

LIST OF FIGURES

Fig. 1.	Map of Kenya showing the location of the study area	4
Fig. 2	Portable spectroradiometer	18
Fig. 3	Characteristics of the electromagnetic energy spectrum	19

Fig. 3.10A	Reflectance of background -----	24
Fig. 3.10	Actinolite-schist -----	24
Fig. 3.11	Mudstone -----	25
Fig. 3.12	Ironstone -----	25
Fig. 3.13	Garnet-schist -----	26
Fig. 3.14	Nephelinite -----	26
Fig. 3.15	Biotite-muscovite schist -----	27
Fig. 3.16	Phyllite -----	27
Fig. 3.17	Chlorite-schist -----	28
Fig. 3.18	Quartz-muscovite schist -----	28
Fig. 3.19	Hornblende-schist -----	29
Fig. 3.20	Quartz -----	29
Fig. 3.21	Quartz-monzonite -----	30
Fig. 3.22	Garnet-hornblende gneiss -----	30
Fig. 3.23	Quartz-muscovitite -----	31
Fig. 3.24	Quartz-feldspar-biotite schist -----	31
Fig. 3.25	Grit -----	32
Fig. 3.26	Tholeiitic dolerite -----	32
Fig. 3.27	Pegmatite -----	33
Fig. 3.28	Migmatitic granodiorite -----	33
Fig. 3.29	Meta-dolerite -----	34
Fig. 3.30	Muscovite-schist -----	34
Fig. 3.31	Garnet-hornblende schist -----	35
Fig. 3.32	Crush granite -----	35
Fig. 3.33	Mylonite -----	36
Fig. 3.34	Olivine-dolerite -----	36
Fig. 3.35	Banded ironstone -----	37
Fig. 3.36	Hornblende-gneiss -----	37

Fig. 3.37	Metamorphosed granodiorite -----	38
Fig. 3.38	Grass -----	38
Fig. 3.39	Soil (Kasarani area, Nairobi) -----	39
Fig. 4.00	Drainage patterns as depicted by Multispectral scanners (MSS) imagery -----	42
Fig. 5	Stereopairs of aerial photographs covering Webuye town and its environs -----	45
Fig. 6	Interpretation of aerial photographs in figure 5 (scale 1 : 25,000) -----	46
Fig. 7	Stereographic projections for 50 readings of strike and dip -----	78
Fig. 8	(a and b): Rose diagrams for strike measurements -----	78
Fig. 9	Wave interaction with an interface -----	A1.1
Fig. 10	Reflection coefficient -----	A1.1
Fig. 11	Water molecule fundamental vibrational modes	
Fig. 12	Spectral signature diagram of a variety of geological materials -----	A1.5
Fig. 13	Multispectral scanner systems -----	B1.2
Fig. 14	Thematic mapper system -----	B1.2
Fig. 15	Spot satellite platform and image swaths acquired in the nadir viewing position ---	B1.4
Fig. 16	Capability of SPOT to revisit localities --	B1.6
Fig. 17	Off-nadir viewing capability of SPOT -----	B1.6

APPLIED ACRONYMS

EM	Electromagnetic
um	Micrometers
IR	Infrared
VNIR	Very near infrared
SWIR	Short-wave infrared
MSS	Multispectral Scanner
TM	Thematic Mapper
SPOT	System Probatoire d'Observation de La Terre
ERTS	Earth Resources Technology Satellite
NOAA	National Oceanic and Atmospheric Administration
DMSP	Defence Meteorological Satellite Program
CII	Clear composite images
HRV	High Resolution Visible
IFOV	Instantaneous field observation view
CCD	Charge coupled detectors
MM	Multispectral Mode
HRP	High Resolution Panchromatic
NASA	National Aeronautics and Space Administration
T	Absorption feature
h	Planks Constant

(Geological map at the back of thesis)

1. OBJECTIVES OF THE STUDY

Basic geological mapping using conventional field techniques is a slow task requiring boundaries and distinctive outcrops of rocks to be followed painstakingly. For example, exploration focused on the eventual discovery of petroleum deposits involves extremely costly methods. The role of remote sensing in this context is two fold: first it allows observation from a limited number of field locations to be extrapolated over large areas and makes the work of geologists more efficient and frees them to make more detailed observations on areas of great interest. Secondly, it helps to identify unusual geological features to which resources may be related. This cuts down the area over which high-cost exploration methods need to be deployed.

Remote sensing, as an emerging applied science is presently used to interpret the environment more than in the past. However, its techniques cannot be used effectively in geological mapping exercises in the absence of conventional field techniques. Both are applied concurrently in the field.

The application of aerial photographs, satellite imageries (Landsat programme) and spectroradiometry in the study of this area will make it easier to understand its geomorphology, structural geology and other geological parameters.

Geological mapping is to be accomplished by applying conventional, photogeology and remote sensing techniques in the field of research. Below is a breakdown of the objectives.

- 1). To use aerial photographs and satellite imageries in mapping the geology of the Webuye-Bungoma area.

- 2). To compare the results of Landsat (MSS, TM, and SPOT) data.
- 3). To establish and interpret spectral data of rocks through computer data modelling.

1.1. Introduction to the study area.

1.1.1. Location

The study area (fig. 1.0) is located south-east of Mount Elgon. It is bounded by longitudes $6^{\circ} 79'$, $7^{\circ} 04'$ and latitudes $0^{\circ} 89'$ and $0^{\circ} 64'$. It is partially covered on the Kenyan Survey sheets of Kimilili (88/1), Kiminini (88/2), Bungoma (88/3), and Lugari (88 / 4).

1.1.2. Climate and vegetation

The area receives maximum rainfall in April and May and has an annual rainfall of about 1400 mm. It has localised showers in the dry seasons, one of which reports a maximum temperature peak in June and the other in December and January. The short rain season runs from August to November. Although the latter period appears long, the amount of rainfall recorded is much lower than that recorded in the rain season of April and May.

Overall, there is a 0-10 % probability of obtaining less than or more than 750 mm of rain a year. The minimum annual mean temperature is $10-14^{\circ}\text{C}$ and the maximum annual mean temperature $26-30^{\circ}\text{C}$. Mount Elgon area alone has a $6-10^{\circ}\text{C}$ range for the former and an $18-22^{\circ}\text{C}$ range for the latter.

The following formula can be applied where recorded values of temperatures do not exist:

$$T = 30.2 - 6.5 \times E(^{\circ}\text{C}) \quad (\text{National atlas of Kenya, 1970})$$

where E is the elevation of the station above mean sea level in thousands of metres and T is the temperature at that elevation.

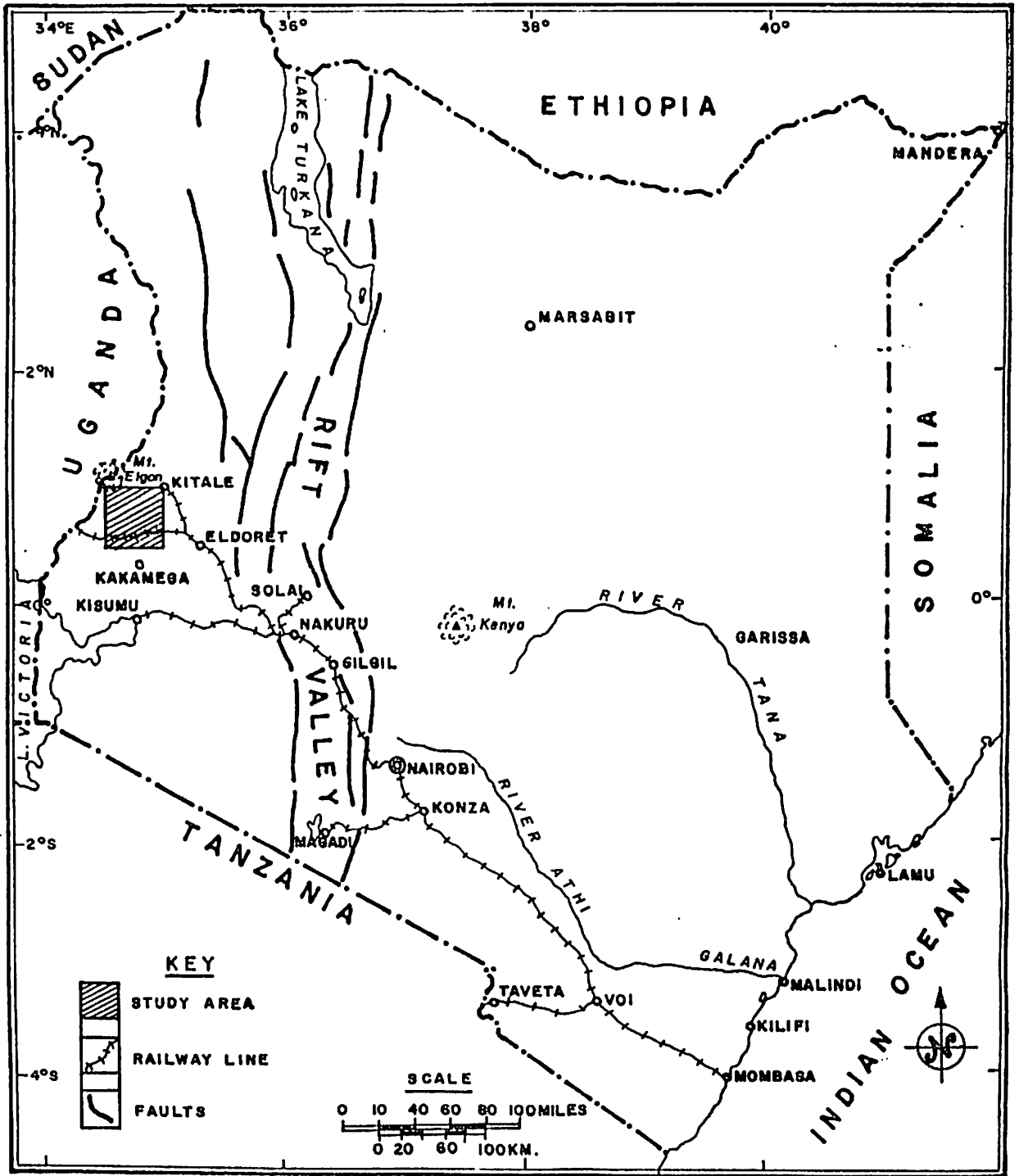


Fig. 1 Map of Kenya showing the location of the study area

The climate is generally pleasant, the average daily temperature showing a slight increase to the south-west with decreasing elevation.

Vegetation types are physiognomic, based on the relative contribution of woody plants vis-a-vis grass and other herbs. There are three main types of vegetation in the research area:

1). Forest

This has a closed stand of tall trees with an interlaced upper canopy, rising 7.5-40 metres or more in height on the slopes of Mount Elgon. The ground cover is dominated by herbs and shrubs. Lianas and epiphytes are characteristic.

2). Wooded grassland

North of Nandi escarpment to the north there is a grassland with scattered or grouped trees. The grass is conspicuous with a canopy cover of less than 20%.

The Nzoia peneplain has grassland with scattered or grouped shrubs, the shrubs are mostly conspicuous but having a canopy of less than 20%.

1.1.3. Communication

The area is well served by roads and trucks. An all weather tarmacked road links Bungoma, Webuye and Kimilili towns. The Great North road passes through this area. There are secondary roads and trucks.

1.1.4. Physiography

The area has four main topographic divisions: a). Slopes of

Mount Elgon. b). Nandi escarpment. c). Uasin Gishu plateau. d).
The peneplain.

Slopes of Mount Elgon rise abruptly from the peneplain as steep cliffs, cut by deep river gorges with frequent waterfalls. The Nandi escarpment rises 330 metres above the neighbouring topography and trends in a north-westerly direction, decreasing steadily in height until it ceases to be a noticeable feature. A manifestation of the escarpment is seen in the famous Broderick Falls, a feature located east of Webuye town along River Nzoia.

The Uasin Gishu plateau is a flat topped area bounded by fairly steep cliffs which vary in height from 15 to 60 metres. The rest of the area is the remains of a gently sloping erosional surface. This is a peneplain with wide nearly flat divides separated by broad shallow river valleys.

1.1.5. Drainage

Rivers and streams exhibit radial drainage from Mount Elgon. Most of them are of the perennial type. Majority of the rivers north of the Nzoia reach a stage of maturity on the peneplain, meandering in broad valleys but rejuvenation has re-excavated their beds so that they now flow in gorges. Kipkaren, Kibisi, Kuywa and Chwele are the main tributaries of river Nzoia.

2. LITERATURE REVIEW

2.1. A Review of the Geology

The geology of the area has been mentioned briefly by early workers like Elliot and Gregory (1895), Gregory (1921), Odman (1929), Hitchin (1937) and Shackleton (1951). There was a suggestion that Nandi escarpment follows a line of a reversed fault by Shackleton in 1951. Later on more serious work was undertaken by various geologists. Gibson (1954), established that Broderick Falls area has granites and granodiorites which intrude Kavirondian sediments west of the Nandi escarpment. He suggested that the escarpment could be having a western downward throw of over 300m and that the area between what is seen as sub-parallel normal faults consists of steeply inclined eastward dipping thrust sheets. Gibson and Huddleston (1954), established that rhyolite overlies the crest of the Nandi escarpment and extends southwards into the Kakamega area.

Holmes' (1951) proposal that the Kavirondian and Nyanzian Systems were older than the Basement System were rejected by Gibson who concluded that there was no evidence for a superposition of the Mozambique strike on the Nyanzian and Kavirondian System. This was backed by the evidence that Nyanzian rhyolite was unaltered regardless of the area having undergone regional metamorphism and metasomatism. Besides Gibson argued that the low-grade metamorphism in the Kavirondian and Nyanzian as well as the high-grade metamorphism of the Basement System showed that the former Systems were younger. This was supported by Huddleston (1954 p.

14) who noted that if the Mozambique Belt was younger north-south strike should be superimposed on the Nyanzian and Kavirondian Systems- apparently this was lacking in Kakamega area. Huddleston also suggests that granitisation of the Kavirondian System is restricted by the intense granitisation of the Basement System. Related work was carried out in the Miller (1954) and Sanders (1963).

To avoid the above confusion, Sanders (1965) revised the geology of this area and came up with the following: that the Nandi escarpment does not divide the goldfields formations in the west from the Basement in the east and that the crust east of the escarpment is actually a rigid unmoved granite mass. He noted that the crust east of the escarpment is dominantly Nyanzian in character with granite and granodiorite and small areas of Nyanzian volcanics and sediments. With increasing distance eastward from the escarpment thick metasediments overly the granite. Other findings by Sanders state that the Nandi escarpment marks a great thrust and wrench- fault zone; the thrusts being expressed in the rocks for a farther 60km to the east. Normal faulting parallel to the escarpment is not observed nor inferred. He reckons that what earlier geologists observed as rhyolite faulting into the escarpment is actually a sheet of steeply eastward dipping mylonite and ultramylonite occupying the zone of maximum cataclasis between the Nyanzian foreland and the imbricated margin of the mozambique Belt. The stress transverse to the orogenic margin was ultimately released in the sole thrusts, thus there are no north-south

Mozambique structures in the Nyanzian or Kavirondian Systems west of the zone of imbrication; whereas in fact Nyanzian rocks situated farther to the east have participated in Mozambiquian folding. Attempts to correlate relative ages with granitisation proved impossible because while Nyanzian and Kavirondian rocks are almost wholly thermal without traces of deep-seated dynamic metamorphism, the Basement System has suffered both thermal and dynamic metamorphism and is a deeply eroded root zone of a fold mountain chain built in a comparatively thick crust against at least one rigid margin. The igneous intrusion effecting the Nyanzian and Kavirondian Systems cannot be applied to granitisation as applied to the Basement System which implies that the transformation of the folded metamorphosed and metasomatised rocks into granite or granodioritic migmatite.

The Bukura and Mbesa area in Kakamega District has been studied by Ichangi (1983), who established that the pyrite mineralisation is of a hydrothermal nature and that the water in the fluid was of magmatic and metamorphic origin. The geology and geochemistry of the late Greenstone Belt of Maseno area in western Kenya was studied by Opiyo (1988). He showed that the source of iron found in chert or similar rocks like silica rich banded ironstone found east of Nandi escarpment is volcanic in origin (hydrothermally derived) due to their close proximity to basalts. He notes that the Mozambique rocks were formed under normal orogenic events with the Nyanzian System only acting as a stable craton along which the Mozambique was

thrusts but not as a source for volcanic material. Ngecu (1991) in studying the Kavirondian System used lithostratigraphic techniques which have necessitated the use of lithostratigraphical terminologies. He found that the Nyanzian Group is composed of tholeiitic and calc-alkaline volcanic rocks and is unconformably overlain by clastic sediments of the Kavirondian group. Lithological formations show that the Kavirondian Group consists of four Formations; Shivakala, Igukhu, Mroda and Mudaa.

2.2. Previous geological studies in remote sensing

In Remote Sensing, Mineral exploration, structure detection and aerial geology mapping have been done in the 3-5 micrometre and 8-14 micrometre bands by using IR Scanners. Early morning imagery have been used to distinguish between limestone and dolomite (Rowan et al, 1969; Sabin, 1978; Hunt, 1977).

Radiometric temperature differences among rock units and rock materials have been used to identify structures (Rowan et al, 1969). Sabins (1969) describes the discovery of a faulted plunging anticline, undetectable on conventional photography or in the field.

Condit (1970) and Goetz (1976) measured reflectance spectra of wet, dry sandy soils and typical volcanic and sedimentary rocks while Hunt (1980), studied spectral data of small pulverised non-weathered samples

Surrogate such as surface-form characteristics visible on conventional photography have been used to distinguish between

igneous and sedimentary rocks (Lillesand, 1987). Visual enhancement of relief by imaging radar has been utilised to identify landform provinces, categorise drainage systems and infer lithology from differences in texture signatures. Success in automated computer mapping of terrain types through digital processing of multispectral scanner (MSS) imagery has been achieved, Smedes et al. (1969).

In Ethiopia, an area previously mapped as basalt was found to be 'Basement System' when imageries of Apollo 9 were used, Barnett (1971). In eastern Kenya, Miller (1975) proposes the use of Landsat images in defining some large sedimentary basin. They have also been used for mineral exploration in relation to lineaments, Bhattarai (1983), Sabins (1978) and Goetz (1976). Correlations of lineaments to known geological, oil and gas fields, minerals, faults and volcanic eruptions are areas where Landsat data can be applied, Fillipone (1986).

Using Landsat (MSS) and aerial photography (Cole et al, 1974) showed that geobotanical anomalies are associated with mineral deposits. Onywere (1990) applied remote sensing techniques in geological mapping with emphasis on landform provinces in the Nairobi and its surrounding areas. He proved the use of remote sensing techniques in establishing not only the geology of this area but also its land-use. Kilonzo (1992), successfully applied geographical Information Systems (GIS) in establishing the stratigraphical units as well as water quantities in Nakuru area.

3. METHODOLOGY OF STUDY

3.1. Rock sampling and analysis

Sampling was carried out insitu on solid rock along rivers and streams, on rock cuttings along roads and on rock exposures on land. The labelling of samples was based on a BW/N format where BW stands for Bungoma-Webuye and N stands for sampling station. Out of one hundred and twenty samples originally sampled and studied macroscopically, thirty representative samples were studied spectroradiometrically and microscopically..

3.2. Photogeology

First order approach was used in studying aerial photographs. They were matched mechanically. They were viewed singly, as mosaics or in stereo. They were used to establish valuable relations of geological and associated features. In stereo, a combination of relief and tonal variations was presented. The combination of geomorphic and structural analysis was used for recognition of rocks. Other factors considered were climate, erosional characteristics, bedding traces, outcrops, superficial cover, lineaments, depth of weathering, texture and colour, and reflectivity. Tonal values are related to the composition of the rock. In brief aerial photos (Allum, 1966) are studied via **accomodation** (focusing of objects at different distances so that they are seen clearly), **convergence** (bringing lines of site onto the objects on which attention is focused) and **fusion** (merging or recombining of two slightly different perspective views).

3.3. Multispectral Scanner System (MSS), Thematic Mapper Scanner (TM) and SPOT images

To accomplish lithological mapping from images, analysis and interpretation of the spectral and spatial information within the images in relation to the terrain present, climatic environment and history, and the prevailing geomorphic processes and their stages of development were considered. Consideration was also given to the environment and operational factors affecting instrument response, the spectral region being recorded and the characteristics of data display. It is vital to understand that the spectral and spatial information available to the operator of lithological identification is expressed by landform development, drainage density and pattern, vegetation differences and spectral reflectivity, all interpreted in the context of climatic effects (Barry et al, 1980).

Clear composite images (CCI) of the above sensors were studied. CCI is an infrared photography of the ground having a combination of four spectral bands for MSS, seven spectral bands for TM and three spectral bands for SPOT. Infrared is the electromagnetic radiation with wavelengths of 0.7 to about 1400 micrometers. All materials continuously emit this radiation as long as they have a temperature above absolute zero in the kelvin scale (Barnett, 1971, Elachi, 1987). This radiation involves molecular vibrations as modified by crystal lattice motions of the material.

Vegetation is more strongly discriminated when the ratio between very near-infrared and red reflectance is displayed as an image (Cole et al, 1974). This ratio forms one of the several vegetation indices and is high where vegetation is most dense and low where it is absent, thereby giving a semi-quantitative nature of the density of plant cover. The subtle differences between different species of plants in this part of the spectrum also allows differentiation between two types of vegetation (Thematic Mapper, appendix two).

3.4. Lithological interpretation

This interpretation included all features found in the field; for example topographic expression, rock and soil colouration, vegetational Zoning, primary and secondary structures, and solution depression.

These features were useful in recognising sedimentary rocks either as consolidated or unconsolidated, igneous rocks and rock bodies as volcanic, hyperbasal or plutonic and metamorphic.

3.5. Structural geology interpretation

The determination of solid rock geometry involved differentiation and correlation of lithologic units distribution and attitude (Drury, 1990). They were verified from direct exposure, outcrop pattern, drainage pattern, topographic expression and dip and strike data. Other features were joints, fractures, faults, folds and flectures and unconformities.

a). Bedding

To interpret bedding, it was vital to realise that stereo-model of aerial photographs depict dipping, heterogeneous sediments as parallel ridges and valleys which are a result of differential weathering (Allum, 1966). Rocks which differ in their mineral constituents also differ in their erosional qualities; resistant beds tend to form ridges and eroded beds tend to form valleys. Aerial photographs were therefore used to provide evidence of bedding which may not be available from field observations. The persistence of particular ridges, which is obvious only on aerial photographs is itself evidence that the ridges represent individual lithological horizons and therefore probably beds.

b). Dip

Dip slopes provided indications of direction of dip. In practise they are more obvious on stereo-model than in the field since vertical exaggeration makes all vertical structures appear to dip towards the principal point of the photographs.

c). Foliations

These are segregations of platy or elongate minerals into thin layers or folia. Schistosity is the parallel orientation of such minerals. On aerial photographs they occur parallel to one another and are numerous in occurrence.

d). Faults

These are fractures which show some form of slipping against one another. They appear as straight negative features.

e). Folds

On aerial photographs these were to be realised from areas where structures could not be noticed in the field.

f). Joints

Useful characteristics of joints included their identification on stereo-models as straight, negative features and their similarity to faults in photographic appearance without evidence of movement.

3.6. Spectroradiometry

In Radiometry, reflection and absorption are used to process spectral reflectance curves for each rock sample collected in the field.

To acquire spectral data a portable spectroradiometer (fig. 2) is used. This instrument has a radiation stabiliser which has three windows representing three radiation bands of green, red and infrared. The wavelengths of these bands are shown in figure 3 as shaded. The windows stabilise radiation from the sun according to their wavelengths. The data display system has a computer and power unit. The former has three windows which display data released by the sensor and the latter accommodates batteries which supply electrical power to the computer. Lastly, the sensor has green, red and infrared bands incorporated in the windows. The radiation stabiliser and sensor are connected to the display system. When the instrument is working (power on), the reflectance data is acquired by directing the radiation stabiliser to the sun while the sensor is directed to a rock sample lying on a black background. The emittance (change in radiant flux per change in area) that is diagnostic of the minerals present is then converted into spectral reflectance and displayed by computer. The reflectance (%) values are plotted against the wavelength (micrometers) using lotus programme in the computer. Since only three reflectance values are acquired per rock sample, the lotus programme is used to model the data in order to produce reflectance curves. In the final reflectance curves, minimas represent absorption features T. These represent small

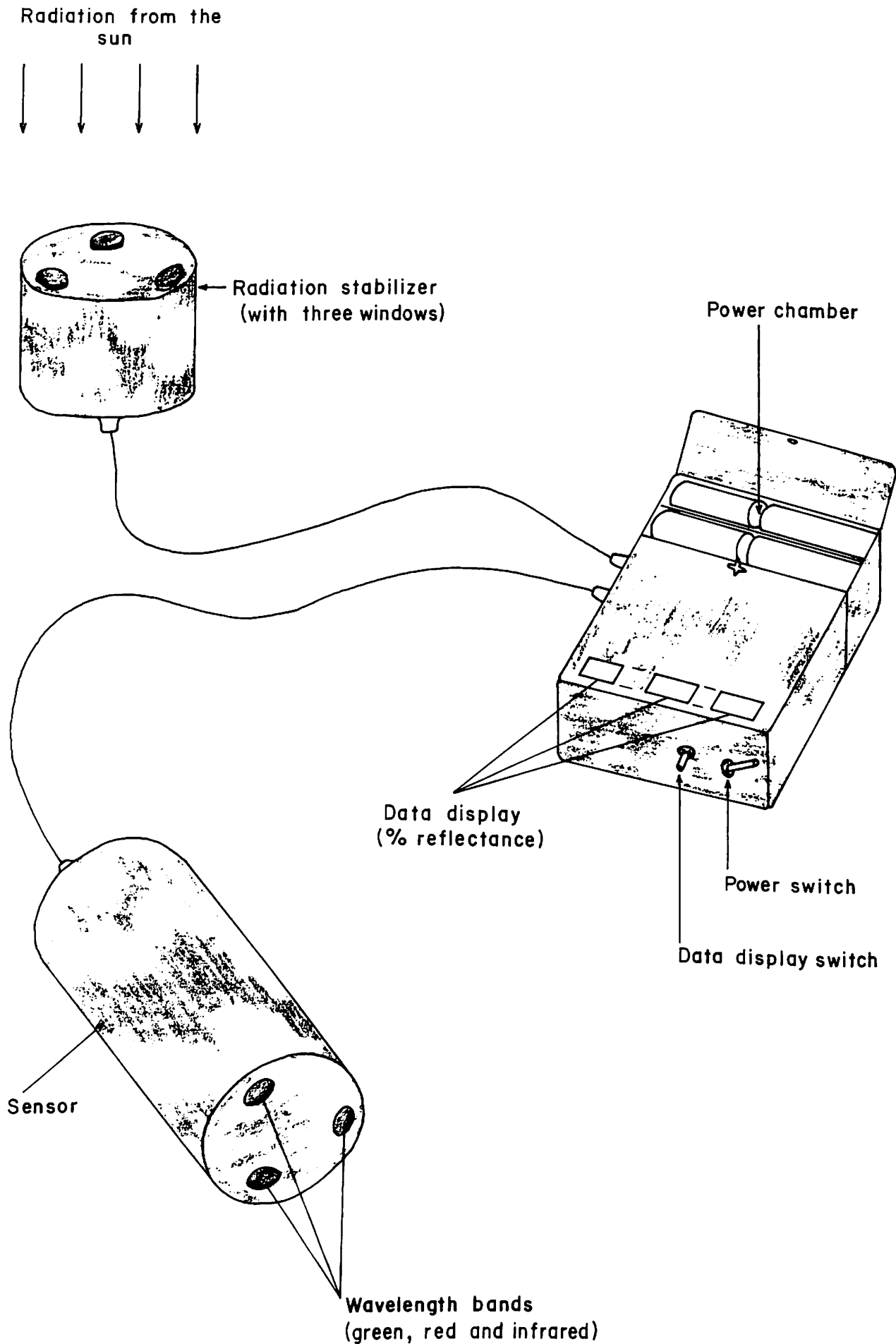
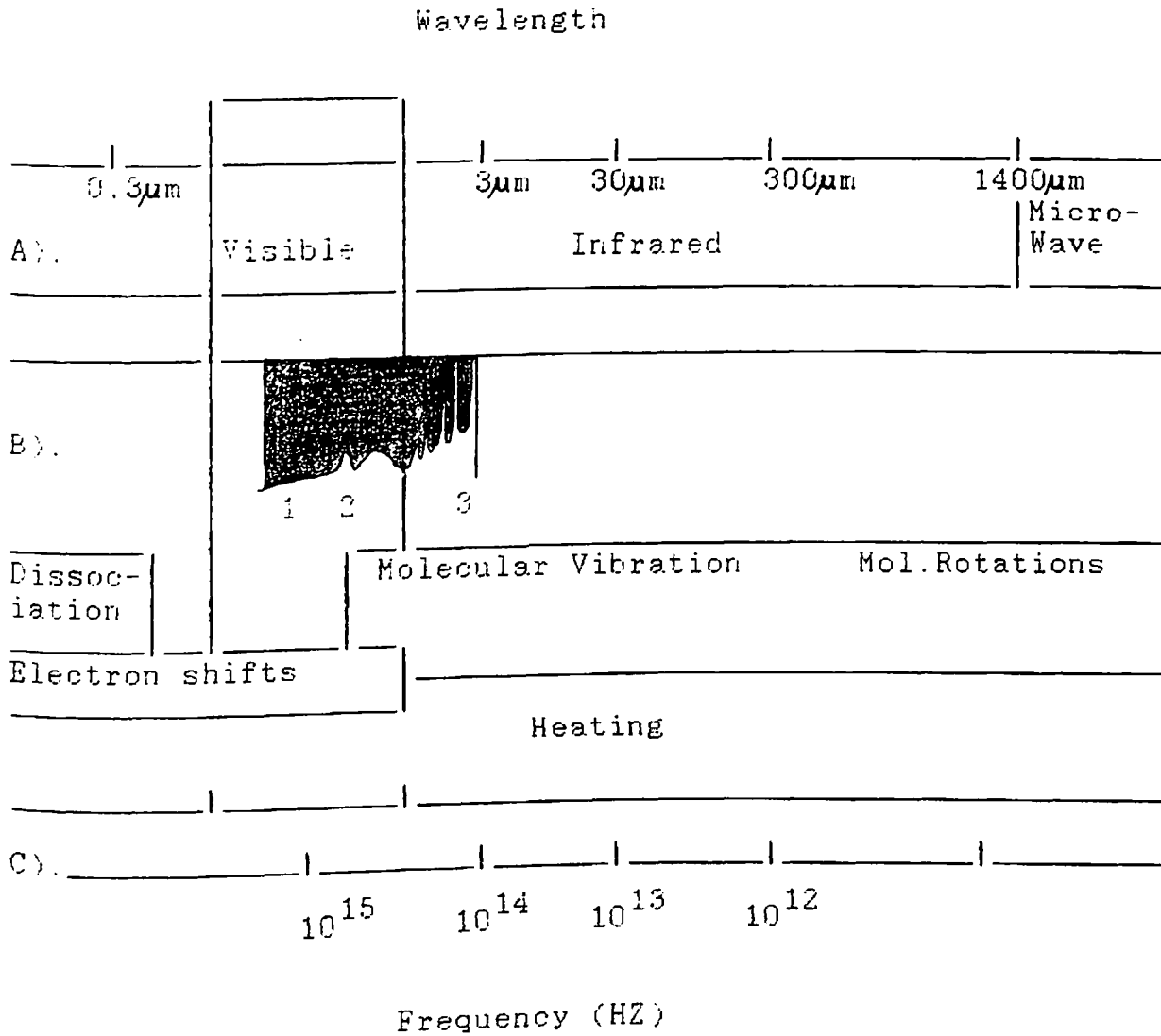


FIG. 2 : PORTABLE SPECTRORADIOMETER
(Based on Sabins, 1987)

Figure 3

Characteristics of the electromagnetic energy spectrum which are of significance.



KEY

μm — Micrometer

HZ — Hertz

A - Regions of electromagnetic spectrum (EM)

B - Shaded areas show regions of the applied spectroradiometry in chapter 3 whose main bands are: 1 - Green, 2 - Red and 3 - Reflected infrared (VNIR)

C - The phenomena detected

(Sabins, 1987)

displacements (vibrations) of the atoms from their equilibrium positions. Examples of molecular vibrational modes are given in appendix one.

All materials are intrinsically unique spectrally (Hunt 1977, Goetz 1976). The spectral reflectance of rocks rise steadily with wavelength to a peak then fall off once more, without having a sudden jump at the boundary between red and infrared.

It is the fine detail in the spectral reflectance curves of rocks and soils that is used to identify minerals. On weathering nearly all iron minerals break down to give oxides and hydroxides. Complex interactions between radiation and both the iron atoms and the molecular structure of iron minerals produce absorption features in the VNIR whose wavelength, breadth, and depth characterise the different mineral species.

Sharp absorption features mean that the molecules are located in well defined, ordered sites or they may be broad showing that they occupy unordered or several equivalent sites. Literature on the wave-surface interaction mechanism is discussed in appendix one.

3.6.1. Reflectance data

In the table below: X-axis represents values for wavelength in micrometers, F (rows) represent figures of reflectance curves, for the Y-axis, columns under F represent reflectance values (in %) for fresh and weathered samples respectively.

Table 4: Reflectance data for sampled rocks

X-axis	F 3.10		F 3.11		F 3.12		F 3.13		F 3.14	
.45	13	7	6.5	5	5	4.4	11	8	5.5	11
.5	12.5	8	7	5.1	5	5	11.5	9	5.2	10.9
.55	12.4	8.3	7.7	5.3	5.1	5.5	12.3	9.8	4.7	10.8
.6	11.5	9	10	6.2	5.4	6.5	12.8	11	4	10
.65	10	9.2	12.1	8	6.2	7.5	13.2	12	3.8	9.5
.7	9.6	9.5	14.2	9	6.5	8.5	13.5	13	3.6	9.1
.75	9	10	14.3	9.7	7.2	9	14.6	14	3.5	9.1
.8	8.5	10.8	13.5	10.5	8.0	9.5	16	15	3.5	9.5
.85	8.5	13.5	12.7	11.7	8.5	9.5	17	16	3.5	9
.9	8.5	16.5	12	13	9	9.5	18	17	3.5	8.9
.95	9	20.2	11.5	13.2	9.1	9.4	19.1	17.7	3.5	8.8
1	9.9	24	11	14	9.3	9.3	20.3	18.4	3.6	8.7
1.05	9.9	26.5	10.5	14.5	9.8	9.1	22.2	19.2	3.8	8.6
1.1	10	29	10	15	10	9	24	20	4	8.5
1.15	11	30	9.7	15.5	10.2	8.8	26	20.5	4.5	8.3
1.2	12	31	9.5	16	10.5	8.5	28	21	5	8

F 3.15		F 3.16		F 3.17		F 3.18		F 3.19	
19.5	20	13	6.5	13	11	18	8	25	15
20	13	14	7	14	10	17	8.5	24.2	14.5
20.4	14.4	14.6	8	14.4	9	16	9.1	23.5	14
21	16	15	9	15	7.7	15	9.6	21.5	14
21	19	14.7	9.6	15.8	7.3	16	10	20.4	14
21.1	20.8	14.3	10.2	16.6	7.2	17	10.3	19.3	14
21.8	19.9	13.6	10.1	16.3	9.1	19.5	11.2	17.7	13.8
22.5	19	13	10	16	11	22	12	16	13.5
23.2	17	12.5	9.5	15.9	13	25	12.3	14.5	13
24	15	12	9	15.8	15	28	12.5	13	12.5
25.6	13.9	11.7	8.2	15.6	17	30	12.6	12.5	12.3
27.2	11.8	11.5	7.6	15.5	19	32.1	12.8	12	12
28.6	10.9	10.7	7	15.4	20	33.5	12.9	11	11.5
30	10	10	6.5	15.3	21	35	13	10	11
31.5	9.7	9.8	6.3	15.2	21.8	36	13.2	9.5	10.5
33	9.5	9.5	6	15	22.5	37	13.5	9	10

F 3.20		F 3.21		F 3.22		F 3.23		F 3.24	
14	17.5	20	10	10	9.5	41	20	10	15
13.5	17	20	11	11	10	38.5	21	10.7	15.2
20.9	16.8	20.1	12	11.6	10.6	34.6	21	11.3	15.4
12.4	16.7	20.6	14.6	12	11	30	21.5	12	15.5
11.9	16.6	20.7	17.6	12.5	11.3	24.4	21.8	12.3	15.6
11.9	16.6	20.8	19.5	13.1	11.5	19.2	22.2	12.6	15.7
11.9	16.7	22.4	20.7	14.5	11.8	18.5	21.9	12.8	15.9

12	16.8	24	22	15.5	12	19	21.5	13	16
12.7	16.9	25.5	22.5	16.5	12.3	20.7	21	13.1	16.1
13.5	17	27	23	17	12.5	22.5	20.5	13.2	16.3
15	17.1	29.7	23.2	17.6	12.6	25.7	20	13.3	16.4
16.5	17.2	32.5	23.4	18.1	12.7	29	19.5	13.5	15.6
17.7	17.9	34.7	23.9	19	12.9	31.2	18.2	13.8	16.8
18.7	19	37	24	20	13	33.5	17	14	17
19.6	20	39	24.8	20.5	13.3	35.2	16.2	14.3	17.1
20.3	21	41	25	21	13.5	37	15.5	14.5	17.3

F 3.25 F 3.26 F 3.27 F 3.28 F 3.29

14	6.5	7.5	13.5	19	26	11	10.8	8	10.3
15	7	8	13.3	20	25.5	10	9.8	8.9	9.9
17.2	7.9	9.1	12.5	21.3	25	9.2	9.3	9.3	9.5
20	9	10	11	22.5	23.5	9	9.5	9.2	9
23.9	10.1	10.5	9.9	23.5	22.5	8.8	10	9.2	8.8
27.8	11.2	11	9.1	24.5	21.5	8.5	10.4	9.3	8.6
28.4	12.1	11.5	8.8	25.2	21.3	9.2	10.7	9.7	8.7
29	13	12	9	26	21.5	9.8	11	10	8.7
29	13.7	13	9.3	26.7	23.2	10.5	11.2	10.5	8.9
29	14.5	14	9.5	27.5	25	11	11.4	11	9.3
28.5	14.8	14.6	9.9	27.9	27.1	12.3	11.6	10.9	9.9
27.9	15	15.3	10.3	28.3	29.3	13.6	11.8	10.7	10.7
27.4	15.2	16.7	10.9	28.9	31.1	14.3	11.9	10.9	11.1
27	15.5	18	11.5	29.5	33	15	12	11	11.4
26.5	15.8	19	12	29.8	34	15.5	12	11	11.7
26	16	20	12.5	30	35	16	12	11	11.9

F 3.30 F 3.31 F 3.32 F 3.33 F 3.34

27	5	9	13	13	9.5	20	13.5	15	8
26.5	6	8	13.5	13.2	9.7	19	12.5	14.4	7.9
25.3	7.1	7.3	13.8	13.6	10.1	18.1	11.8	13.5	7.9
24	10	7	14	14	11.6	17	10.5	12	7.9
23.4	13.1	6.9	14.3	14.2	13.5	15.8	10	11.6	7.8
22.7	16.2	6.9	14.5	14.4	14.6	14.6	9.6	11.2	7.8
17.9	16.6	6.5	14.6	14.7	14.8	14	9.3	11.3	7.7
17.2	17	6	14.7	15	15	13.5	9	11.5	7.7
19.5	16.2	5.8	14.9	16	15	14	8.8	11.8	7.6
26	16	6	15	16.8	15	14.5	9	12	7.6
27.2	15.9	6.5	15.3	17.2	15.1	15.3	9.8	12.7	7.5
28.4	15.8	7	15.6	17.4	15.1	16.2	10.6	13.4	7.4
29.3	14.9	7.5	16.3	18.4	15.3	17.6	11.3	14.1	7.3
31	14	8	17	19.5	15.5	19	12	15	7.2
31.7	13.5	8.5	17.7	19.8	15.8	20.5	12.7	16	7.2
32.5	13	9	18.5	20	16	22	13.5	17	7

F 3.35 F 3.36 F 3.37 F 3.38 F 3.39 F 3.10A

12	11	17.5	15.5	17	12.5	9	3.5	5.5
----	----	------	------	----	------	---	-----	-----

11.5	11	17	15.2	15.5	13.1	7.5	3.6	5
11.1	11.1	16	14.9	15	13.7	6.8	4.3	4.7
10.5	11.5	15	14.8	14.6	14.5	6	6	4
10.2	11.6	14.1	14.7	14.8	14.9	5.5	7.3	3.9
10.3	11.8	13.1	14.7	14.9	15.3	4.9	8.6	3.7
10.5	12.1	13	14.6	14.9	15.4	6.7	9.5	3.5
10.6	12.5	13	14.6	15	15.5	8.5	10.5	3.4
11.3	12.8	13.5	14.5	15.3	15.5	11.7	11	3.4
12	13	13.8	14.5	15.5	15.6	15	11.5	3.5
12.9	13.7	14.1	14.5	16.2	15.7	20.2	11.8	4
13.7	14.4	14.3	14.5	16.8	15.7	25.3	12.1	4.4
14.9	15.2	14.6	14.4	17.9	15.8	28.2	12.3	5
16	16	15	14.4	18	15.9	31	12.5	5.5
18.5	17.2	15.5	14.3	18.5	15.9	33	12.8	6
21	18.5	16	14.2	19	16	35	13	7

NB Columns under F 3.38 rep. data for green grass

F 3.39 rep. data for loam soil

F 3.10A rep. data for standardised background

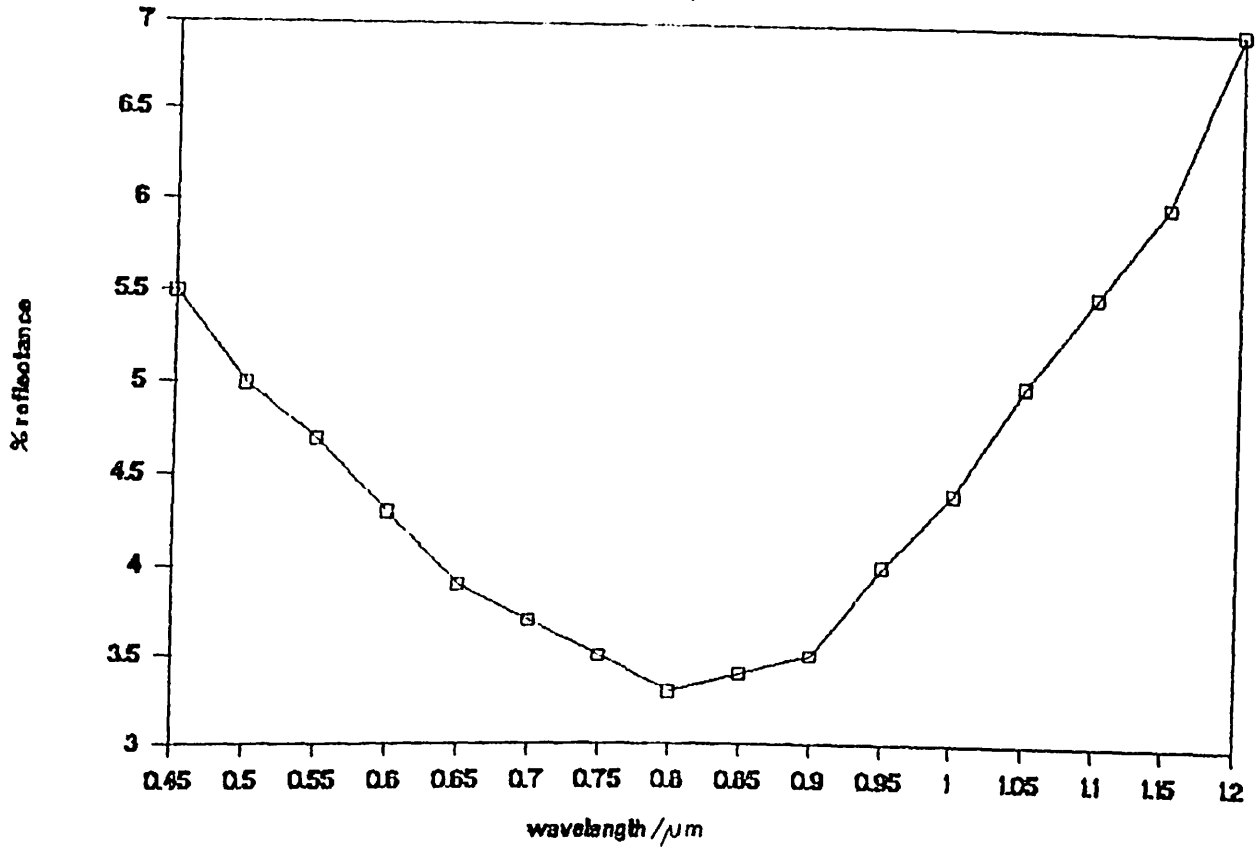


Fig. 3.10 A Background

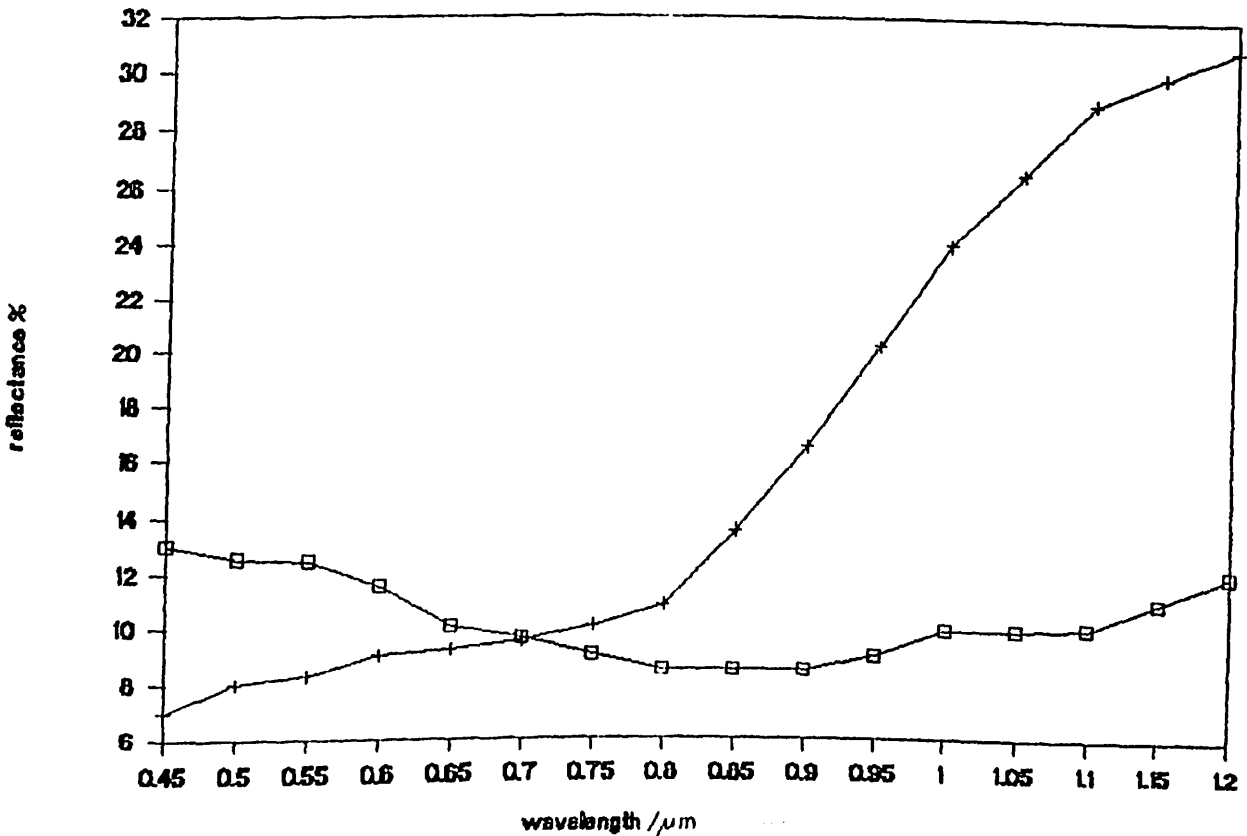


Fig. 3.10 Actonilite schist

NB. For figures 3.10 - 3.37,

- — □ rep. fresh rock sample
- + — rep. weathered rock sample
- T rep. absorption feature

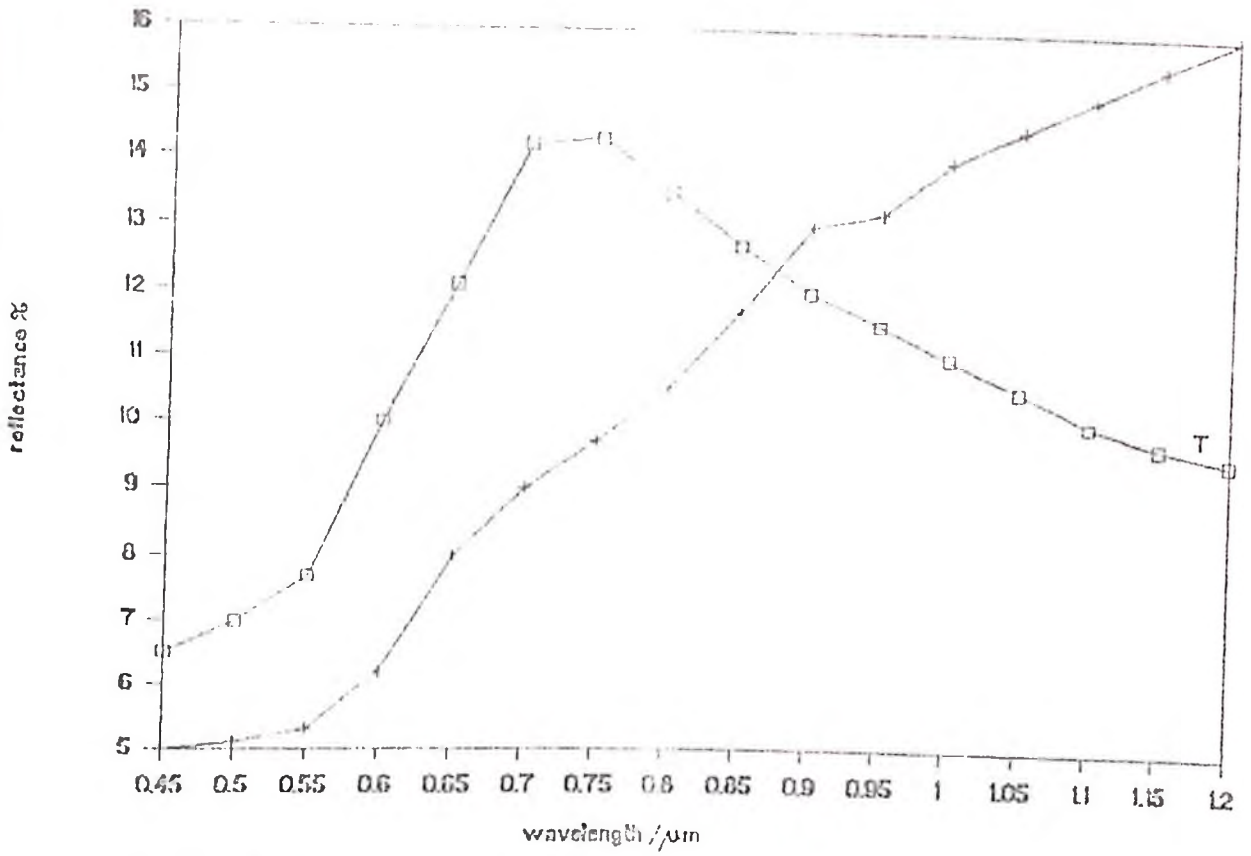


Fig. 3.11 Mudstone

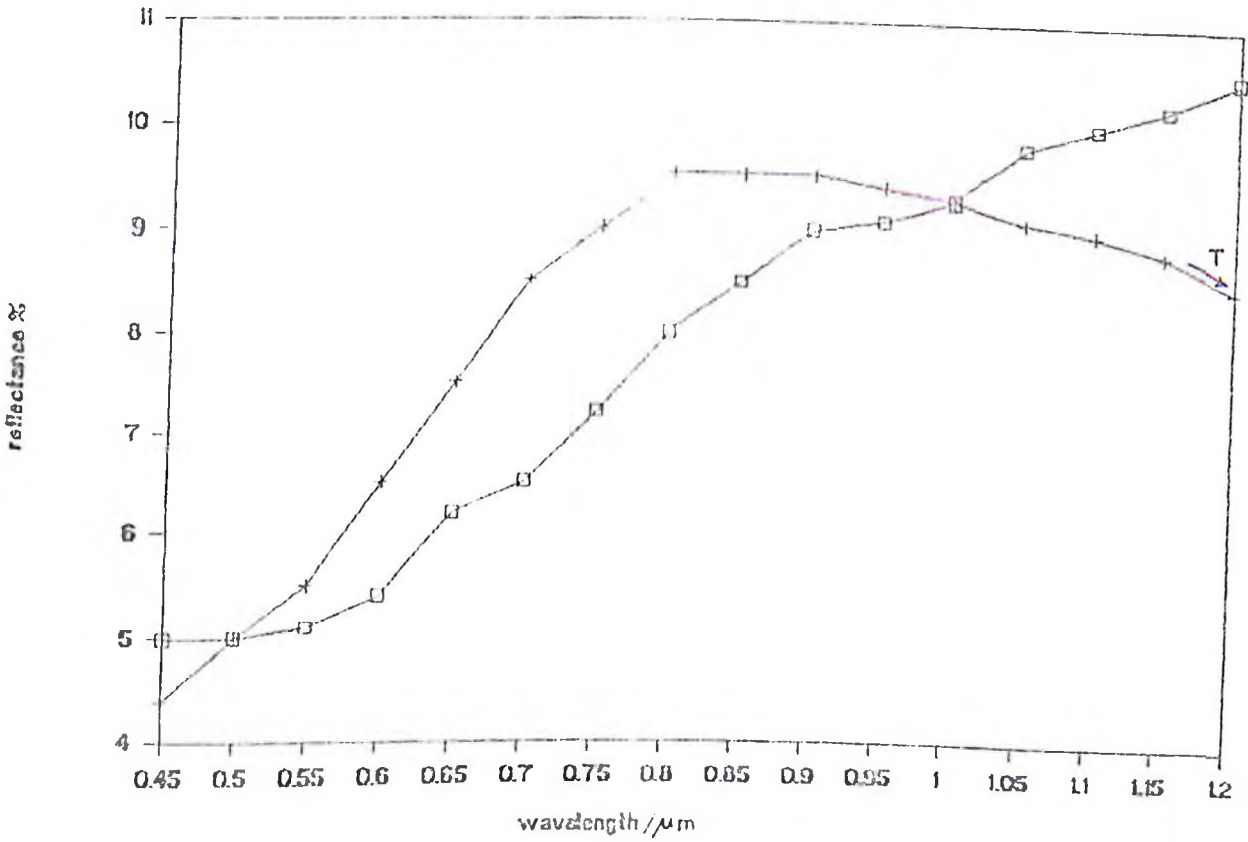


Fig. 3.12 Ironstone

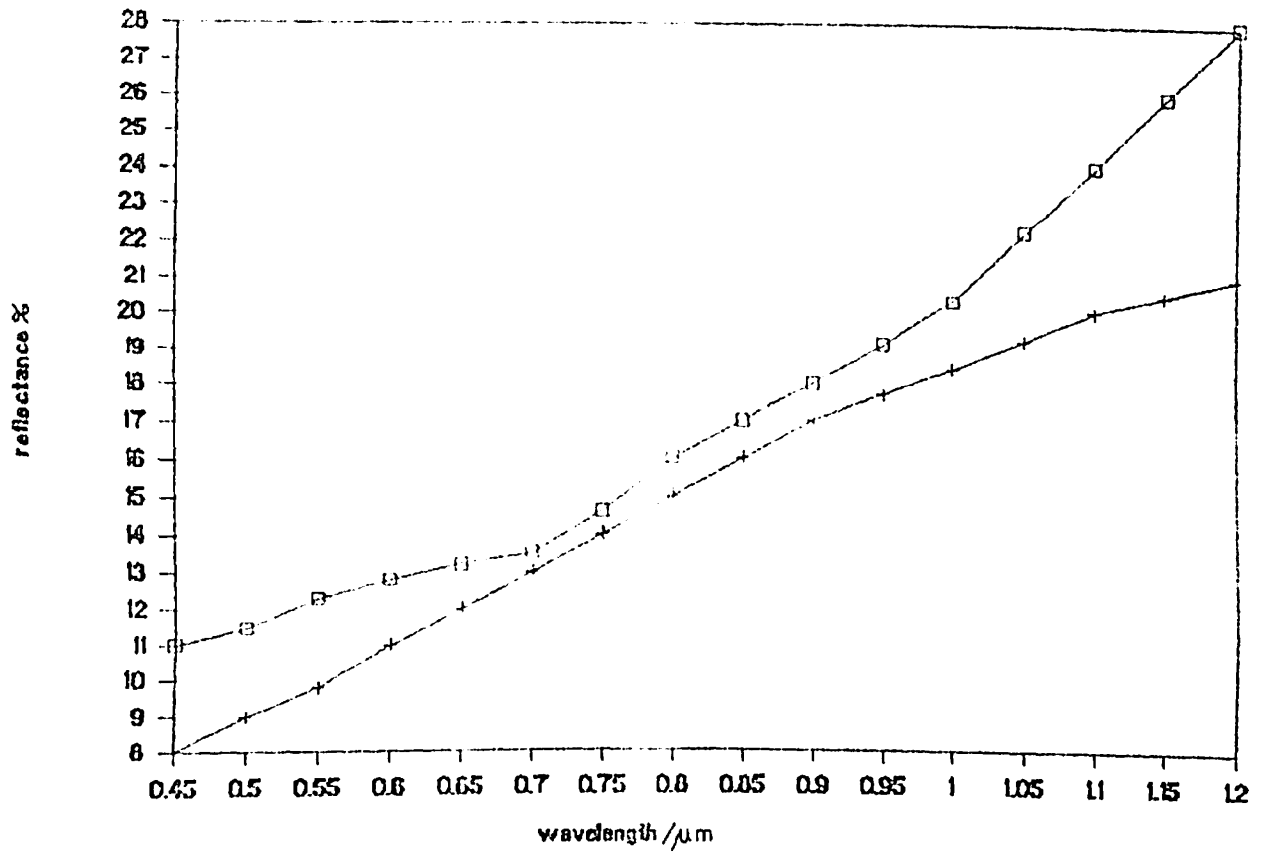


Fig. 3.13 Garnet schist

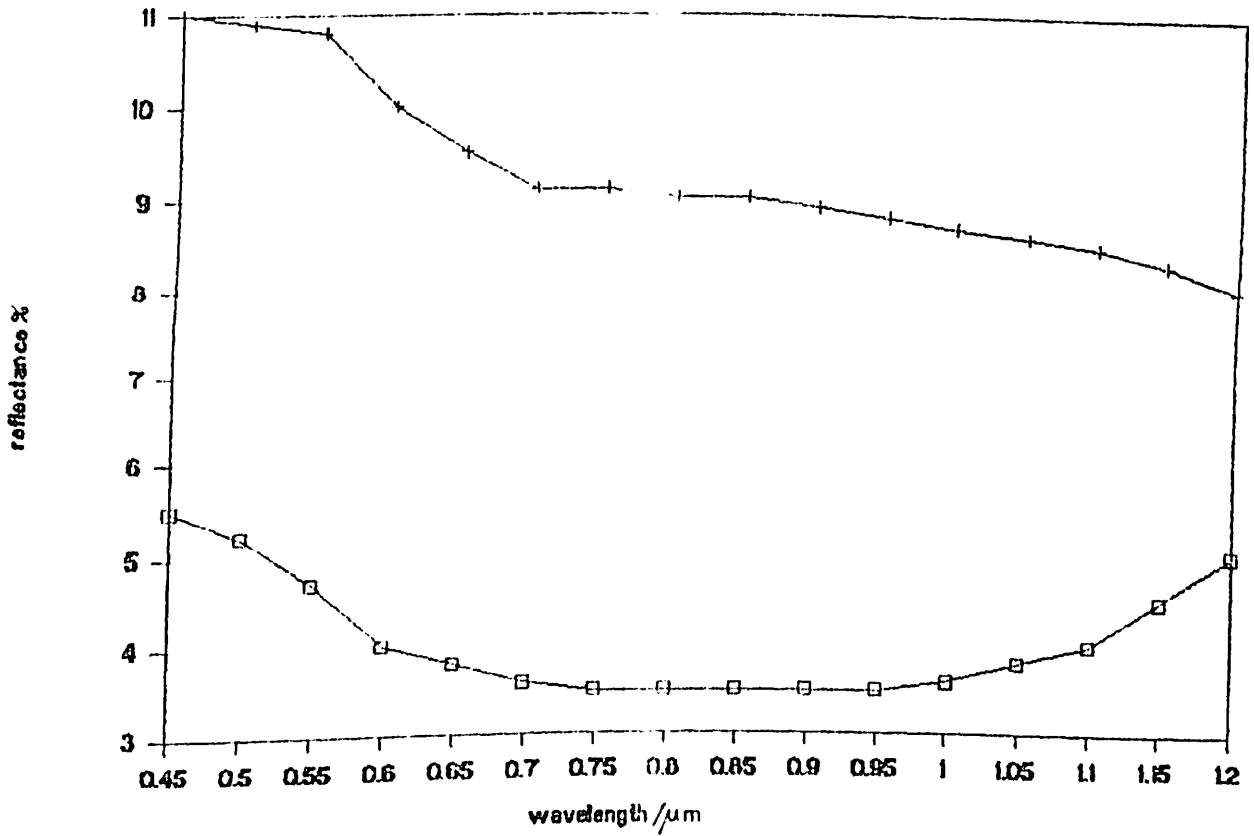


Fig. 3.14 Nephelinite

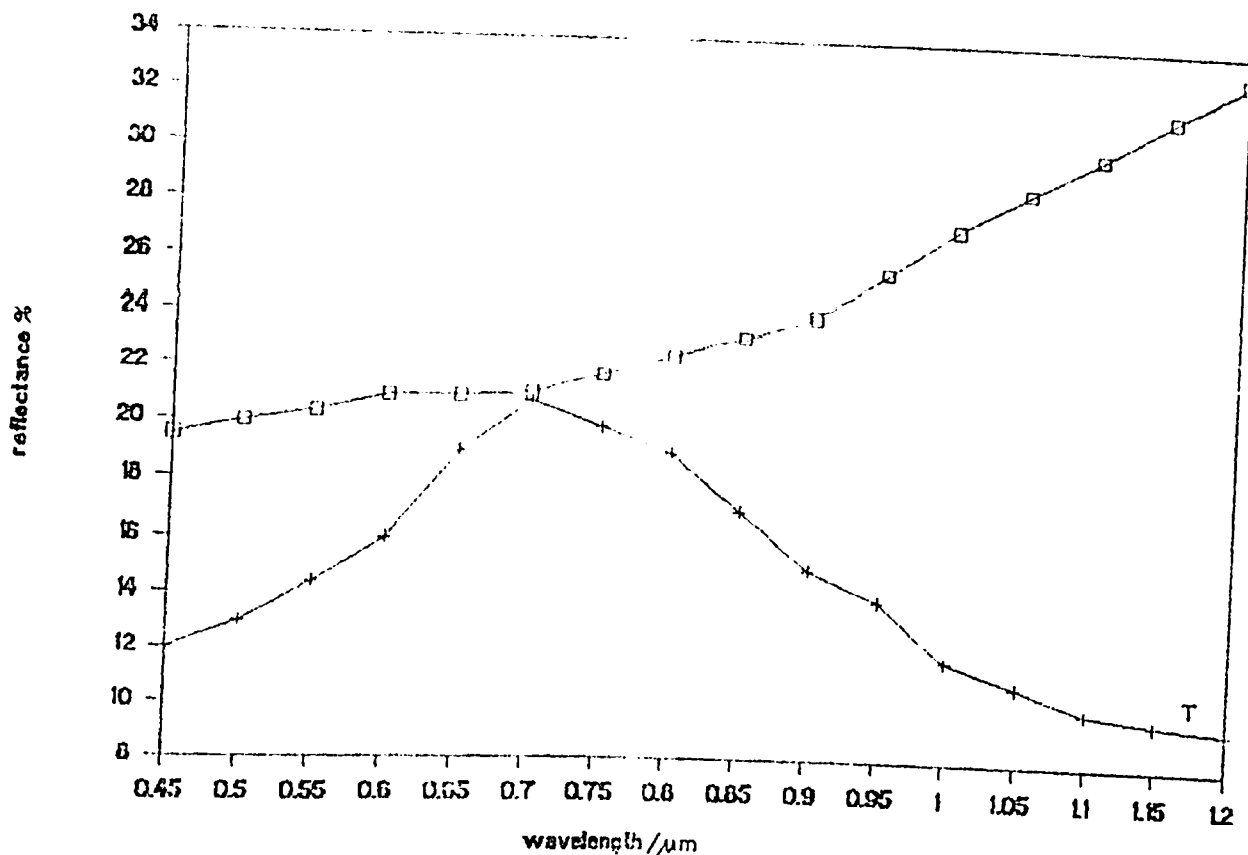


Fig. 3.15 Biotite-muscovite schist

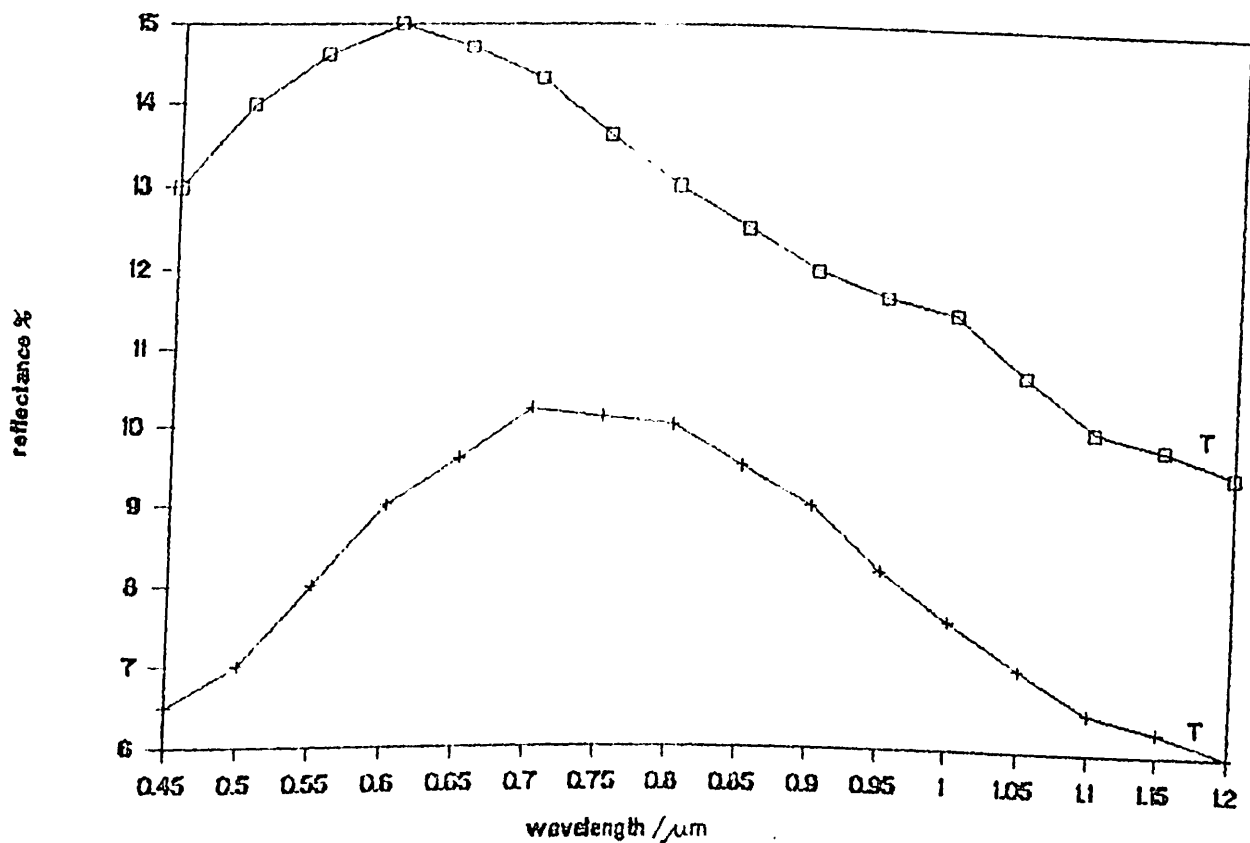


Fig. 3.16 Phyllite

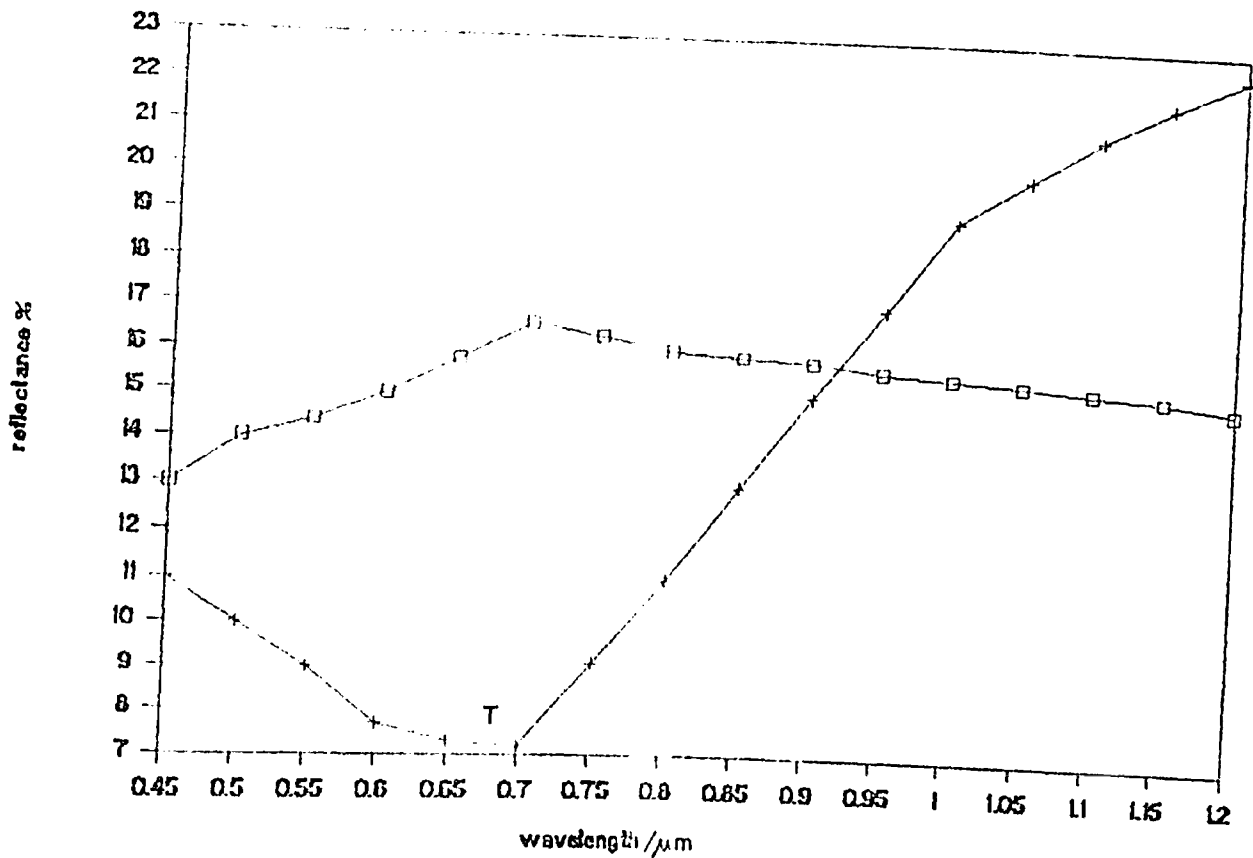


Fig. 3.17 Chlorite schist

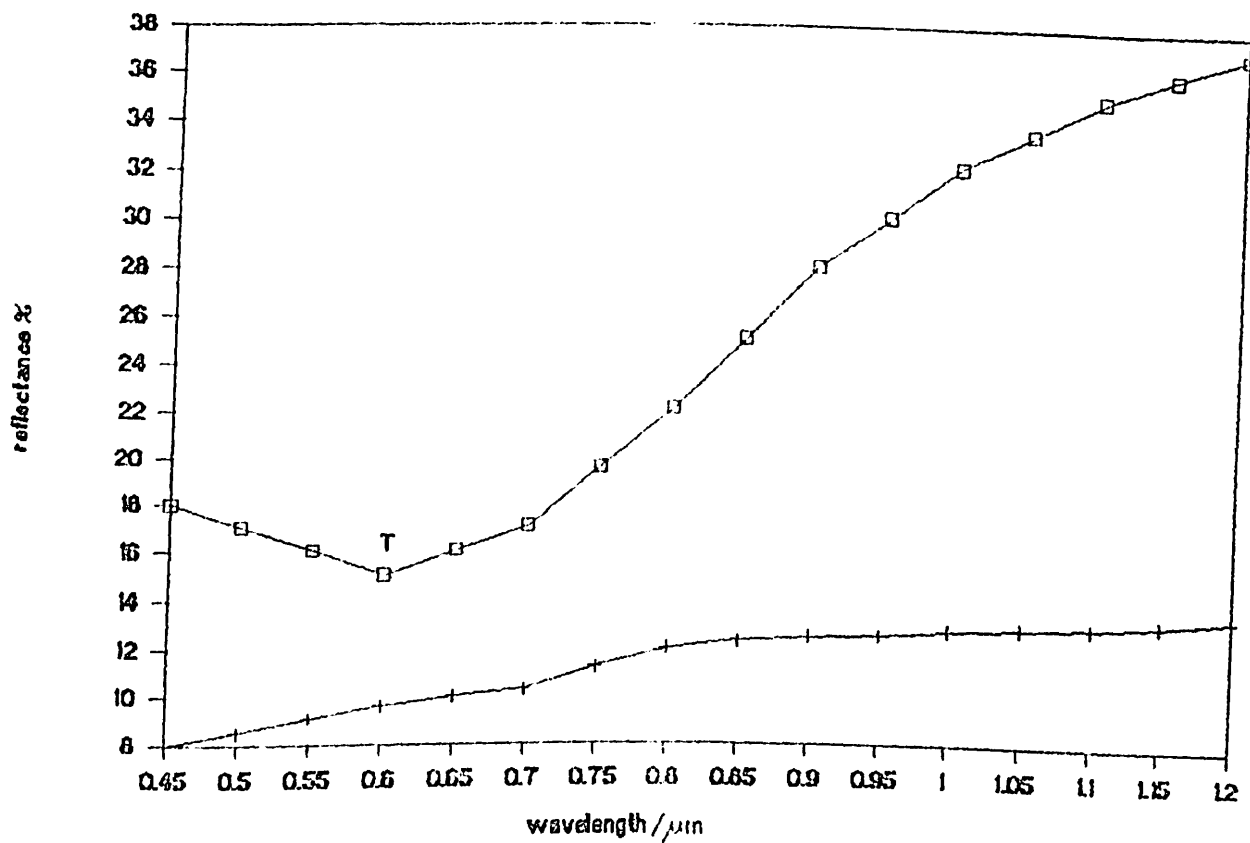


Fig. 3.18 Quartz-muscovite schist

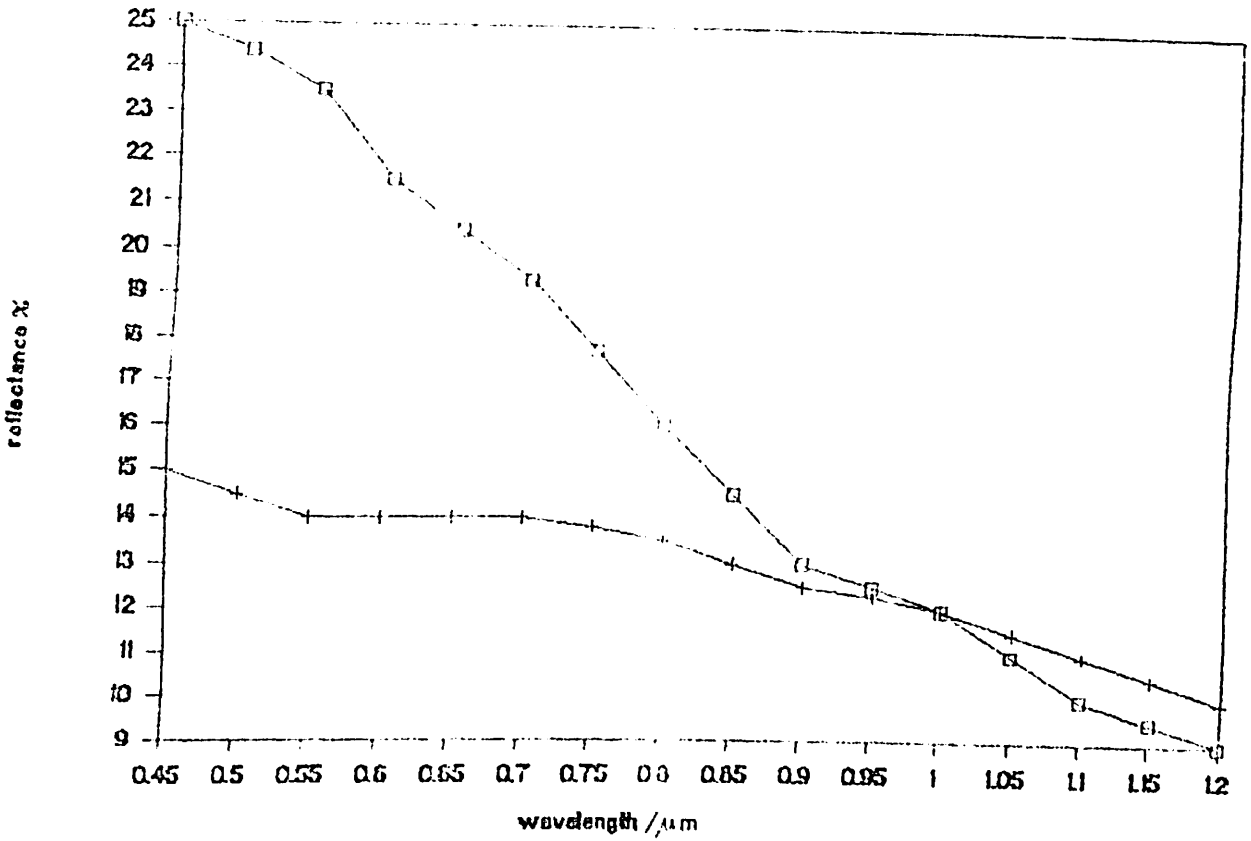


Fig. 3.19 Hornblende schist

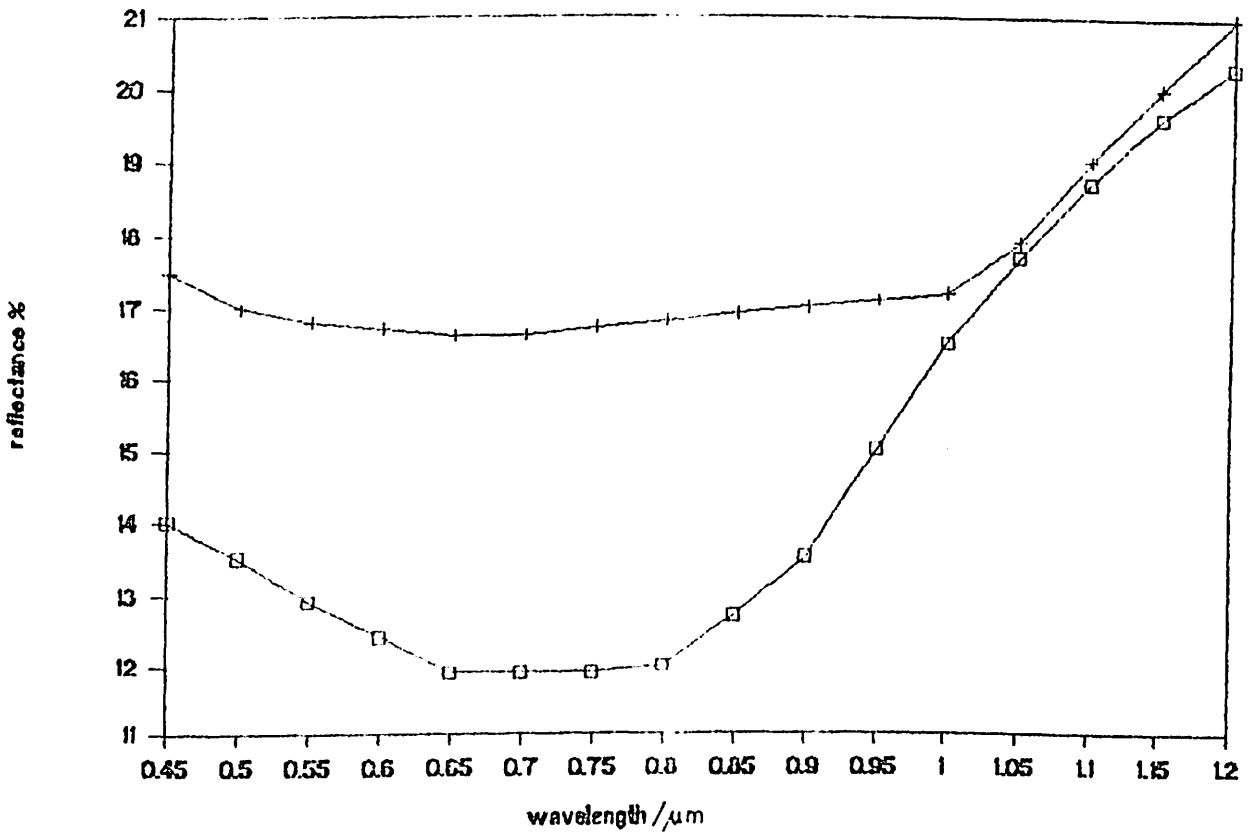


Fig. 3.20 Quartz

Fig. 3.21 Quartz-monzonite

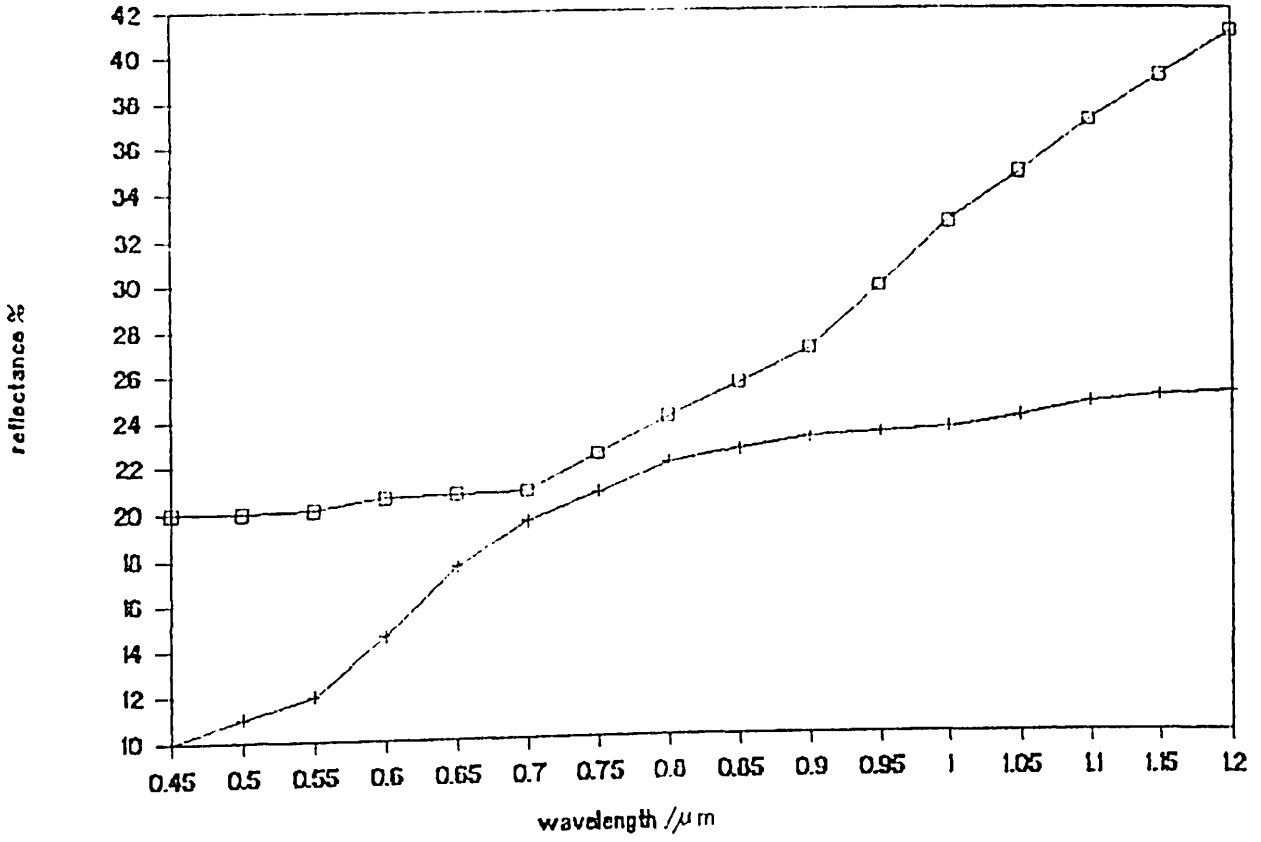


Fig. 3.21 Quartz monzonite

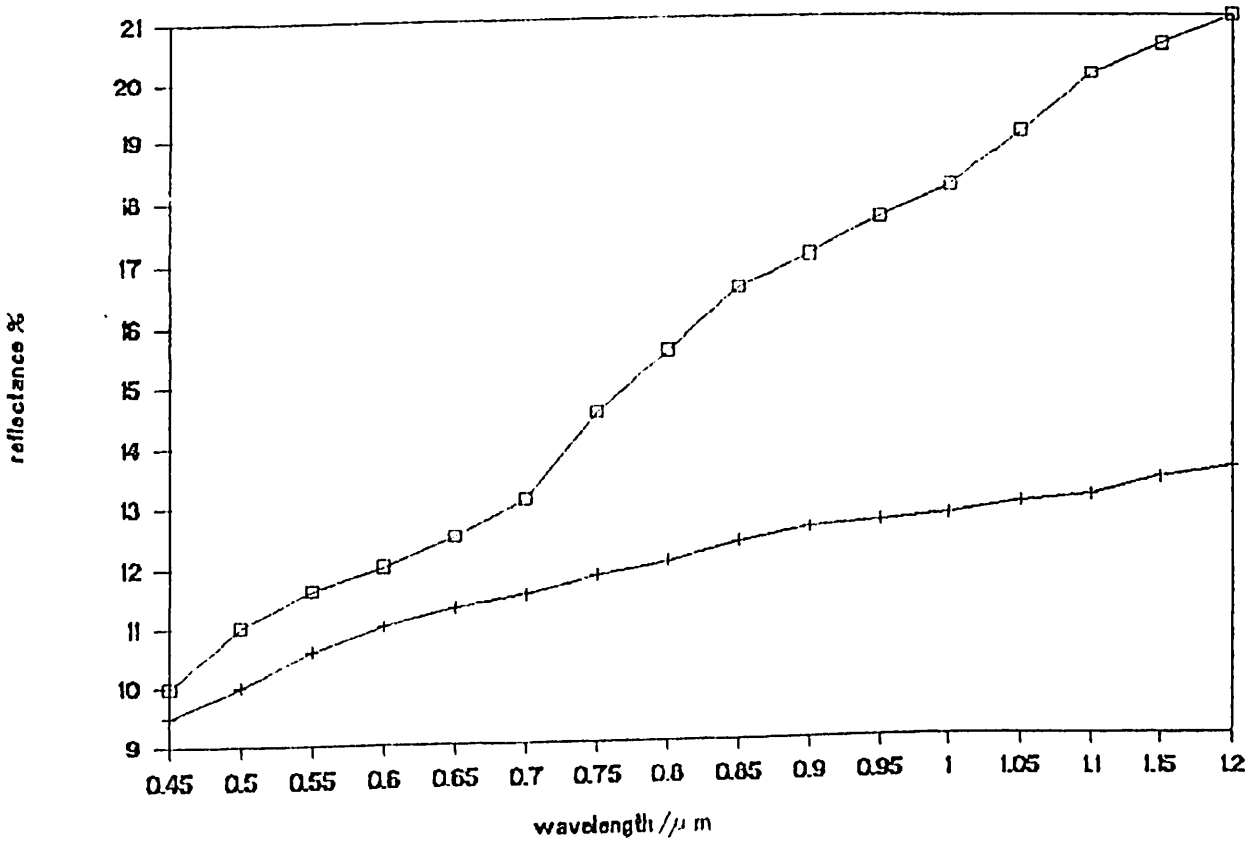


Fig. 3.22 Garnet-hornblende gneiss

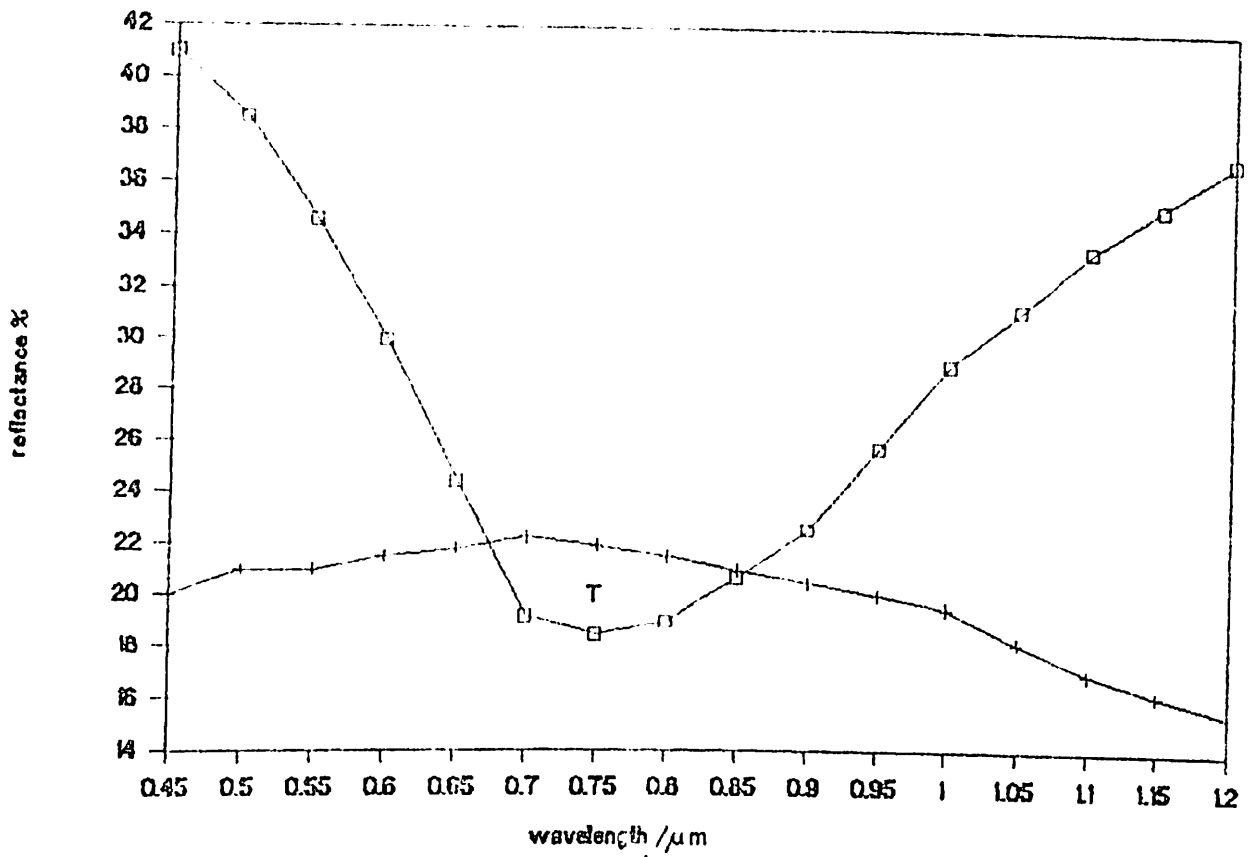


Fig. 3.23 Quartz-muscovite

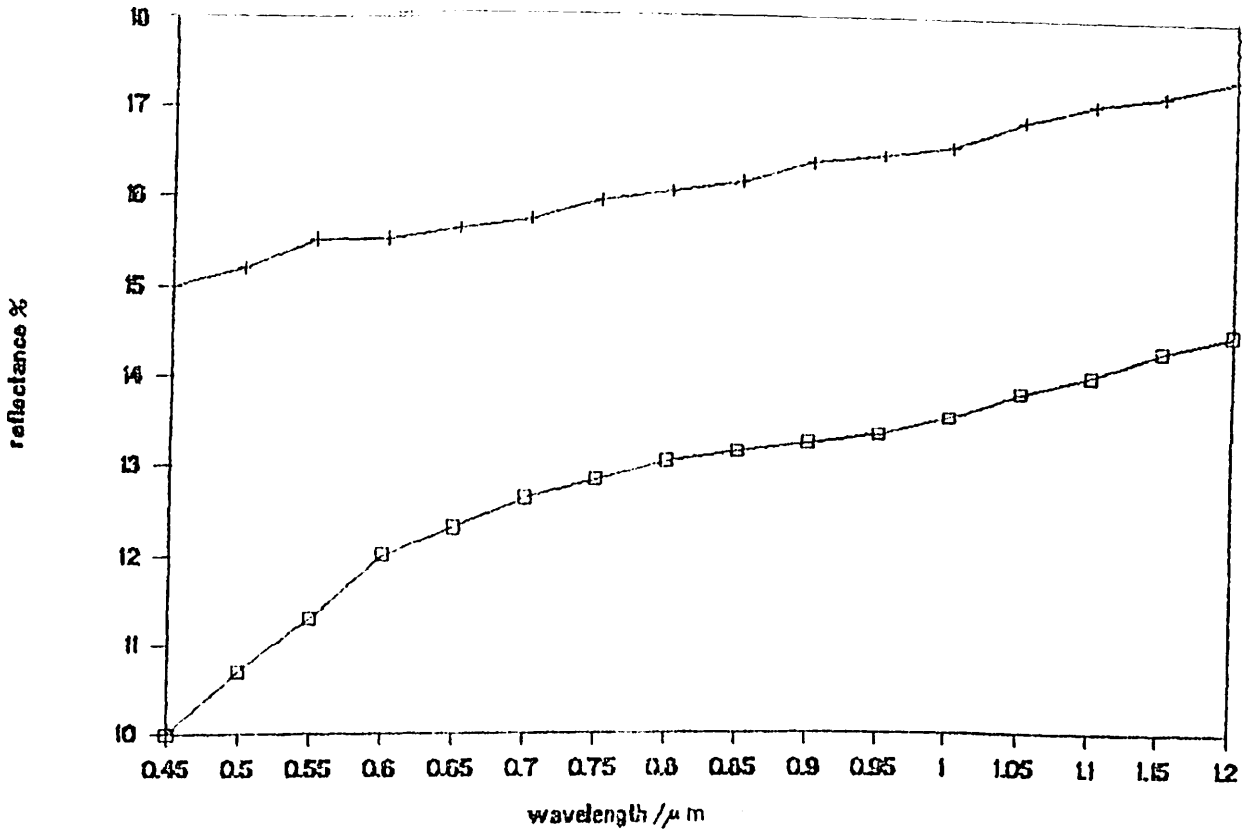


Fig. 3.24 Quartz-feldspar-biotite schist

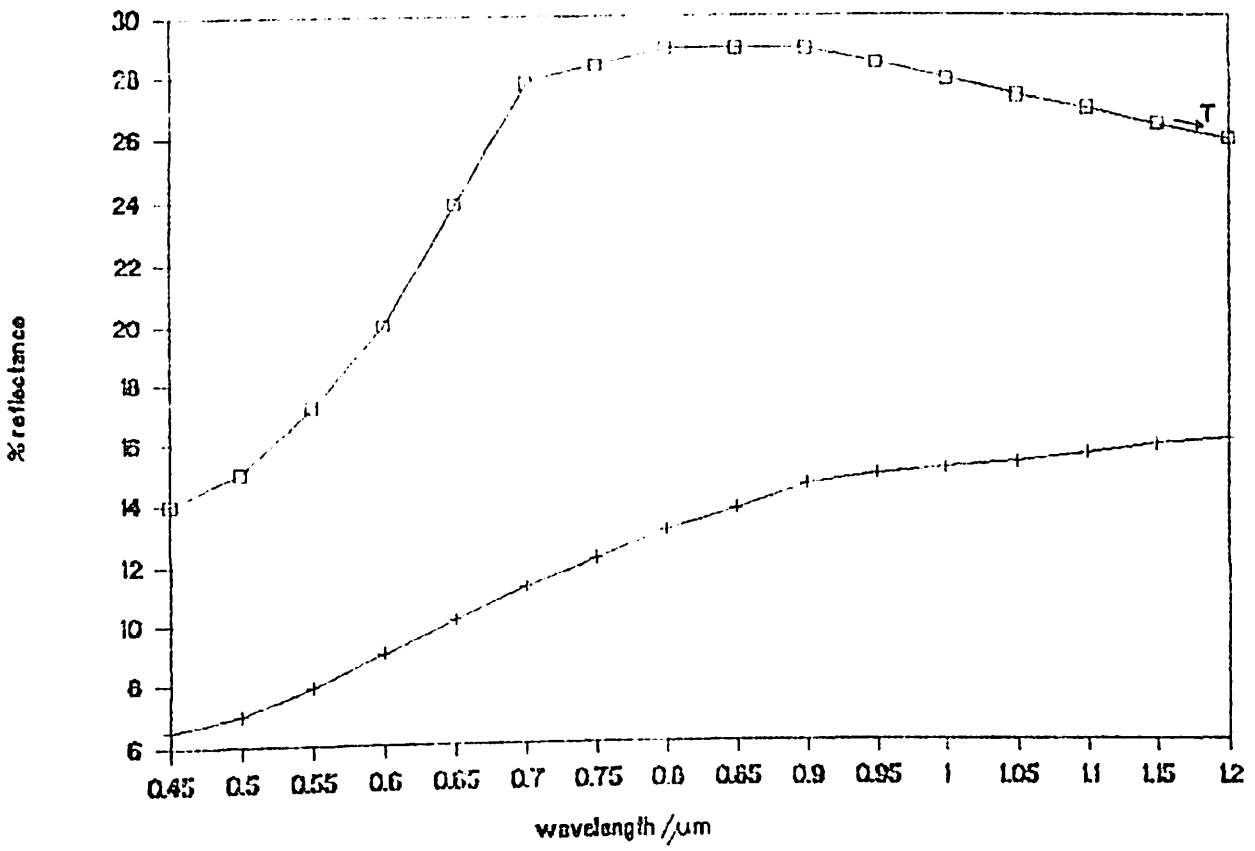


Fig. 3.25 Grit

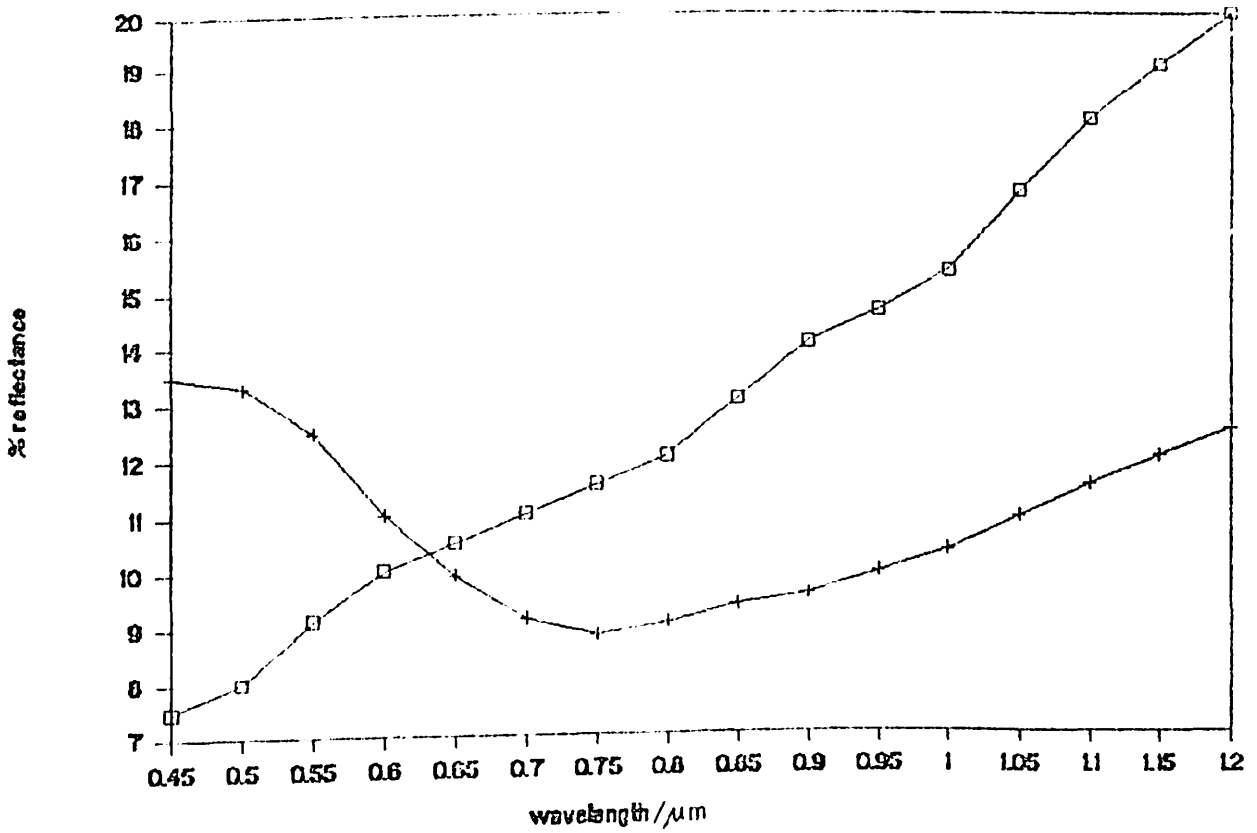


Fig. 3.26 Tholeiitic dolerite

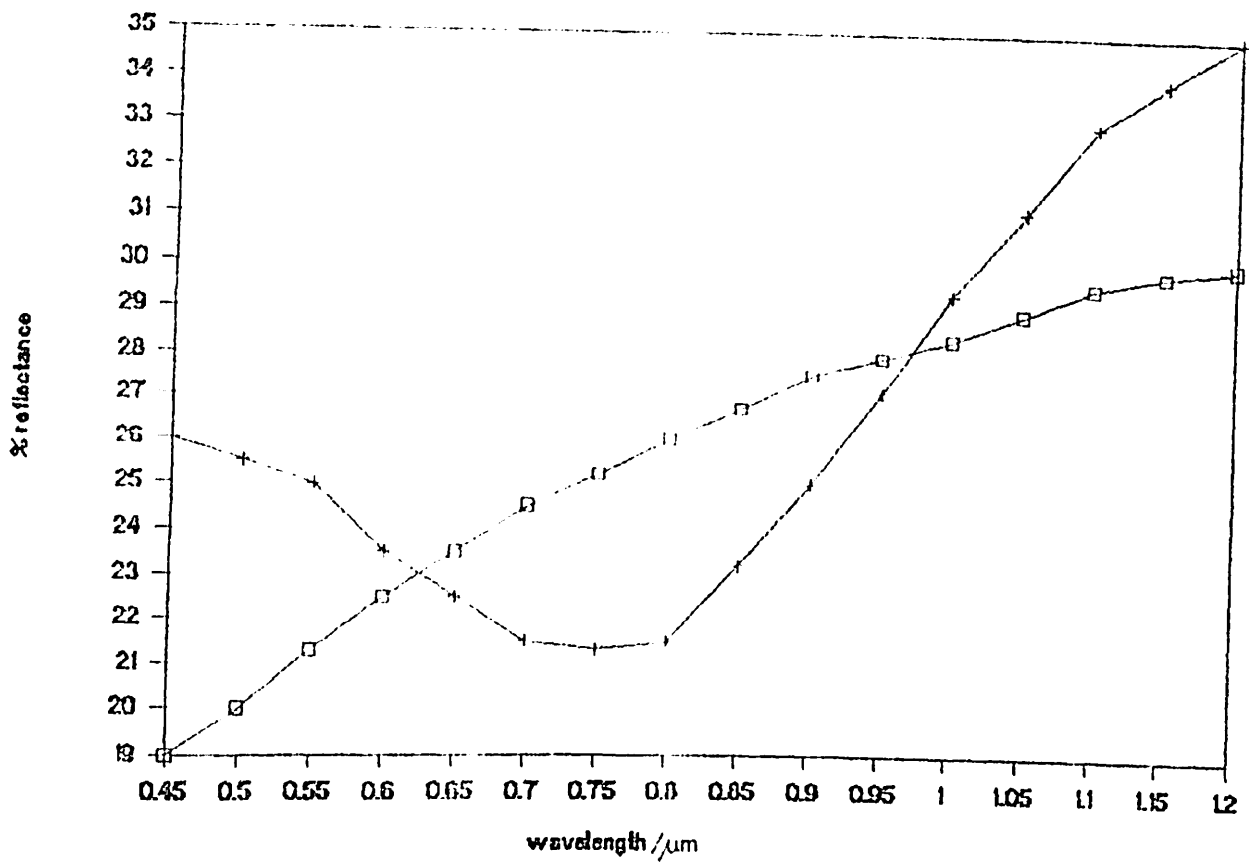


Fig. 3.27 Pegmatite

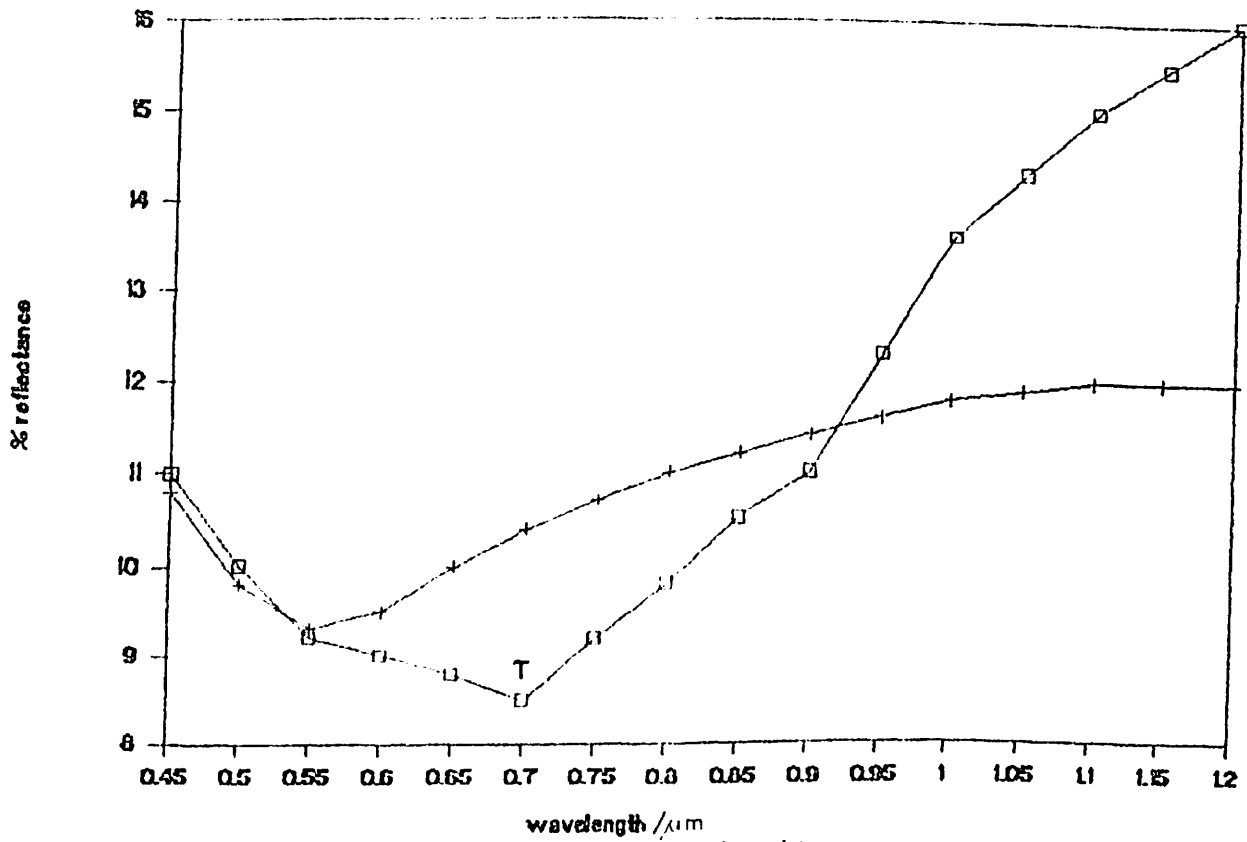


Fig. 3.28 Migmatitic granodiorite

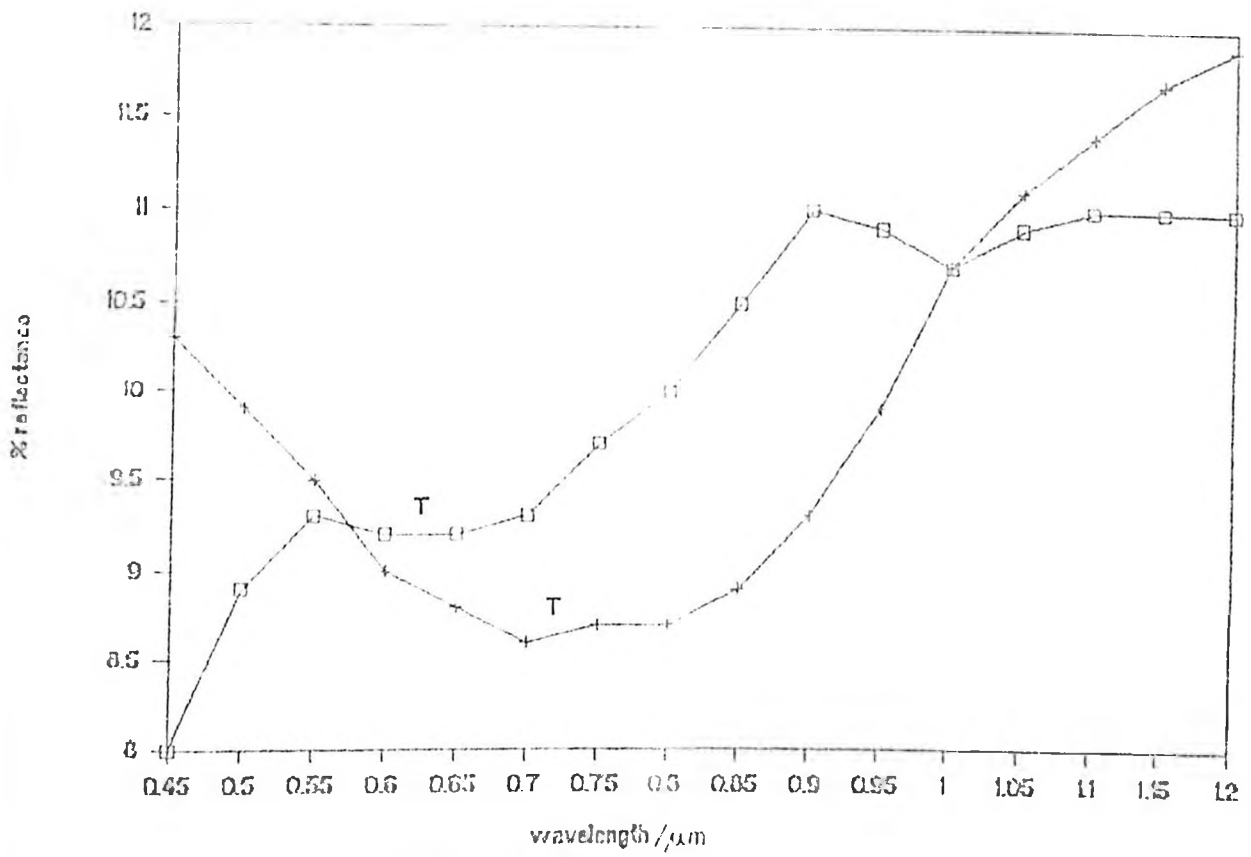


Fig. 3.29 Meta dolerite

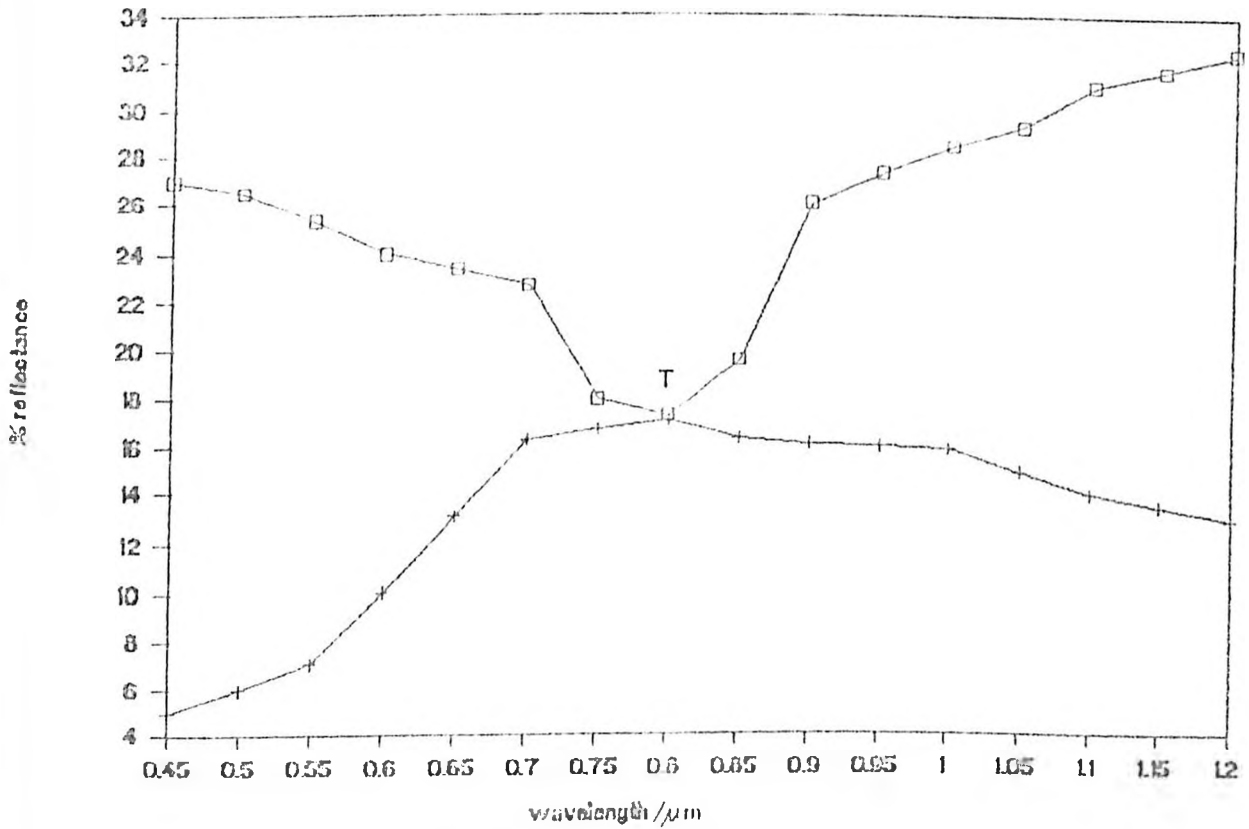


Fig. 3.30 Muscovite schist

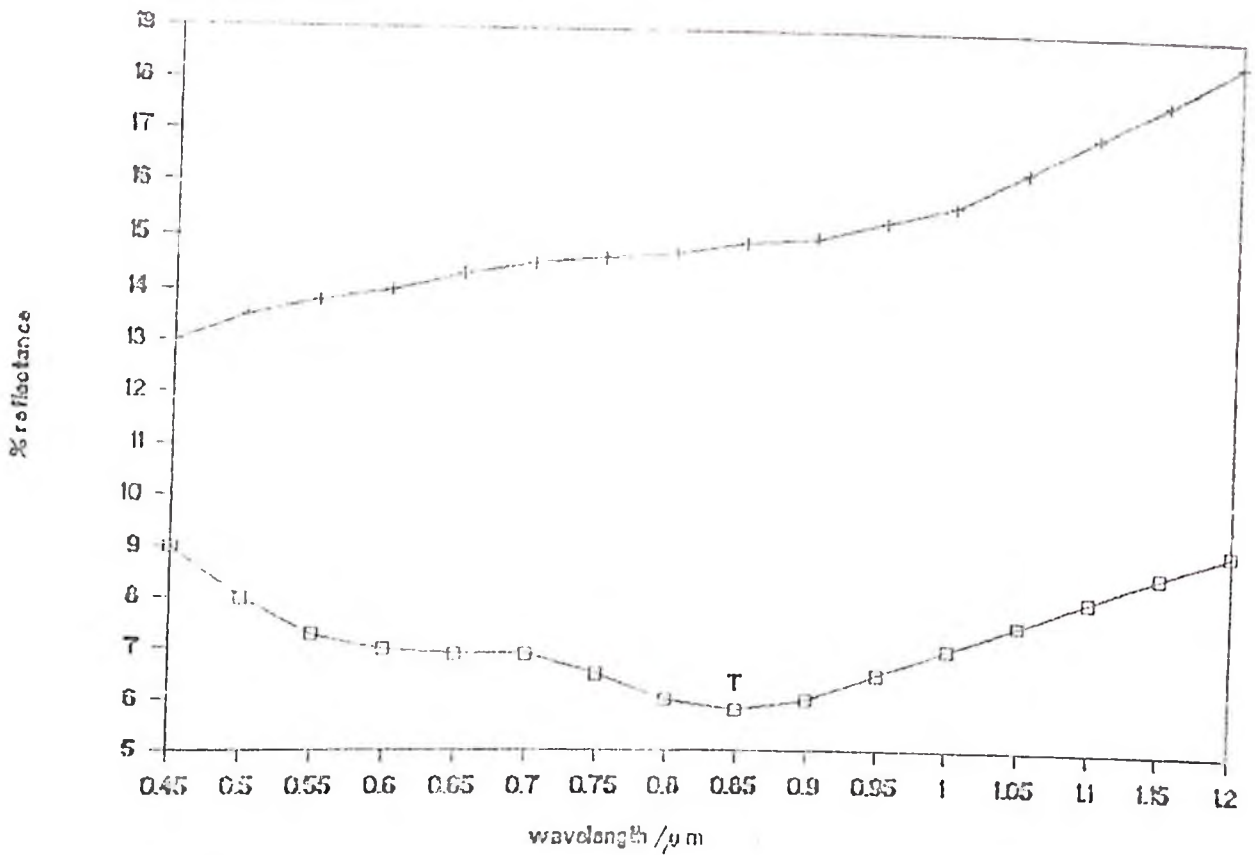


Fig. 3.31 Garnet-hornblende schist

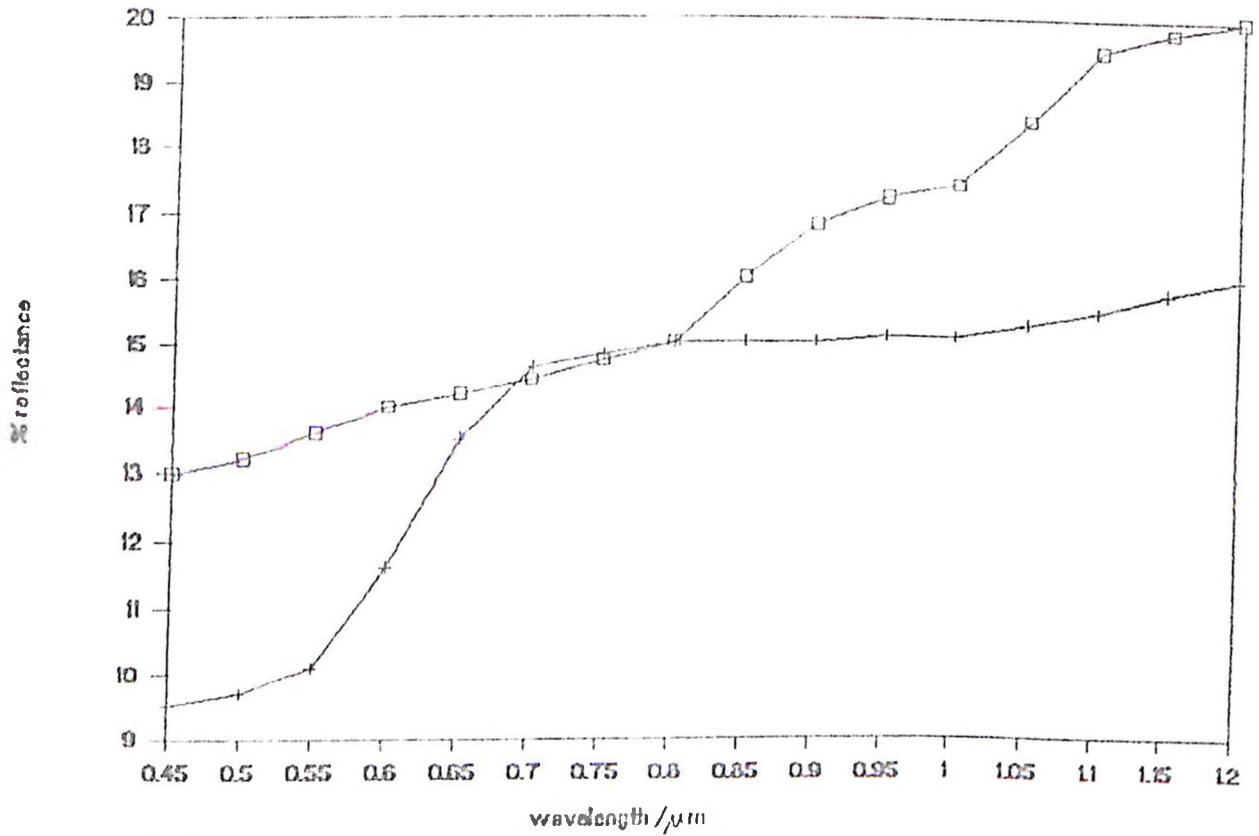


Fig. 3.32 Crush granite

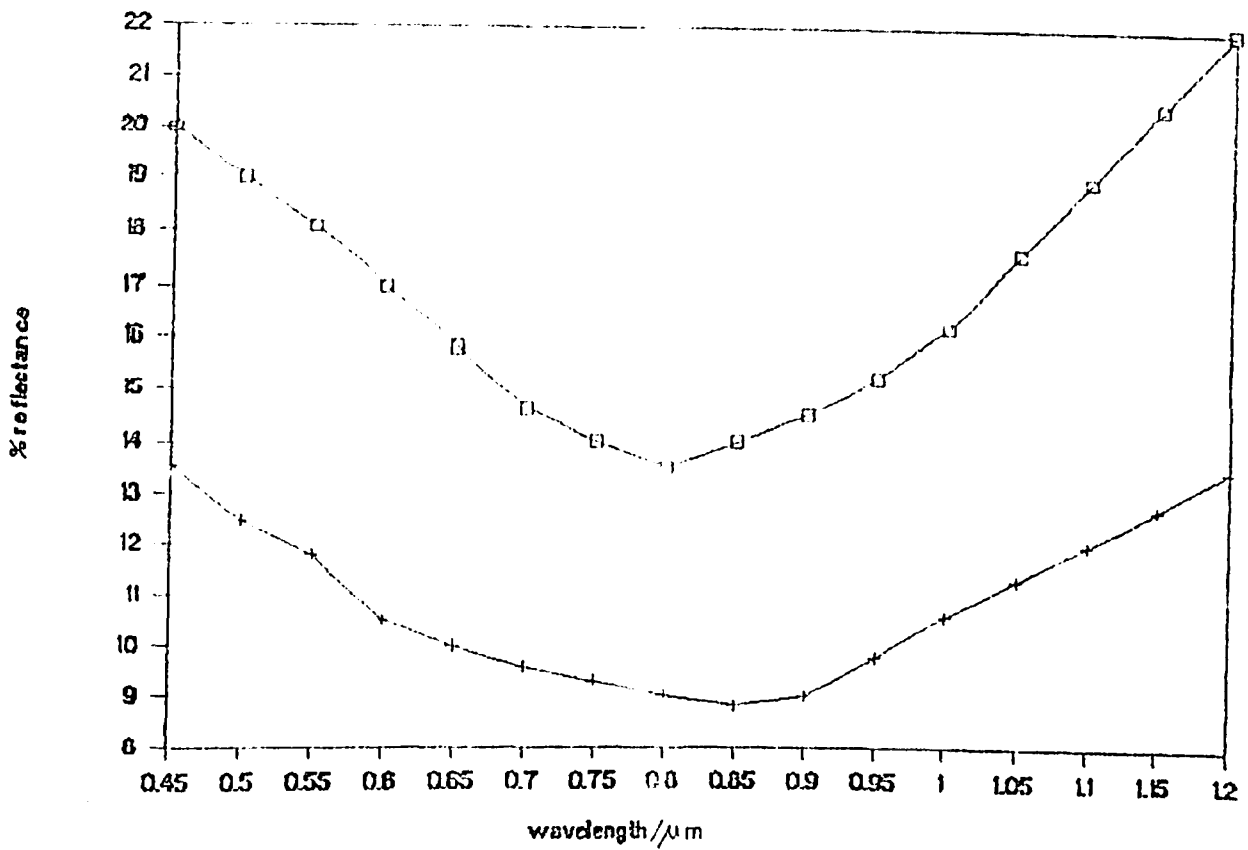


Fig. 3.33 Mylonite

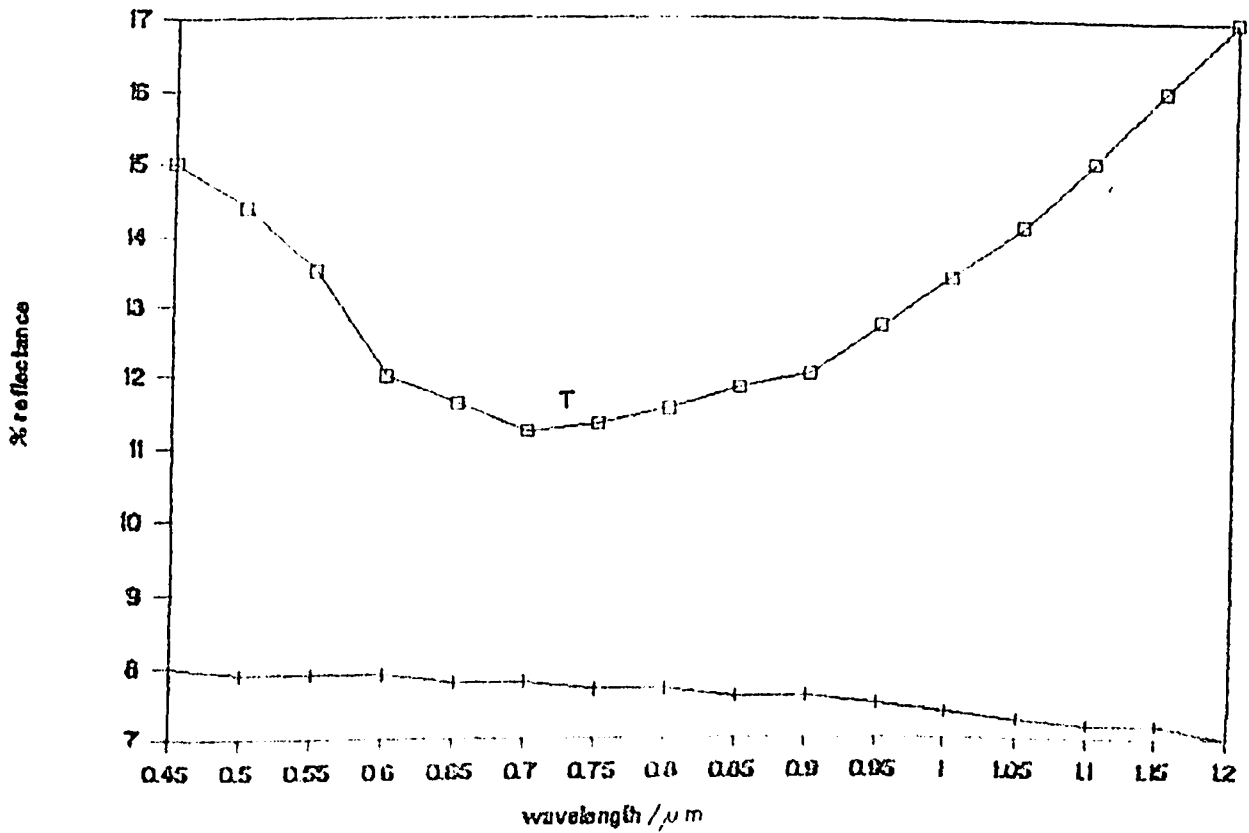


Fig. 3.34 Olivine dolerite

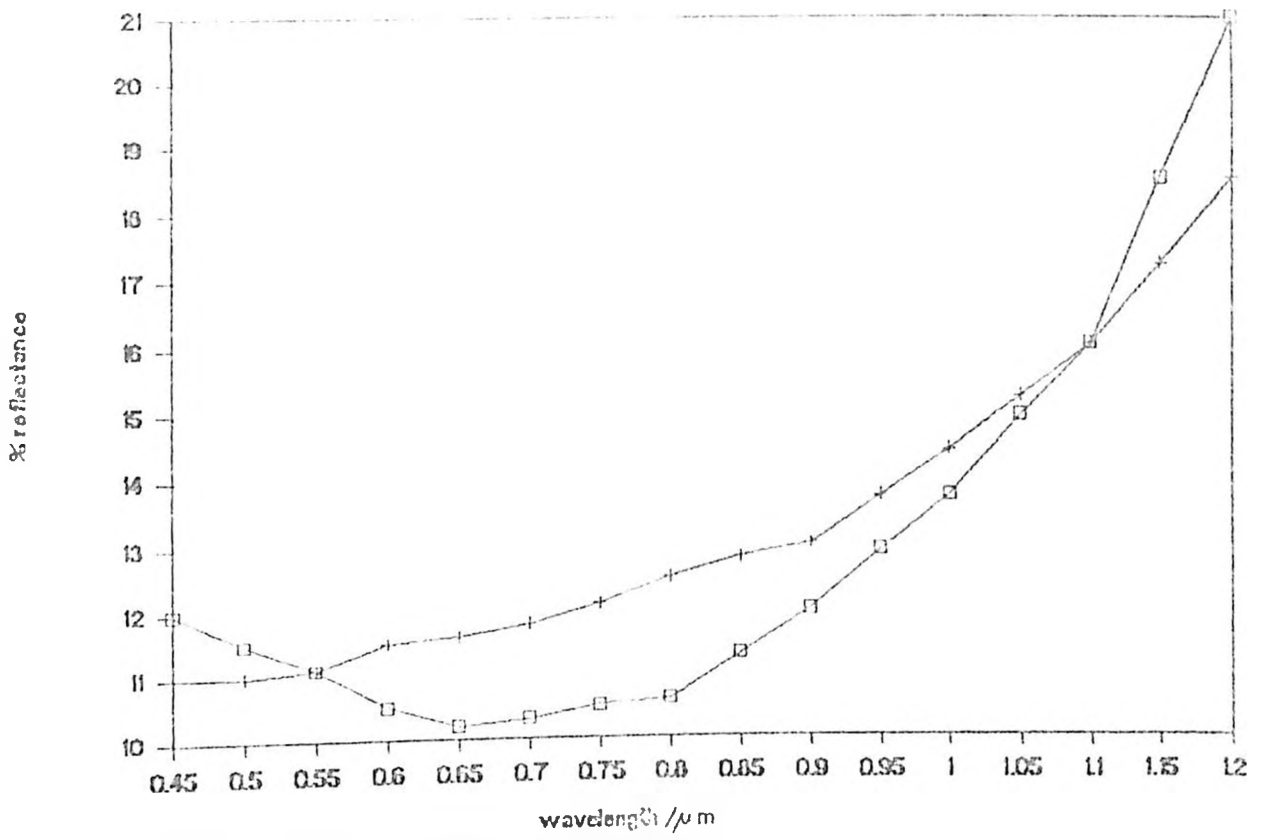


Fig. 3.35 Banded ironstone

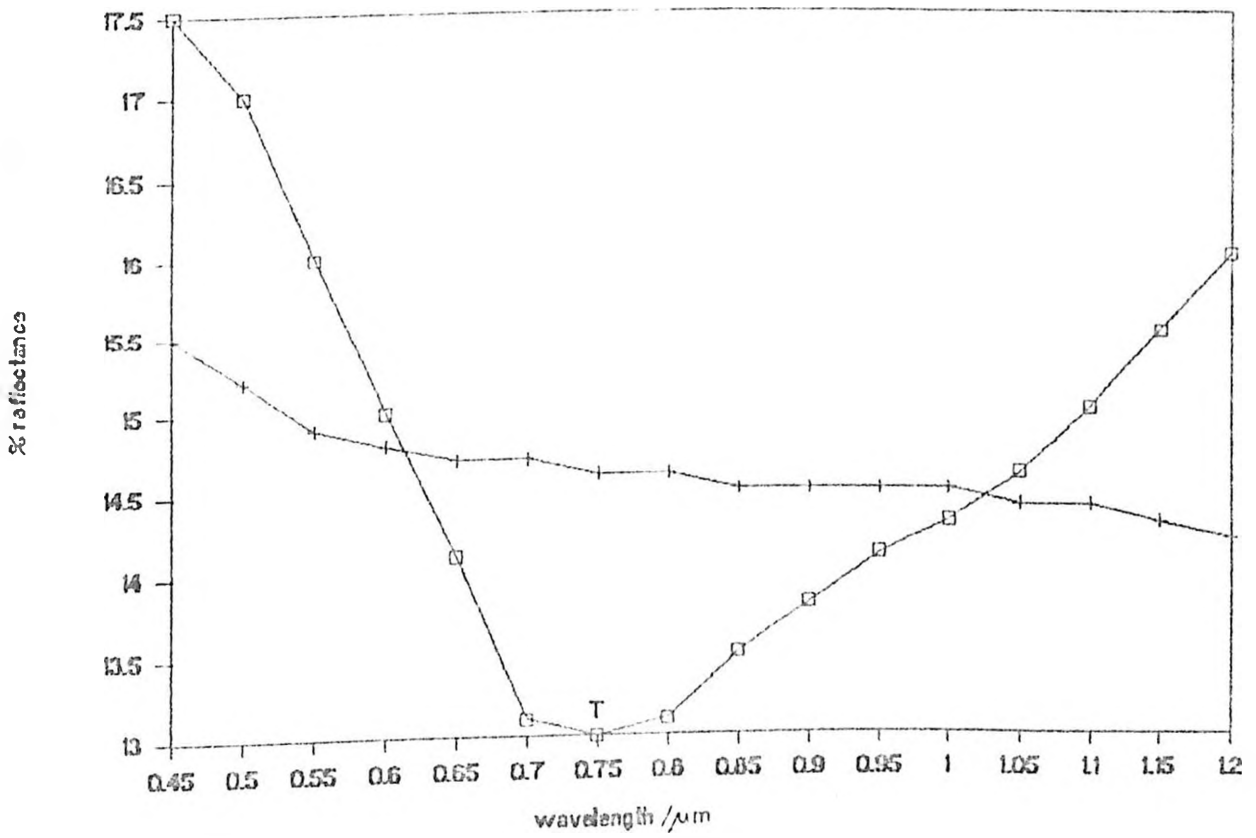


Fig. 3.36 Hornblende gneiss

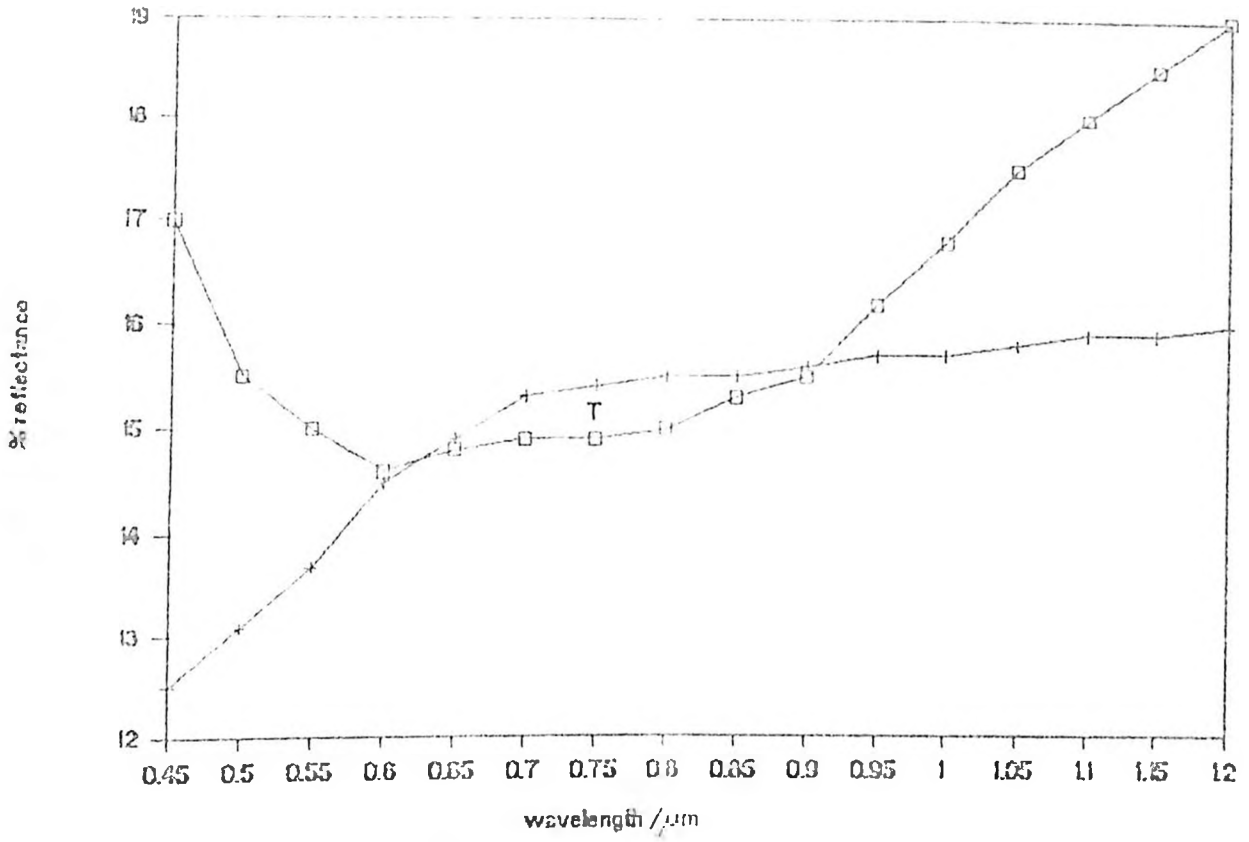


Fig. 3.37 Meta (gneissose) granodiorite

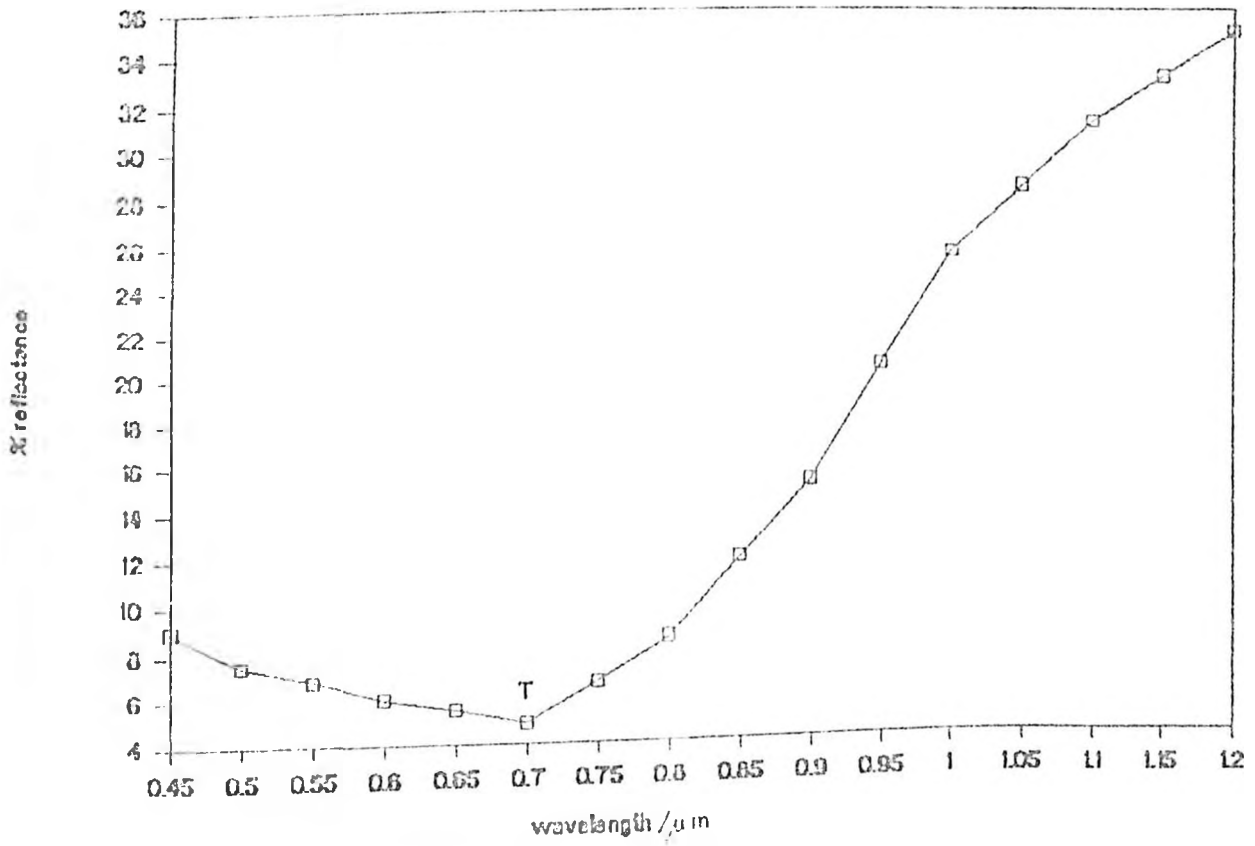


Fig. 3.38 Grass

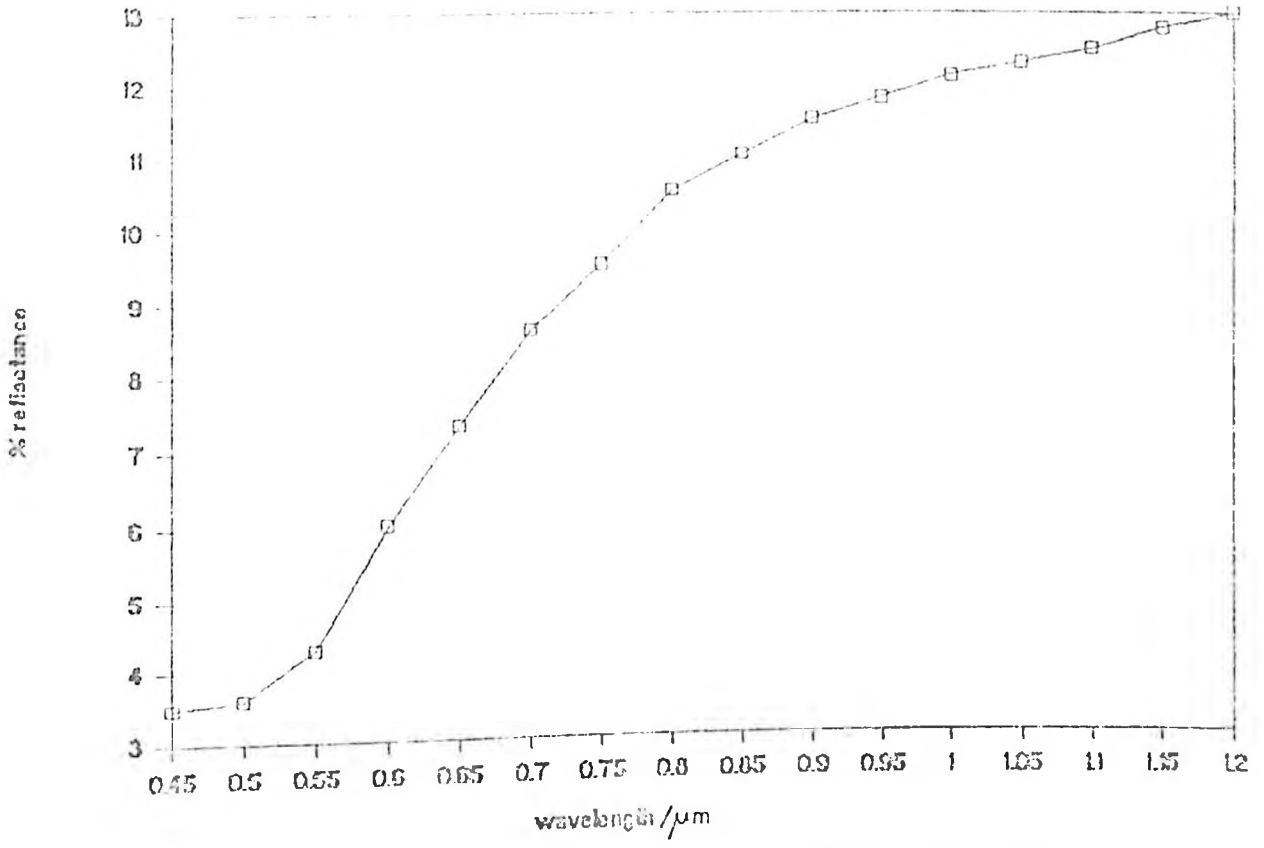


Fig. 3.39 Loam soil, Kasarani area (Nairobi)

4. GEOLOGICAL INTERPRETATION

4.1. Introduction

In the field seeing connections over distances between geological features on the ground is hindered by topography and vegetation. In this case any clues to continuity and variation over wide areas that an image from the air or space reveals make the work of a geologist easier and more efficient. Rocks of different compositions respond to weathering and erosion differently depending on the chemical composition and physical structure of their constituent minerals. This means that the intricacies of land surface are frequently controlled by the underlying rocks and the structures in which they are disposed (Drury, 1990).

Fractures in the crust, in the form of faults across which large masses of rock have moved relative to one another, produce zones of altered and shattered rocks that are easily exploited by erosion (Drury, 1990). Where faults are steeply dipping they outcrop as sharp, almost straight lines. Steep slopes are probably the most readily identified geological features on remotely sensed images. When they dip at shallow angles, their outcrops are more intricate and do not exert such a strong control on the appearance of terrain from above.

The composition and internal structure of rocks controls the finer details of the surface, particularly the drainage patterns which develop upon them (Thornbury, 1969). Rocks that are impermeable to surface water, like clay-rich sediments or crystalline igneous and metamorphic rocks retain all rainfall

at the surface and so have fine, intricate drainage patterns (fig. 4.00).

Structures in geological units can be inferred from drainage patterns. Uniformly dipping layered sequences of different resistant rocks have developed a parallel or trellis-like pattern of streams (Nandi escarpment). Outcrops of homogeneous rock show no clear arrangement having instead a drainage network like the veins in a leaf- (dendritic pattern). Large upstanding masses of resistant rocks like mountains and hills are remnants of volcanoes are drained by streams that define a radial system of valleys. A typical example of this is the drainage in Mount Elgon area; there is a radial system of drainage emanating from the mountain. The drainage channels form tributaries of the river Nzoia. These channels drain water in a south-easterly direction (fig. 4.00). Besides, the composition and internal structure of rocks have an effect on the local products of erosion. Some rocks produce quite smooth weathered surfaces while others are characterised by rough surfaces (Hills, 1956 and 1963).

The Nzoia peneplain has a dendritic drainage pattern characterised by irregular branching of streams, with leaf appearance. This drainage has developed in flat-lying areas of more or less uniform composition (see geological map). This suggests the availability of massive intrusive rocks and / or strongly metamorphosed sedimentary rocks. The former are metamorphosed granodiorites and the latter are the phyllites / greywackes / grits.

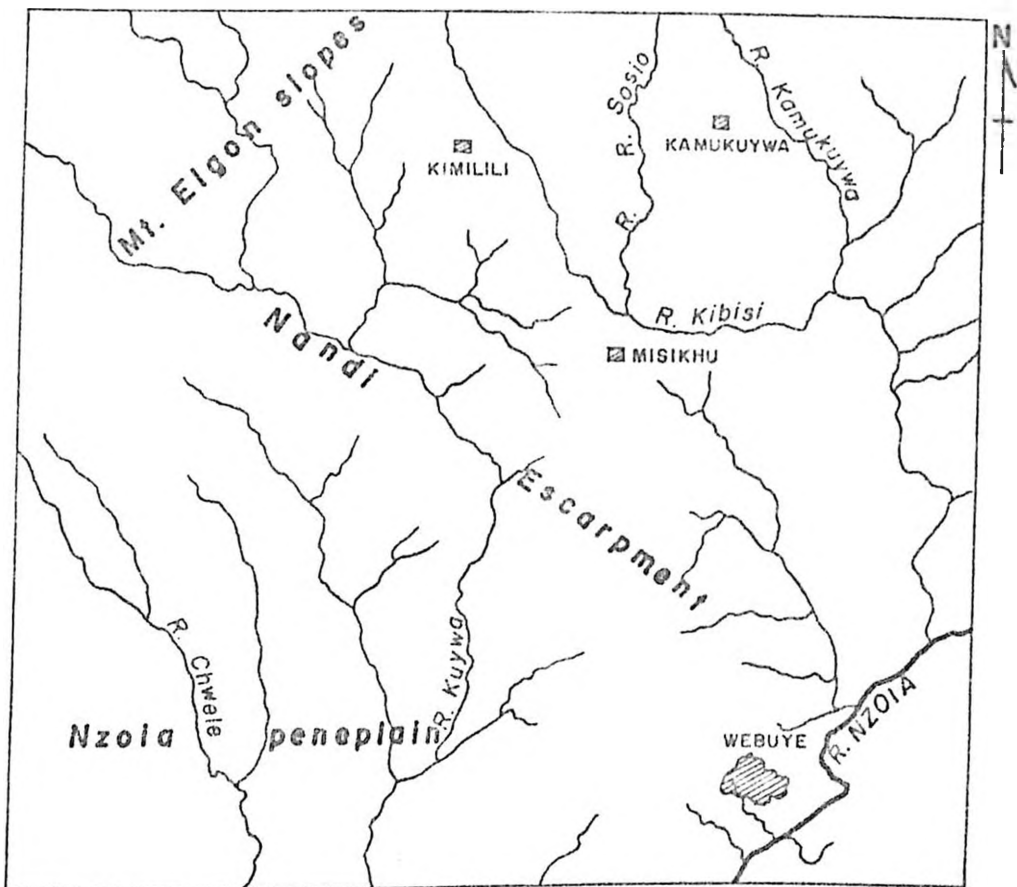


Fig.4.00- Drainage patterns as depicted by Multispectral scanners(MSS) imagery (acquired , Dec.1975) .

- Scale : 1 / 250,000

Type of drainage

- Nzoia penoplain - Dendritic
- Mt. Elgon slopes - Radial
- Nandi escarpment- Trellis

The main agent contributing to land forms in humid areas, both temperate and tropical is flowing water. In the tropics there is increased weathering of rocks by chemical means. In these areas heavy loads of sediments in running water gives an MSS image of pale colour, while more or less clean water gives black colour. At the surface of the earth, dense vegetation both binds the soil and reduces the speed at which rainfall flows over land. In densely forested areas of the tropics, this allows steeper valley slopes to be better preserved than in more temperate areas where the angles of slope are reduced both by erosion and the downward creep under gravity of wet soil and other surface debris.

In vegetation, chlorophyll has its maximum precipitation in red, green and blue band and plant cells reflect most radiant energy here. The abnormally low reflectance of plants in red and their very high infrared response causes vegetation to be rendered in the false colour composite (FCC) as various shades of red while other surfaces appear in greys, blues, yellows and browns.

4.2. Detailed Photogeology

The interpretation keys applied to aerial photographs were based on Allum (1966).

Kazik, (1955) has recommended that colour photography for geological processes be limited to a scale of 1 : 10,000 and larger than this. The scale used in this study is 1 : 25,000.

Aerial photographs used in this research were prepared before the rainy season. This is because it is possible to observe prepared fields; which have a light grey tone with sharp boundaries. The interpretation of a stereopair of aerial photographs for the Webuye area is shown in figures 5 and 6. The forests around Mount Elgon appear dark, a photograph manifestation of the trees. Features of high relief can be seen clearly like Mt. Elgon and the Nandi escarpment. Thus it is possible to identify features of low or high relief (Cater, 1951).

Strong colour contrast of varying grey is observed on the Nzoia peneplain. It reveals that this area is typical of the sedimentary rocks. Colour contrast is influenced by humidity, soil and rocks. South of Webuye town, mudstone is exposed to rapid erosion and some mass movement. It is a dissected area with broad open valleys.

Igneous rocks appear massive and weather along fractures. They are coarse with regular dissection of dendritic drainage. There are narrow steep sided valleys in the mountain slopes. Metamorphic rocks are resistant to erosion and exhibit upward bending nature at the contact metamorphic zones. They have distinct relief in veins, crumbling and mineralisation slumping. There is an overall differential erosion.

The valleys can be differentiated from other areas on the mosaic by their colour which is light-grey with sharp



→ North

X- Air sortie position



Figure 5 : Stereopair of aerial photographs covering Webuye town and its environs. Scale 1:25,000

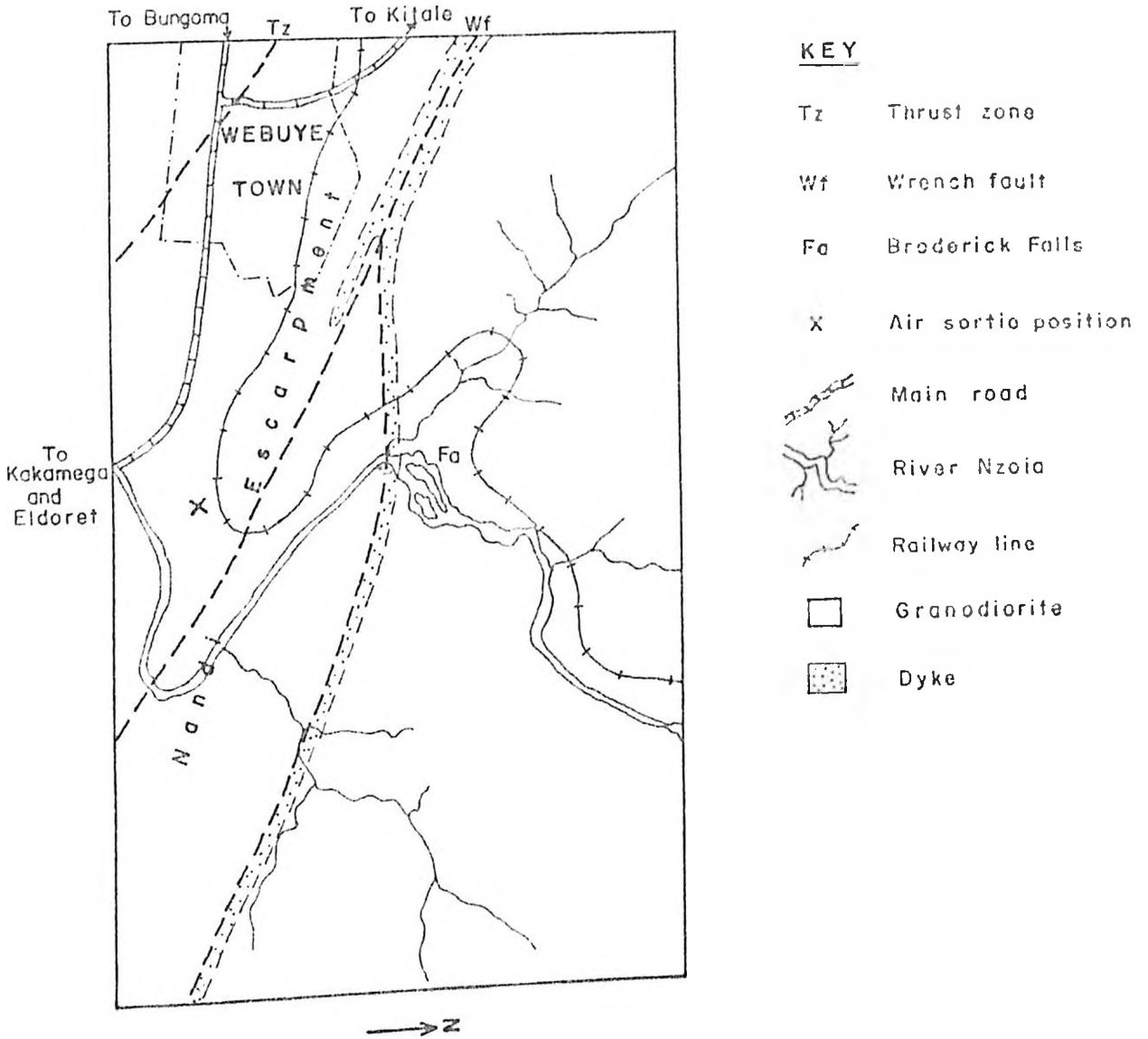


Figure 6 : Interpretation of aerial photographs in figure 4.20a. Scale 1:25,000 .

boundaries. This is attributed to the presence of sediments (Rich, 1951).

Texture which can be fine, course, rough and fluffy has been used in relation to soils and density of drainage network. Wide spacing of streams is typical of this area and shows coarse texture while close spacing of streams which is basically a revelation of fine textures of drainage is somewhat absent only being revealed in the northern part of the suffocated escarpment.

The orderly spatial arrangement of geological, topographical or vegetational features is "Pattern". Spatial arrangement can be both two or three dimensional. They may represent faults, joints, dikes or bedding.

By considering factors like lithological character of the underlying rocks, altitude of the rock body, arrangement and spacing of the planes of lithological and structural weakness encountered, it is found that stream patterns in this area are controlled by the underlying structure and rock type. The faults found here are oriented in the south-east direction which is also the direction taken by the streams which empty their waters into the river Nzoia, so does the orientation of the major rock types. Patterns of vegetation reflect structural conditions or lithologic character types. This is true of the Nzoia peneplain which has more or less southerly drainage network and hosts very few rock types with minor variations up to the Nandi escarpment. Soil patterns reveal information of

direct use in engineering geology studies, as in the location of granular materials. Soil patterns are vital in suggesting the distribution of certain rock types which may reflect geologic structures. For example, the slopes of Mount Elgon which have nephelinite and agglomerates are covered by a dense forest meaning that their weathering products are quite fertile.

As a recognition element, shape is useful in relief or constructional landforms, such as volcanic cones like the Mount Elgon volcanic cone, river terraces and certain glacial features. It is also useful in differentiating rock units where a formation is expressed in bold cliffs and overlies a second formation that shows a lesser angle of slope or where adjacent rocks show significant differences in topographic relief. Bold cliffs are shown by the topographic relief exhibited by the Nandi escarpment and Broderick Falls. Slopes of gully cross-section are important to the interpretation of surficial materials for engineering geology.

In terms of size, recognition of geological features from aerial photographs is appropriately considered in relation to thickness of strata. The size of features such as Mount Elgon volcanic rocks and rock displacements have been ascertained to good accuracy from aerial photographs. Studies in quantitative geomorphology suggests that size, in terms of definite measurements, may be a vital parameter of geological interpretation of aerial photographs.

4.3. Geology

4.3.1. Summary of geology

According to geological findings, this area mainly consists of igneous and metamorphic rocks. There are some sedimentary rocks mainly in the south of the area.

To the west of the Nandi escarpment, the Nyanzian and Kavirondian rocks are poorly exposed and are only seen to advantage in some scattered exposures on land and in the Nzoia river and its tributaries. There are outcrops of non-metamorphosed granodiorites, medium-grained greywacke, fine-grained argillite and meta-basalts.

To the east of the escarpment, low-grade metamorphosed lavas and sediments having ironstone extend in a north-westerly trend. The gneisses and schists referred to as part of the Greenstone belt are believed to be derived from progressive and constructive dynamic metamorphism of the Kavirondian and Nyanzian rocks. There is progressive change from greenschist facies in the west to epidote-amphibolite facies in the east with increasing eastward plastic deformation and strain-slip cleavage.

The Nandi escarpment is occupied by a granite-migmatite complex which exhibits mylonites that are a clear indication of extreme shear. An examination of the metamorphosed granodiorites along the escarpment and the migmatitic granodiorite found south of Kamukuywa shows that there have been metasomatism and deformation episodes. This is due to the available

porphyroblastic feldspars which retain original twinning. Differential movement is also exhibited in the rock fabric by the available quartz.

Differentiated metasediments found east of the granite-migmatite (granodiorites) complex are referred to as "supercrustal folded metasediments. The "Basement" in this area is the granite-migmatite complex which blends into the recognisable Nyanzian and Kavirondian rocks to the west.

The dolerite dykes scattered in the area east of the granite-migmatite complex have undergone slight to intense metamorphism according to the degree of metamorphism of the surrounding host rocks. The less metamorphosed dolerites have ophitic texture and contain pale-green augite partly replaced by hornblende.

The isotopic ages determined (cahen, 1966) and reported by Sanders (1965) show that:

- i). Ages range between 410 and 635 million years from feldspars and micas in the Mozambique Belt.
- ii). Deformed granite and granodiorite of the Nyanzian Shield and the western orogenic front of Mozambique Belt range between 710 and 1060 million years.
- iii). Rocks of the Nyanzian Shield range between 2510 and 3150 million years. There is a younger limit of 2550 million years for the Nyanzian and Kavirondian rocks.

On the whole, it is difficult to decipher the true order or

superposition of rock contacts in the major formations because the area is envisaged to have "tectonic rock contacts". Chronologically, it is true from the evidence in isotopic age determinations, structures and metamorphism that the Nyanzian Shield is older than the Mozambique Belt. This study area marks the "contact between the Nyanzian Shield and the Mozambique Belt in western Kenya".

Absorption features observed in spectral reflectance are generally broad meaning that molecules occupy unordered or several equivalent sites. What is observed in the near infrared (T features in figures 3.10 to 3.39) serves to identify overtones and combinations involving materials with very high fundamental frequencies. Groups providing this are those with O-H stretching modes like clays and micas. In the spectra of minerals containing ferrous ions, absorption features are due to the spin-allowed transitions.

Rock Chronology (Based on Sanders, 1965)

Recent	Ironstone
	Mount Elgon Series
Tertiary	Nephelinite
	Turoka group
	Muscovite-quartzite
Lower Palaeozoic	Quartz-muscovite schist
and Upper	Biotite-muscovite schist
PreCambrian	Muscovite-schist
	Garnet-schist

Quartz-feldspar-biotite schist
Hornblende-gneiss
Garnet-hornblende gneiss
Hornblende-schist
Garnet-hornblende schist
Migmatitic granodiorite
Mylonites and crush granite

Kavirondian Group

Grits and phyllite
Mudstone

Archaean

Nyanzian Group

Actinolite-schist
Chlorite-schist
Banded ironstone

Intrusives

Granodiorite
metamorphosed granodiorite
Olivine-dolerite
Meta-dolerite
Tholeiitic dolerite
Quartz-monzonite

4.3.2. Detailed geology

Detailed rocks examinations reveal that this area consists of Nyanzian Group, Kavirondian Group, Turoka group, Mount Elgon Series, Intrusives and Iron Formation

NB Group is a lithostratigraphical terminology which is defined by regions of complex stratigraphy. It is limited by aerial extent of features chosen to characterise and distinguish it. Group represents a principle stratigraphical unit in the hierachial ranks of the lithostratigraphical classification. Boundaries of lithostratigraphical cut across isochronous surfaces and lithological features are repeated time and again in the lithostratigraphical sequence. The term **group** is an informal unit of a Group.

4.3.3. Nyanzian Group

There are two rock types in this Group; schists (actinolite and chlorite schist) and banded ironstone

4.3.3.1. Schists

There are four types of schists in the Nyanzian Group:

- (i). Actinolite schist (BW/25).
- (ii). Chlorite schist (BW/18).

These rocks are characterised by a high content of actinolite, and chlorite. Feldspars, quartz, micas and iron oxides are present in low quantity.

The effect of actinolite is that it stabilises the reflectance spectra (fresh actinolite schist, figure 3.10). The weathered sample has abundant chlorite, an alteration product of actinolite and feldspar. It gives an absorption feature "T" in the VNIR region of the spectrum. In figure 3.17, the absorption feature "T" is more to the right of the curve for the fresh sample while it is in the red band for the weathered sample.

The reflectance pattern of fresh mudstone (figure 3.11), is similar to that of chlorite schist.

4.3.3.2. Banded ironstone (BW/20)

The iron formation is composed of recrystallised chert, haematite and magnetite. There is general development of granules, mainly of iron silicate. They are ovoid or bean-shaped and range from a fraction of a millimetre to few millimetres. They do not display concentric or radiating structures.

Even though it is found in association with thick volcanic sections or even interbedded with them, it is curious to note that elsewhere ironstone formations have been formed without such trace of volcanic material or characteristic. There is no sufficient correlation with igneous activity to justify the conclusion that it is the principal source of iron and silica. It is quite evident that periods of iron formation development follow the exposure of large amounts of basic lavas to the effects of weathering. This may be the most plausible factor in the development of iron-rich deposits. The deposition of iron takes place as a ferric hydroxide, ferrous carbonate, ferrous silicate or pyrite depending upon the pH and Redox potential of the environment. The presence of "banding" shows that the rock was deposited in relatively quiet and deep water condition.

It is not known when the typical minerals of the iron formations occurred. It has been argued that the haematite and magnetite are partly primary and partly due to

recrystallization; minnesotaite and stilpnomelane are probably products of mild metamorphism. Banded ironstone is a Precambrian iron formation similar to those in North America.

The iron oxide displays an absorption feature "T" in the VNIR region of the wavelength. This reflectance is due to energy being absorbed to accomplish a distortion in the Fe-O bond. The lower values of reflectance in the green band are related to the bonding in the mineral chert and the red colour imparted during weathering.

4.3.4. Kavirondian Group

This Group consists of mudstones, grits and phyllites. With the exception of schist, other rocks take up a large part of the southern region. The schist is found in the higher part of the Nandi escarpment, north of Wajimoi market. It forms a lense 200m thick, in the metamorphosed granodiorite that stretches east-west.

4.3.4.1. Mudstone (BW/42)

The clay-rich mudstone lacks fissility and or bedding. The diagenesis of montmorillonite has produced the chlorite that constitutes 80% of the rock composition. Other minerals present are quartz, feldspar, micas and actinolite. The rock forms a northward trending lense in the vast grits and phyllites. Huddleston (1951), has reported the presence of mudstone in the Kakamega area.

A reflectance "minima" or absorption feature "T" in the fresh

sample (fig. 3.11) stands for the distortion of the AL-OH bonds of the clay minerals by radiation. It has been established that the reflectance curve for a soil sample (fig. 3.39) collected from Kasarani, Nairobi (Kenya), is similar to that of weathered mudstone. This resemblance is related to the similarity in the composition of both samples.

4.3.4.2. Grit (BW/34)

This is an incoherent deposit compacted by silica as cementing matrix. There is abundant quartz as well as some micas (muscovite and biotite), feldspars (microcline and aperlthite) and rock fragments. Accessories include zircon, tourmaline and apatite. Muscovite is distorted with bent flakes while biotite entered in as an accessory and takes up a small percent.

The texture is such that the groundmass has been modified by pressure solution (Huddleston, 1951) and secondary growth. The presence of quartz feldspars and micas reveals that this rock was derived from metamorphic and igneous terrains.

There is nothing special in the reflectance curves for this rock because of its mixed up composition with variegated and changing phases of the mineral content (fig. 3.25). However the fresh sample gives a reflectance maxima in the red band. This maxima may be due to the reflective nature of the quartz mineral and silica cement. The weathered sample gives green < red < infrared reflectance values.

4.3.4.3. Phyllite (BW/11)

The principal minerals in phyllite are: quartz (15 %), feldspars (35 %, in small grains), chlorite and micas related to clays (30 %). Chlorite is fine grained and almost isotropic in character. The accessories present are; iron oxides, zircon, garnet and tourmaline. These accessories have made the rock coarse-grained. The rock has undergone a more advanced grade of metamorphism. This is shown by the presence of biotite.

The rock has a silky sheen of the cleavage surfaces due to the coarser texture of the micas. The cleavage that is parallel to the original bedding is well developed due to the parallelism of the mica and chlorite flakes. Further, bedding has become so transposed that the original structure can no longer be deduced. Resistant grains such as large quartz grains and magnetite crystals have been rotated in some cases without being shattered. The grains have been enclosed in eye-shaped pressure shadows filled with introduced quartz, chlorite or mica flakes.

In figure 3.16, of the fresh sample, a reflectance maxima is found in the green and red bands. This is due to the energy released via the Si-O bond of the quartz. In the same curve, within the infrared band, energy has been absorbed by the AL-OH bond of the clay minerals. The weathered sample gives a similar curve but with lower values. This means that the alteration has not added anything significant.

4.3.5. Mount Elgon Series

4.3.5.1. Nephelinite (BW/30)

This is a basalt (Plate 1), in which there is abundant nepheline with little augite. Feldspars and quartz are generally absent.

The nepheline (sodium aluminosilicate) has some kaliophilite (Potassium aluminosilicate). It occurs in anhedral grains often interstitial or vaguely elongated. There is poor cleavage parallel to prism and base. The low relief, low birefringence and negative uniaxial figure are diagnostic of this rock. Nepheline alters to zeolites.

Melilite is an abundant accessory mineral and gives single cleavage cracks occupying the centre of the crystal with pervoskite distributed along it. It is negative angle length slow because when it is examined in crossed nicols (xpl) with a quartz wedge it gives a high interference figure. Olivine and leucite are present. The former is partially altered to serpentine while the latter is in small crystals in the rock matrix.

The abundance of the feldspathoids (nepheline and leucite) and clinopyroxene gives a reflectance curve (fig. 3.14 for fresh sample) similar to that of background of figure 3.10A. This also defines the reflectance pattern of ultrabasic rocks. They have much more opaque materials and Fe^{2+} bearing minerals and consequently the ferrous iron bands are more pronounced. Alteration minerals of nephelinite give higher reflectance

values because of the reflective zeolites that result from alteration of nepheline.

There is no precise mode of occurrence for nephelinite. Desilication of basic magma by limestone has been proposed. In many instances, the availability of limestone seems questionable. There are suggestions that some alkali rocks of this sort result from the assimilation of granitic material by a very basic magma. In Navajo desert, the presence of phenocrysts of granitic material supports this hypothesis. The occurrence of nepheline in dolerite (diabase) intruding chalk at Scawl Hall, Ireland is clear evidence that under suitable conditions, reactions with limestone can produce highly undersaturated rocks.

4.3.6. Turoka group

Turoka group consists of schists, gneisses, (garnet and hornblende-rich), plutonics and related rocks and quartz-muscovite.

4.3.6.1. Schists

Based on the grades, the schists are:

- (i). Muscovite schist (BW/9a).
- (ii). Biotite-muscovite schist (BW/12).
- (iii). Quartz-muscovite schist (BW/4a).
- (iv). Garnet schist (BW/4).
- (v). Hornblende schist (BW/9).
- (vi). Garnet-hornblende schist (BW/48).
- (vii). Quartz-feldspar-biotite schist (BW/40).

These schists (i-vi) are characterised by a high content of micas, quartz, garnet and hornblende. Quartz and feldspar occur as lenticular streaks or lenticles of either or both minerals. In the garnet schist, recrystallization continued after the activity of regional stress had ceased making unoriented metacrysts. Metacrysts (garnets) have enclosed grains of quartz and feldspars.

The schists in the Archaean Shield (Huddleston, 1951) of Kakamega area have abundant quartz, muscovite and hornblende.

The schists owe their origin to recrystallization under conditions of active shearing or active orogenic pressure which made minerals with shiny properties like micas and amphiboles to crystallise in an orientation normal to the shortening direction of the rock. Quartz and feldspar occur as separated grains or aggregates. The former forms vein-like bands in hornblende schist or as inclusions in micas.

Linear structures have been strongly developed in some schists (hornblende and garnet-hornblende schists). These structures have developed from intense crumbling or intersection of cleavage and bedding planes or two or more cleavage planes. There are also lineations due to the orientation of acicular minerals such as hornblende and elongation of sand grains and pebbles. Regional metamorphism is manifested well in the formation of these rocks.

Garnet is poikiloblastic with many inclusions particularly of quartz and feldspar in the garnet-hornblende schist. Some sections of garnet are free from inclusions.

1

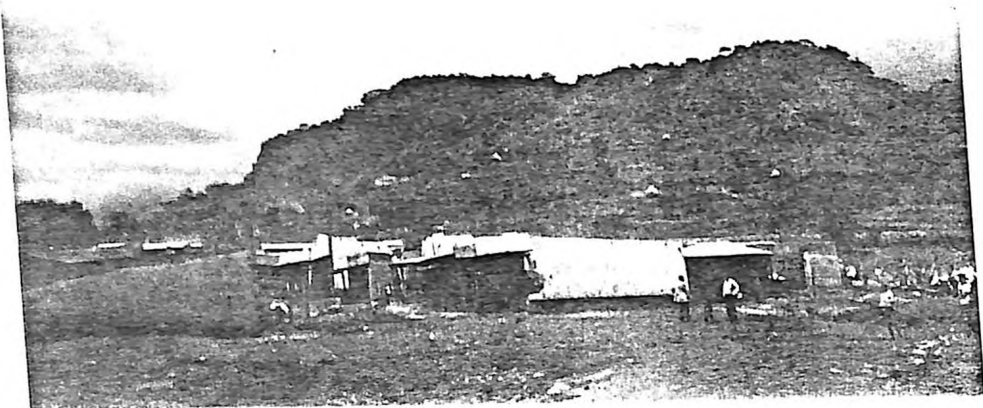


Plate 1: Nephelinite rock on the slopes of Mount Elgon at Kapkateny Market (camera facing north-west).

2

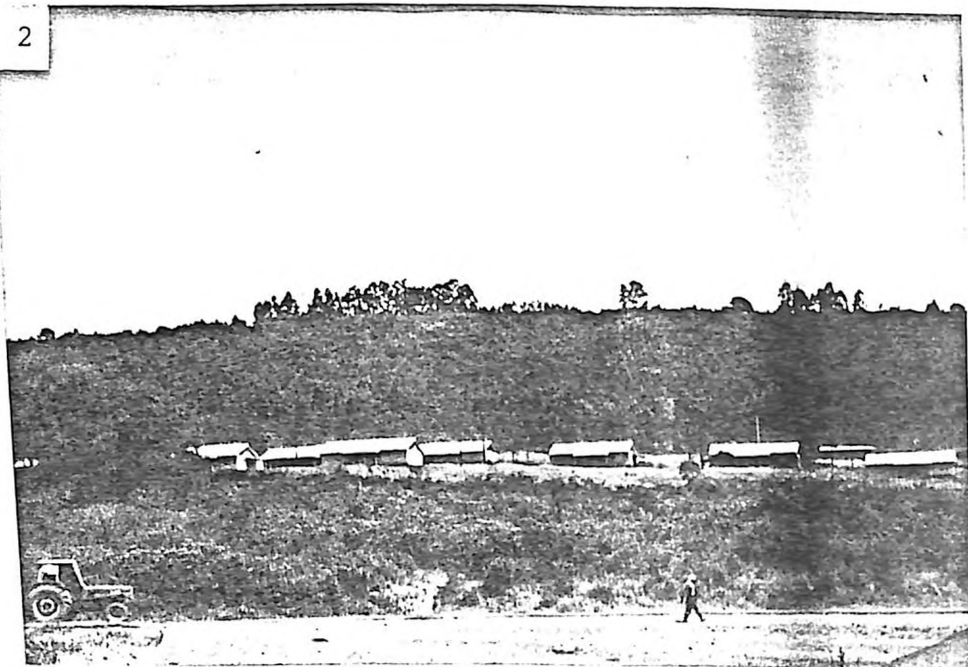


Plate 2: Nandi escarpment:- Granodiorite-rich area overlooking the Nzoia peneplain (photo. taken from west).

3

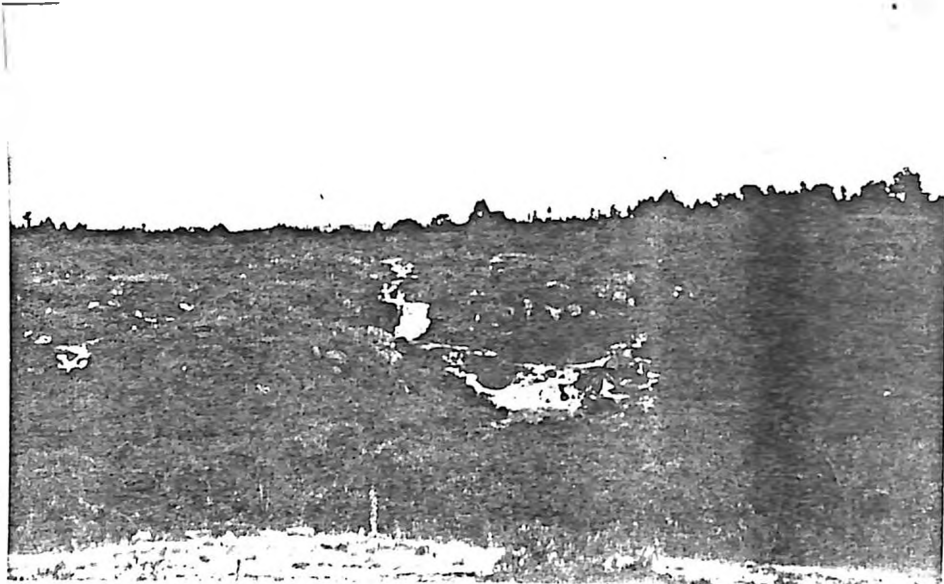


Plate 3: Broderick Falls along river Nzoia. This area has unique rolling scenery with hydroelectric potential (photo. taken eastwards).

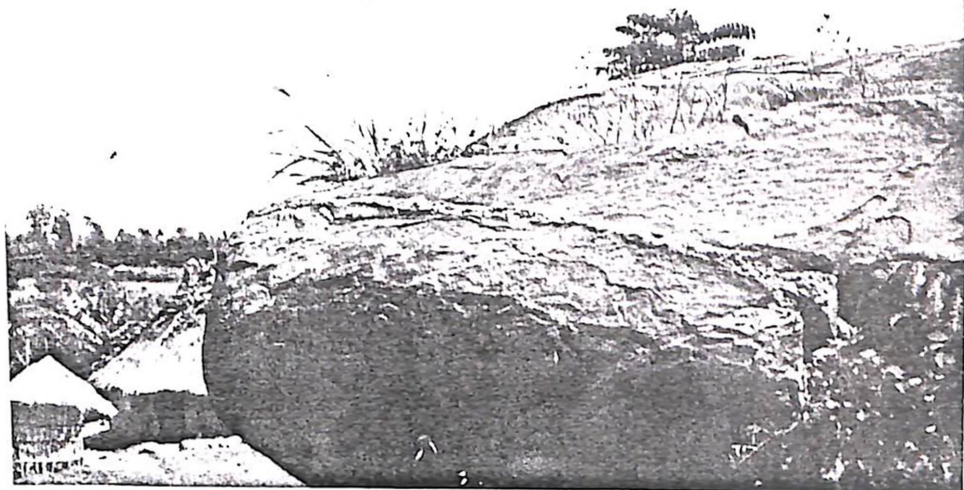


Plate 4: Granodiorite with xenoliths and dioritic mixing found 1.5 km north-east of Wajimoi Market along the main road (camera facing north).

Plate 5: Dolerite (Tholeiitic intrusion):- Hard course-grained mass exhibitng quartz veins (photo. taken from south-east).

Plate 6: Nzoia peneplain:- located to the west of Nandi escarpment, the peneplain has soil that is suitable for growing sugarcane (camera facing west).

5



6



At the immediate north of the confluence of Vilivili stream and Kibisi river, there is metamorphosed pillow lava overlying the garnet-hornblende schist. The source of this lava is not yet established except that it is relatively younger than the schists.

Muscovite is about 85 %, biotite 5 % with little sodic feldspar, quartz and accessories like chlorite. The reflectance spectra has an absorption feature "T" in the VNIR region. Distortion of the Mg-OH bonds by radiation occurred in the micas. The reflectance green > red < infrared relationship justifies this phenomena. For the weathered sample there is a reflectance maxima in the red band. An absorption feature that is supposed to be present (due to clay AL - OH bonds) in the weathered sample has been displaced to the right of the VNIR region (fig. 3.30).

In the Biotite-muscovite schist, the micas (biotite > muscovite) are about 45 % of the whole mineral composition. The reflectance values (fig. 3.15) are affected by the high percentages of the reflective quartz and sodic feldspars. There is no absorption feature that may arise from the micas because of the presence of the reflective minerals. In the weathered sample, there is a reflectance maxima in the red band and an absorption feature "T" due to the distortion of the AL-OH bonds in the available clays. This is found in the VNIR region.

The quartz-muscovite schist and garnet schist have quartz (25 %), muscovite (45 %) and garnet (45 %) respectively. The fresh

sample of the former (fig. 3.18) has an absorption feature "T" arising from the distortion of the Mg-OH bonds of the micas. The weathered sample gives green < red < infrared reflectances thus proving that some reflective material is present. Garnet is known to give green < red < infrared reflectance relationship regardless of its presence and whether in weathered or fresh samples. This gives a reflectance minima (figures 3.13, 3.22). In these rocks, weathering serves to reduce reflectance in all the three bands.

The availability of the Al-OH bond of the clays and its ability to be distorted by radiation gives the absorption feature "T". In the hornblende schist, hornblende (figure 3.19), masks the reflectance to give a minima in the VNIR region. This minimises the values as the wavelength increases. The weathered sample gives generally lower values of reflectance than the fresh one. There could be a replacement of hornblende by chlorite, epidote and possibly biotite. Garnet and hornblende in figure 3.31 produce gradual increase in the reflectance values. The particulate effects of garnet and hornblende cancel each other to give gradual increase in the reflectance.

Quartz-feldspar-biotite schist (BW/40)

Abundant micas (biotite > muscovite, 35%), feldspars mainly of labradorite type (30%) and quartz (20%) define the groundmass of this schist. In the latter, two minerals occur as lenticular streaks or lenticles of either or both minerals. The micas and amphiboles have crystallised as oriented metacryst. This is because recrystallization continued after the activity of

regional stress had ceased. There are iron oxides, clays (chlorite), augite and apatite. Little weathering change in the rock (fig. 3.24) gives a less significant absorption feature "T". This feature is due to the AL-OH bond distortion in the clays (alteration products of feldspars and micas). There is virtually no unique feature in the reflectance of the fresh sample except with the similarity observed in both curves which comes from the "green < red < infrared" reflectance values. Owing to the abundance of the reflective quartz and sodic rich feldspars, the expected absorption features have been cancelled.

4.3.6.2. Gneisses

Hornblende gneiss (BW/21) and garnet-hornblende gneiss (BW/7) fall in this category. In these rocks, dark and light minerals are segregated into layers with a massive character due to interlocking of the mineral grains. In the groundmass, streaks, lenses and dykes of pegmatitic material are observed. The cleavage is less easy. The presence of more or less flat-lying foliation testifies to recrystallization under a very thick cover of younger rocks. This phenomena usually called "load metamorphism" is well exhibited by the gneiss, 1 km north of Makunga market.

In the foliated variety, there is little or no tendency for pegmatitic material to inject or segregate in the rock. Biotite and amphibolite crystals show parallelism. In the garnet-hornblende gneiss some banding is observed. The massive variety gives vague foliation in the outcrop. There is a transition

into granulite facies (hornblende gneiss). The abundance of the minerals has been used as a basis of naming for example a rock having 60% hornblende and 15% garnet is called garnet-hornblende gneiss. Feldspars, apatite and accessories such as actinolite and iron oxides are present. Miller (1952), reports gneisses with abundant garnets, hornblende, biotite, quartz and muscovite in the Cherangani area.

The reflectance spectra for both rocks are quite different even though they are gneisses. In figure 3.22 of garnet-hornblende gneiss, the values of reflectance increase with increasing wavelength i.e. green, red and to infrared bands. This is true for the fresh and weathered samples. In figure 3.36 the fresh sample of the hornblende gneiss has an absorption feature T due to the distortion of the Mg-OH bond of the micas. Such a distortion is little in the former rock type. Garnet is the only determining factor in these schists and therefore, the differences in the reflectances are directly related to it. This mineral records high reflectance in the red band thus maximising sensed radiation.

4.3.6.3. Plutonics and related rocks

These are crush granite, migmatitic granodiorite and mylonite.

(i). Crush granite (BW/15)

A coarse-grained rock containing about 8 % quartz, feldspar of which 2/3 or more is potash feldspar or albite-oligoclase and small percentages of biotite and hornblende. Sodic oligoclase is the chief plagioclase of the granite. There is a microperthitic texture in the potash and sodic feldspars.

The quartz does not show crystal boundaries except when enclosed by microcline. The biotite has built roughly hexagonal plates which cut across and give an elongated section showing basal cleavage. The fresh biotite has deep brown colour with intense pleochroism as well as with inclusions of apatite, zircon and magnetite. Muscovite forms ragged flakes posterior to biotite or partly in parallel intergrowth with it. It is clear in thin sections.

The crystals of hornblende are irregularly bounded and at least without terminal planes. They show prismatic cleavage and the lamellar twinning that is parallel to the orthopinacoid in some cases. This mineral has green colour with marked pleochroism and an extinction angle of about 15° . Magnetite shows opaque to deep brown colour. The presence of tourmaline shows that this rock has undergone modification.

The reflectance curves for crush granite (fig. 3.32) and quartz-monzonite (fig. 3.21) are similar. This means that the minerals are the same except in the percentage composition. It also automatically means that their respective alteration products are the same. Absorption features are lacking because of the shelving capability by the reflective sodic feldspars and quartz minerals.

(ii). Migmatitic granodiorite (BW/10)

Characterised by sheet and vein reticulates, this granodiorite contains microcline (30 %) around which there are rounded grains of quartz. A perthitic texture exists as an intergrowth

between the orthoclase and other minerals. The grains of quartz are anhedral and are characterised by a wandering extinction. Hornblende and biotite are accompanied with pyroxenes. Both have inclusions of accessories of apatite, zircon and iron oxides which are brown and dark respectively. Muscovite is found in patches enclosing biotite. Phenocrysts of the feldspars are zoned: the zoning arising from the sodic feldspars of orthoclase and microcline. Although the borders of the grains are somewhat corroded by quartz and alkali feldspars, they are euhedral to subhedral and rectangular in form. The micas in this rock give an absorption feature "T" due to the distortion of their Mg-OH bond by radiation (fig. 3.28). The weathered sample gives a reflectance minima in the green band. The little alteration that has occurred in this rock has given lower overall reflectance values. The rock is generally hard and therefore quite resistant to weathering.

Igneous rock varieties have absorption features in the infrared region of the spectrum. These are due to vibrational overtones and combinations of OH^- and H_2O . Those with much less water like biotite granite have diminishing absorption bands.

(iii). Mylonite (BW/49)

The rock is intensely fractured and brecciated making it hard to decipher its mineralogy. However from the micro-examination of the rock, there is abundant quartz, little feldspar, micas and amphiboles. Intense movements have accentuated the quartz grains so that this mineral is now fragmented parallel to the

strain shadows. There has been an attrition of the augen. The rock however falls short of the "hartschiefer" structure typical of pronounced banding.

The reflectance is similar to that of melanocratic rocks like nephelinite, only that reflectance values of mylonite are higher (fig. 3.20). The reflectance values for the weathered sample of mylonite are higher than those of the fresh sample because of what may be the "reflective nature" of quartz.

(iv). Quartz-muscovitite (BW/2)

This rock is composed mainly of quartz and muscovite. It is shiny white and forms a lense in the hornblende gneiss. There is little sodic feldspar (microcline) in the groundmass.

A reflectance minima exists in the red band. This is an absorption feature "T" resulting from the distortion of the Mg-OH band in the muscovite of the fresh sample. The weathered sample gives a reflectance maxima in the red band and what appears to be an absorption feature to the right of the VNIR region. Chlorite may be responsible for this feature.

4.3.7. Intrusives

The intrusive bodies of hyperbyssal origin range from large to small sizes. They include granodiorites, dolerites, quartz-monzonite and granodiorites.

4.3.7.1. Granodiorites

Granodiorites are subdivided into two rock types; "granodiorite with xenoliths and dioritic contamination" (BW/35, Plate 4) and

"metamorphosed granodiorite with xenoliths and dioritic contamination" (BW/12) have been examined. Basically the only difference arises from the shear character of the latter. In the latter, layers of alternating foliations or lenticles of different composition are present. Due to higher interlocking of the quartz and feldspar grains, these rocks split more or less like a gneiss.

Microcline is a dominant feldspar (30 %) with rounded quartz grains around it. Orthoclase, microcline and albite have natured intergrowths of the perthitic texture. Like the migmatitic granodiorite, these rocks have anhedral quartz that is invariably strained by a wandering extinction. Both hornblende and biotite have inclusions of accessories.

The plagioclase is anhedral to euhedral and rectangular in form although the borders are somewhat corroded by quartz and alkali feldspar. Pyroxene is in short prisms generally enclosed in hornblende.

Metamorphosed granodiorite gives an absorption feature "T" (fig. 3.37) in the fresh sample. This feature shown by green > red < infrared is due to the distortion of the Mg-OH bond of the micas. The weathered sample gives green < red < infrared reflectance owing to the the presence of quartz which is a reflective mineral and has shelved the absorption feature in the red band.

4.3.7.2. Dolerites

The dolerites are large intrusive bodies of the hyperbyssal

pyroxenic, hollocrystalline and non-porphyrific variety. Feldspars (labradorites) and clino-pyroxene (augite) are the main constituents. They are idiomorphic with columnar habits. Original hornblende and a little biotite are present. The augite has no crystal outlines. Dolerites have been reported in the Eldoret area (Sanders, 1957).

Olivine has built near rounded idiomorphic crystals that are very pale. There is no quartz in the dolerites. There is an intergrowths of titaniferous magnetite (ilmenite and magnetite). Apatite, the accessory mineral is needle-like.

There is an overall ophitic texture (augite wrapping around feldspars) and idiomorphic habit in the augite. Dolerites are:

(i). Olivine dolerite (BW/43).

Augite occurs in little grains and tends to be idiomorphic as well as forming some micrographic intergrowth with feldspar.

(ii). Tholeiitic dolerite (BW/44, Plate 5).

In this variety, there are lath-shaped plagioclase, augite granules, some magnetite and a brown glass enclosing abundant crystallites.

(iii). Meta-dolerite (BW/17).

In this rock, the relative proportions between crystalline and vitreous parts varies rather widely. It is sheared.

The abundant mafic minerals in the olivine dolerite give a reflectance minima (fig. 3.34) which is noticed in the fresh

nephelinite (fig. 3.14). The weathered sample has very gradual reflectance values even though the green < red < infrared trend is present (fig. 3.34, curve b). The tholeiitic dolerite (fig. 3.26) has green < red < infrared values for the fresh sample while the weathered type has a reflectance minima in the red band that may be due to the reflective effect of the glass enclosing "crystallites". This may further be due to the more mafic content of the resultant products. When the reflectance curves of meta-dolerite (fig. 3.29) are compared with those of the tholeiitic dolerite they exhibit curve similarities.

The ultrabasic rocks have much more opaque materials and Fe^{2+} bearing pyroxene and olivine and consequently the ferrous iron bands are more pronounced.

4.3.7.3. Quartz-monzonite (BW/29)

This granite forms a small body in satellite stock or border facies of batholith masses. The feldspar (microcline) is about 40 % and quartz 35 % in the groundmass. The plagioclase displays its best form with the presence of quartz resulting in a better development of the crystal form. Both are completely zoned and form poikilistic grains in which the other minerals are embedded. Orthoclase and microcline are both perthitic in character. Quartz occurs interstitially in its position.

Diopside occurs as remnants enclosed in amphibole while the latter (hornblende) occurs in irregular plates and in prisms without vertical terminations. Biotite is present along with hornblende and gives a brown colour in micro-observation. Accessories include apatite, sphene and magnetite.

The rock exhibits an intersatal to ophitic texture. It is similar to quartz diorites and granodiorites. Alteration has occurred via albitization and pyroxenes have been altered to amphiboles with some replacement in the latter by chlorite and biotite.

The minerals present in the quartz-monzonite and crush granite are the same. This is exhibited by the reflectances of both rocks (figures 3.28 and 3.32). The reflectance taken in green, red and infrared bands are also the same. Both rocks are hard and therefore quite resistant to weathering. It is really sensible that the reflectances for their weathered samples should not be very different from the fresh ones. This is true for the red band only. The differences in the green and infrared bands may have arisen from the rocks' abilities to weather. In this case, quartz-monzonite weathers faster than crush granite when exposed to the same conditions. There is a wider gap in reflectance (red band) in the former than the latter, so to the reflectance values.

4.3.8. Ironstone (BW/5)

Magnetite takes up a large proportion while its counterpart haematite complements the remaining percentage. The granular texture exhibits ovoid grains which range from a fraction of a millimetre to a few millimetres in diameter. Even though most of the rock is weathered, fresh parts retain this unique structure.

When magnified, sedimentary structures such as cross-bedding,

ripple marks and intraformational breccias are observed. The presence of these structures indicate that the rock was deposited in shallow water where waves and currents were active.

The oxides in the ironstone (non-banded variety) display absorption feature "T" in the VNIR region of the spectrum. The bond responsible for this is the F-O bond. The reddish colour for these compounds (both banded and the non-banded varieties) imparts a general decrease in the reflectance towards the green band (3.12 and 3.35). Weathering has shelved the absorption feature in figure 3.12 b.

This ironstone is thought to be a recent formation because it is directly related to the schists in which it forms a lense-like structure.

4.3.9. Vegetation

Plant communities are specific to rock type or soil. This results from differences in the chemical and mineral composition of the rock or soil and differences in the physical characteristics of the medium.

The areas underlain by granodiorite have a patchy vegetation cover which in places enhances the typical crisscross pattern common to intrusive rocks. The appearance on images of vegetation species associated with residual soils or parent rock materials is seasonally dependent.

In areas where the vegetative cover completely blankets the surface, geologic structures have been recognised by their topographic expression alone for example, most of the Nandi

escarpment north of Webuye town can be noticed both on satellite images and aerial photographs. Within Webuye town, geologic structures such as faults and joints have been enhanced by anomalous vegetation patterns. They have a modest vegetation cover and such patterns reflect the higher moisture content generally found along fractures and fault zones, due to structural control of ground water movement.

On the Nzoia peneplain, vegetation types vary as much as the rock types. More or less short scattered trees can be found overlying the phyllites, grits and greywacke while relatively tall and thick vegetation is favoured by the granodiorites. The northern part of this area is however covered by both thick and scattered trees because of the varying rock types like schists, gneisses and migmatitic granodiorite. The slopes of Mount Elgon are quite fertile and therefore covered by thick forests.

4.4. Structural Geology

4.4.1. Introduction

Vital tools of structural and morphotectonic analyses of large structures in this study are the geometric order, symmetry and the influence of structure on geomorphology.

- i). The "geometric order" of the structure which reflects the geometric order of the movement picture. The rock structure of the rock is related to the deformation that produced it.
- ii). The "symmetry" of the structure is related to the symmetry of the deformative movements. There is a relationship between

the symmetry of cause and effect and by measuring the former we can deduce the latter.

iii). The "influence of structure on geomorphology" is profound, but the expression differs with the condition of internal and external variables.

The main causes of differential erosion are variation in composition, state and climatic conditions. Thornbury (1969), Swain, Davies (1978) and Viljoen, (1975) have recognised these parameters in their texts.

Unlike body sensors and seismic recording arrays which can portray features in space, the remote sensing systems that utilise Electromagnetic (EM) energy, portray rock structures as strictly two-dimensional configuration of some unspecified discontinuity. In structural mapping concern lies on discontinuities that are readily perceived by the naked eye. Primary discontinuities in sedimentary rocks are expressed in the "Griffithsian formula" (Griffithsian, 1961) shown below.

$$D = (c, o, sh, s, p)$$

Where D is discontinuity as a change in composition (c), orientation (o), shape (sh), size (s), or packing (p). Discontinuities are well exposed in the sedimentary as well as all metamorphosed rocks.

4.4.2. Detailed structural geology

The primary discontinuities of most interest are unconformity, bedding surface, or formational boundary and drainage systems

of contrasting types of density. These are well exhibited by Broderick Falls (Plate 3), Nandi escarpment (Plate 2) and the drainage systems (fig. 4.00).

The secondary structural discontinuities of interest involve changes in the state of host rocks imposed during deformation in regional metamorphism. The differences in chemical and physical properties have been induced by comminution and differential strains in fault zones.

The principle of superposition and original horizontality serves to specify the initial condition of primary discontinuities. Primary structural discontinuities are boundaries represented as contacts which show in remotely sensed images on a macroscopic scale. Essentially, secondary structures in this area are deformed primary structures and include imposed features generated on or from the active movements. The latter includes the mechanically induced fractures, intrusive contacts and transposed and recrystallised or redistributed primary structures in metamorphic rocks.

Observations on metamorphosed granodiorites and associated rocks spanning the area in a north-westerly direction (orientation N60°W) show that a whole spectrum of sizes of structures may be generated from a single deformational event as the stress is redistributed and attenuated through inhomogeneities to act on progressively smaller units.

According to the concept of superimposition adjacent to

plutons, migmatites are common and contacts are gradual and generally conformable with foliations developed in country rock. The migmatitic granodiorite located at about a half a kilometre south of Kamukuywa and the metamorphosed granodiorite found at Webuye (see geological map) are some of the examples presumed to be part of plutons at depth. Present are "epizonal intrusions" likely to have had an ambient temperature of 0-300°C which have a discordant habit, distinctive shapes with sharp contacts as well as composition and structure contrast.

The epizone is the upper zone of metamorphism in which distinctive physical conditions are moderate temperature, lower hydrostatic pressure and powerful stress. The rocks produced in an epizone include chlorite schists, mylonites, generally cataclastic rocks and phyllites. These rocks are will represented in this area.

The faults apparent in some of these intrusions typify their sharp separations (faults lying on boundaries of tholeiitic and meta-dolerite dykes).

The escarpment area has had successive or episodic compressional events that have impressed new forms on the earlier structures and produced the interference fold patterns. There is lenticularity in the areas east of the Broderick Falls and the southern periphery of the escarpment:- the "Drag" phenomena (Barry et al, 1980) has been proposed in

line with lateral movement or merely the incomplete preservation of a pitching anticlinal structure, Sanders (1965). Polyphase deformations have resulted in the complex outcrop patterns of the fabric elements. The geometric analysis of polyphase deformation structures is complicated by the new structural or fabric elements and structures induced by each successive deformational event. Stereographic projections carried out reveal that there is such complex folding that can be exemplified through the drag effect that has produced two main fold limbs which dip at:

- i). 40° to the N 60° E and
- ii). 42° to the N 5° W

There is a minor limb that is oriented to $N60^{\circ}W$ and dips at a low 4° . This makes it quite difficult to infer folding in this area since the data: 50 strike measurements with point counting on 2, 3, 4, and 5 poles options were used (fig. 7).

Rose diagrams for the strike measurements were made in two parts: sixty readings covering the whole area (fig. 8a) and forty readings covering the Nandi escarpment (fig. 8b). For the former, an average strike of $N55^{\circ}W$ prevailed over the less significant $N60^{\circ}E$. In the escarpment an average strike of $N60^{\circ}W$ prevails over that of $N85^{\circ}E$.

Thus, it is concluded that the strike of the rocks overlying the escarpment is at $N60^{\circ}W$ while the general strike is $N55^{\circ}W$.

There is need to understand terminology on linear features as implied by many geologists studying aerial photographs. O'Leary

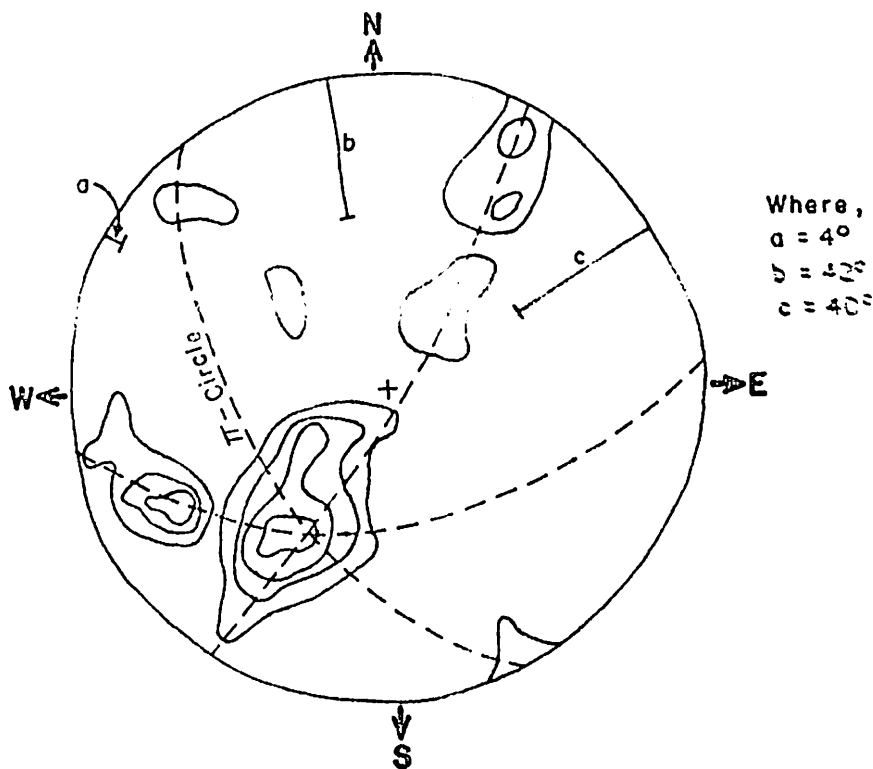
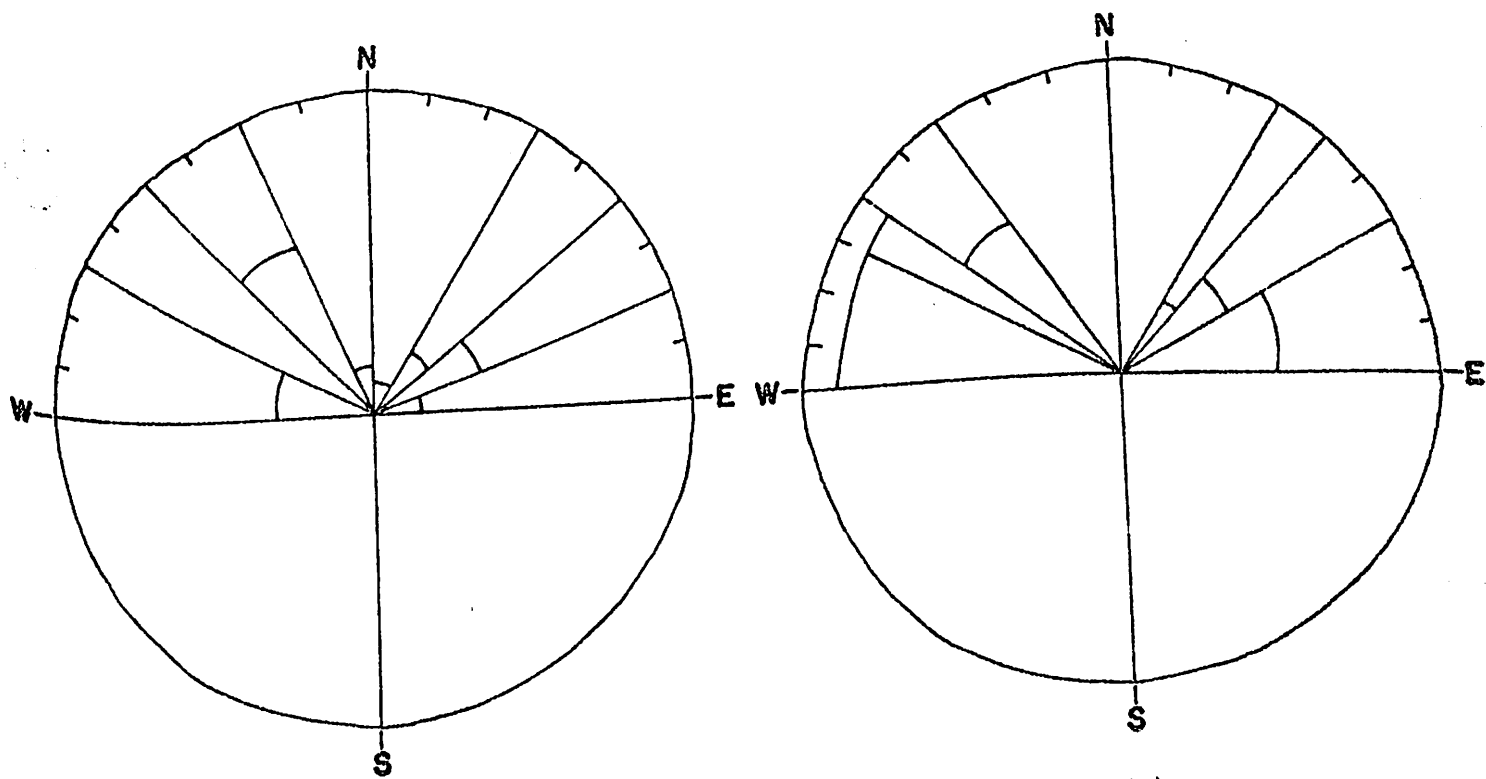


Figure 7 : Stereographic projection for 50 measurements of strike and dip. Point counting done on 2, 3, 4 and 5 poles options.

Figure 8 - Rose diagrams for strike measurements



(A).

60 readings taken for the study area at 0-20°, 21-40°, 41-60° and 61-90° interval. Radius is equal to 19.

(B).

40 readings taken along the Nandi escarpment at 0-30°, 31-50°, 51-60° and 61-90° interval. Radius is equal to 9.

et al (1976), have addressed this problem and defined Lineament "sensu stricto" in a geomorphological sense as a "mappable, simple or composite linear feature of a surface, whose parts are aligned in a rectilinear or slightly curvilinear relationship and which differs distinctly from the patterns of adjacent features and presumably reflects a subsurface phenomena". To restrict the term lineament solely to topographic features fails to accommodate the allied and derived forms. Linear features found in this area can be described in the main categories below:

a). Those defined by point and / or segment alignments like plutons, dykes, topographic depressions and stream or valley segments. The dykes found east of the escarpment are generally vertical while those on the west are inclined. The dolerite dyke at Lugulu market shares the strike with wrench fault.

b). By linear truncations and offsets of contours in topographic maps like Nandi escarpment, Broderick Falls and the Nzoia peneplain (Plates 2, 3 and 6) and Faults. The Nandi escarpment which strikes $N60^{\circ}W$ gives a dip of about 70° to the east. It appears well on all the imageries (MSS, TM and SPOT). Wrench-faults which traverse a proportionate part of this area have more or less the same orientation like the main thrust zone of the escarpment. According to the measurements made on the geological map and by reference to the aerial photographs, the displacement in the rocks ranges from slightly less than a kilometre to more than two kilometres. This justifies the drag

effect that is envisaged to have been responsible for the thrusting of the rocks from the east thereby giving an all eastern dipping characteristic. With opposing forces at about $N60^{\circ}W$, the wrench faults were created. In the field, it was possible to identify and measure rock displacements notwithstanding their gradational. The final measurements realised from the geological map approximated well with those obtained in the field. Rocks like the chlorite schist have 2.75 km displacement while the relatively harder ones like the *granodiorite* have 0.9 km. This means that the drag effect and therefore the displacement is inversely proportional to the hardness of the rocks in the area. The orientation of these faults point to close association of the faults and the drainage on the slopes of Mount Elgon. Faulting has an upper hand on the drainage habits of the rivers in the mountain. And of course the topography has been shaped by faulting, erosion, orientation and weathering patterns of rocks.

c). Linear boundaries in derived maps showing facies, structural domains or strain zones for example, shear in *granodiorites*, *mylonites* and faults along the boundaries of different grades of metamorphic rocks.

The geologic significance of a topographic lineament varies depending on whether it is degradational and aggradational in character. Most of the lineaments are a result of differential erosion and exposure but the streams (tributaries) of river Nzoia arising from Mount Elgon express

several pronounced lineaments. They are also controlled by rock types.

Mylonites (BW/44) are found in and within the granodiorites mainly in Webuye town. There are some pockets of mylonites near Teremi schools. They have a general orientation of $N60^{\circ}W$. This orientation is observed in dykes, faults, shear and granites. There is a small body in satellite stock or border facies of batholith masses represented by quartz-monzonite north of Baraki school.

There are also giant quartz (BW/14) and pegmatite veins (BW/33) in this area. However there are more quartz veins than pegmatite veins. The latter are found at the Namarambi road junction, east of Makotelo market while the former are found south of Makunga market along the main road, south of Lutacho schools and south of Malomonye market, east of Misikhu mixed schools and south-west of Kibingei dispensary. These veins are define segment alignments.

4.5. Economic minerals and water resourcea

4.5.1. Economic minerals

Valuable minerals found in this area include: muscovite, graphite, garnet, zoisite and epidote. There is sand harvesting.

Muscovite is abundant in Misemwa area. Its deposit extends beyond the area covered by Misemwa primary and secondary schools, and the market. It is found in a circular area of about 1km in diameter and forms a sheared flaky mass.

Garnets are found in hornblende schist south of Ndivisi market. They form a porphyritic texture in the schist groundmass. They are also found in garnet-hornblende schist east of Kamukuywa market.

A *small mass* of graphite is located 300m north of Lutacho schools. Its coverage has not been ascertained because of the thick forest cover and overlying soil. Kyanite occupies a small area 2 km east of Ndivisi market along the Ndivisi-Karima road. Epidote and zoisite are located in chlorite schist along Mukhe-Kimilili road and in migmatitic granodiorite at Nakalira west of Kamukuywa respectively.

Sand harvesting has been going on along Kivisi river east of Ndivisi market. There is no sand harvesting in the rivers found on the Nzoia peneplain because they are laden with silt.

4.5.2. Water resources

4.5.2.1. Introduction

A growing population and the desires for improved quality of life are placing increasing demands on our water resources. This places greater demands on scientists and engineers to provide means to observe better observe and make inventory of the amounts of water in the various environments.

Considerable effort and progress have been made in improving the conventional means of observing water resources and associated watershed characteristics. In most cases, these measurements are made at one point only or at widely separated points. Thus it is difficult to adequately monitor the spatial variability in phenomena such as soil moisture or rainfall. Remote sensing approaches offer a capability for repetitively monitoring large areas with a high observational density that can accurately depict spatial and temporal variability.

4.5.2.2. Subsurface Water

The water distribution and deposition in this area is understood via the recognition of the watershed or catchment which respond to the deposition of rainfall by continually, although slowly adjusting its stream network and surface cover to transport the water out of the watershed via runoff, evapotranspiration and ground water fluxes. The watershed geology, soils and vegetation modulate or control the rate at which rainfall is manifested as runoff or the other fluxes. Subsurface water can be described according to the available Physiography.

(i). The Uasin Gishu plateau.

In this area most of the boreholes and wells on average record

a water depth of about 10m except where located within /or in the watershed of the gravity springs. The available metasediments are permeable enough to store ground water. Besides, the soil cover is quite thick and therefore justifies the recorded water level.

The groundwater system is even more complex owing to the fact that the faulting that is envisaged to have accompanied the evolution of the Nandi escarpment and Mount Elgon extends into this plateau. The evidence comes from the displaced rocks and the source of the river Nzoia tributaries up in the mountain. The catchment area is located on the slopes while the watershed is away from the slopes. The gravity springs drain to the south-east and may point in the direction of the watershed.

In the past there have been cases of water pollution e.g. during the 1989 unexpectedly high rainfall, the Kamukuywa and Ndivisi areas reported crude oil leakage into the gravity springs. Oil has been reported as leakage while drilling a borehole for water in Kimilili town (Gibson, 1952).

It was argued that since this area has igneous and metamorphic rocks, oil might have migrated from somewhere else through faults. Present observations show that in this area, water from gravity springs is milky. The source of this colour ought to be established.

(ii). The Nandi escarpment.

Eventhough igneous rocks do not form good aquifers, there are other parameters which ought to be considered. The Nandi escarpment has undergone complex faulting and folding

processes. The former has affected the immediate neighbouring areas like the Uasin Gishu plateau.

The source and drainage of coincide with the faults right along the slopes of Mount Elgon. These faults could be aquifers. The available joints are a positive step in this direction. The orientation of faults coincides with the orientation of rocks as well as the drainage.

(iii). The Nzoia peneplain.

The peneplain has greywackes, grits, mudstones, phyllites and granodiorities. On average, the underground water can easily be found at a depth of 2m in the dry season meaning that it is even better in the rain season. This is possible with the sedimentary rocks than with granodiorities because of their massiveness and resistance to weathering. The effect of thrust forces responsible for the evolution of Nandi escarpment are minimal in this area.

4.6. Discussion

This research covers 750 Km² in the south-east of Mount Elgon, Bungoma district, Kenya.

Aerial photographs and satellite images have been widely used for qualitative and quantitative geological information. It is now established that the amount of information depends on the terrain- whether igneous, metamorphic or sedimentary: the climatic environment and sometimes the the stage of geomorphic cycle. Sedimentary rocks which normally yield the greatest amount of information because of strong differences produced by erosion are quite lacking. These rocks occupy a small area south of Webuye town.

It has been proved that the combination of photographic tone, texture, pattern, colour, shape, size, relation to associated features and vertical exaggeration of rock types and structures are all vital parameters in establishing geology of any area.

By studying strike and dips of beddings as well as stream patterns, it is possible to interpret the existence of certain features like stream patterns on the slopes of Mount Elgon which show that faults are a major reservoir of ground water.

Several aides in the geological interpretation utilised include: macroscopic and microscopic examination of rocks, spectroradiometric data analysis by computer, stereographic projections and rose diagrams. These last two proved that in this area, there are two main plunges of fold limbs at 40^o dip, N60^o E and 42^o dip, N5^oW. The general rock strike of foliation

stands at $N60^{\circ}W$. The naming of rocks examined depended on abundance of minerals and the placement in the chronology was arrived at by data discrimination. Satellite imageries: MSS, TM and SPOT have been compared quite well in terms of improved instantaneous field of view, ground resolutions and picture elements. The Landsat programme has proved that large areas can be mapped as well as major structural and lithological features. Some rock units have been subdivided on the basis of their tone for example, nephelinites found on the slopes of Mount Elgon appear red on all imageries. This has made evaluation and revision of published work easier. However, limitations of Landsat programme in this work show that minor geological structures cannot be delineated. This also applies to many mapped rock units which cannot be distinguished via reflectivities like schists and gneisses. A large part of this area is covered by soil and vegetation thereby masking the underlying rocks. The precision of locating boundaries and identifying small or isolated features is inhibited by small scale and low resolution of imageries. This programme does not allow identification of lithology or rock composition.

On the whole, SPOT provides the best form of geological data, followed by TM and MSS respectively. However, vegetation and drainage patterns are well exhibited by MSS (appendix 2).

It is not easy to evaluate the amount of minerals like Graphite, epidote and kyanite. They are not related to structures and therefore it is difficult to use imageries. Structures seem to play a big role in influencing groundwater.

4.7. Conclusion and Recommendations

This area consists mainly of igneous and metamorphic rocks. Kavirondian and Nyanzian rocks are poorly exposed west of the Nandi escarpment. At the immediate east of the escarpment, low-grade metamorphosed lavas and sediments extend in a north-westerly trend. Further to the east, gneisses and schists of the greenstone Belt are derived from progressive and constructive dynamic metamorphism of the Kavirondian and Nyanzian rocks. There are low to high-grades of metamorphism east of the escarpment manifested in the greenschist (Nyanzian Group), garnet and epidote-amphibolite facies (Basement System) with plastic deformation. The Mozambique rocks were formed under normal orogenic events with the Nyanzian Group only acting as a stable craton along which the Mozambiquian was thrust and as a source for volcanic material. Evidence for metasomatism and deformation episodes arise from metamorphosed and migmatitic granodiorites. Isotopic age determinations, structures and metamorphism show that the Nyanzian Group is older than the Mozambique Mobile Belt.

Absorption features (T) observed in spectral reflectance are broad, meaning that molecules occupy unordered or several equivalent sites. These features were used to identify overtones and combinations involving materials with very high fundamental frequencies. Minerals with O-H stretching modes like clays (Al-OH) and Micas (Mg-OH) have high fundamental frequencies. Spin-allowed transitions give absorption features in the spectra of minerals containing ferrous ions. Generally,

readily detected minerals are those produced by alteration which dominate surfaces and are common in sedimentary rocks.

It is evident that there is complex faulting and folding in this area. This is shown by the degree of metamorphism adduced from minerals like garnets, biotite and shear in the granodiorites, gneisses, schists and mylonites. Other evidence comes from wrench faults and folds with high plunges. The following is plausible enough for further research.

i). Conduct research on "surface and groundwater" along the Nandi escarpment and neighbouring areas. The industrial discharge from Pan paper and Webuye heavy chemicals into river Nzoia and possibly into the underlying faults is of major concern. Complaints of air pollution as well as deterioration of building materials have been reported.

ii). According to claims received in 1989 from people staying in the Ndivisi-Kamukuywa area that there was oil pollution in the ground water during heavy rains, it is imperative that some investigation should be carried out to find out the source of the pollution preferably in both wet and dry seasons. Emphasis ought to be placed on milky water in gravity springs east of Ndivisi market.

iii). The extent of graphite partially exposed north of Lutacho schools should be ascertained by geophysical and geochemical investigations.

iv). The determination of structural geology in this area is vital since there is no detailed work which has been carried out.

References

- ALLUM, J. A. E., (1966). Photogeology and regional mapping, Pergamon, London.
- ASHLEY, R. P., (1979). Relation between volcanism and ore deposition at Goldfield, Nevada Bureau of Mines and Geology, Report 33, p. 77-86.
- BARNETT, J. J., (1971). "Temperature measurement from a satellite" in Environmental remote sensing: Applications and achievements, Barnett, E.C. and Curtis, L.F. (eds), Edward Arnold, London. pp 185 - 214.
- BARRY, S. S. and ALAN, R. G., (1980). Remote Sensing in Geology, Pub. U.S.A, p. 381 - 503.
- BERNEISTEIN, R., and FERNEYHOUGH, D.G., (1975). Digital image processing: Photogrammetric Engineering, Vol. 41, p. 1465 - 1476.
- BHATTARAI, K. D., (1983). Mineral exploration by remote sensing techniques in Nepal. Adv. Space Res. Vol. 3, No. 2 pp. 49-54.
- CAHEN, L. and SNELLING, (1966). Geology of Equatorial Africa, Pub. Willey and Sons.
- COLE, M. M., OWEN-JONES, E. S. and CUSTANCE N. O. E., (1974). Recognition and interpretation of spectral signature of vegetation from aircrafts and satellite imagery in western Queensland, Australia. Symposium European Earth Resources. Satellite Expts. 1974 Proc. European Space Research Organisation Spec. Publ. 100, pp. 243-287.
- DRURY, S. A., (1990). A Guide to Remote Sensing: Interpreting Images of the Earth, Pub. Ox. Univer. Press.

- ELACHI, C., (1987). Introduction to the physics and techniques of remote sensing. Pub. John Willey and Sons, Inc.
- FILLIPONE, W. R., (1986). Practical applications of remote sensing Geophysics. The leading edge of exploration, Vol. 6, No. 12, 1987. pp. 16-22.
- FONTANEL, A. C., BLANCHAT, C. and LALLEMAND, C., (1975). Enhancement of Landsat imagery by combination of multispectral classification and principal component analysis, in Proceeding Symposium of Earth Resource Survey, Houston, Texas, NASA TM X - 58168 Vol. 1 - B, p. 991 - 1012.
- GIBSON, A. B., (1952). Geology of the Broderick Falls area, Report No. 26 Geol. Surv. Kenya.
- GOETZ, A. F. H., (1976). Application of Remote Sensing for resource exploration, present and future, Pub. Willey and Sons.
- GRIFFITHS, J. C., (1961). Measurement of the properties of Sediments : Journ. Geol., Vol. 69, p. 487 - 498.
- HARALICK, R. M., (1984). Digital step edges from zero crossing of second directional filters: IEEE Transaction on pattern analysis and machine intelligence, Vol. PAMI - 6, p. 58 - 68.
- HILLS, E. S., (1956). A contribution to the Morphotectonics of Austria, Journ. Geol. Soc. Austria, Vol. 3, p. 1 - 15.
- HILLS, E. S., (1963). Elements of structural Geology: New York, Wiley and Sons, p. 483.
- HOLMES (1951). Physical geology. Pub. Wiley and Sons
- HUANG S., (1983). Advanced Space Research, Vol. 3, No. 2, p. 91 - 94. Pub. China.
- HUDDLESTON, A., (1951). Geology of Kakamega area. Report No. 28 Geol. Surv. Kenya.

- HUNT, G. R., (1977). Spectral signatures of particulate minerals in the visible and near-infrared, *Geophysics* V. 41 pp. 501-513.
- HUNT, G. R., (1980). Electromagnetic radiation-the communication link in remote sensing in Siegal, B.S. and A.R. Gillespie, eds. *Remote sensing in Geology*; Ch. 2 p. 5-45, J. Wiley & Sons, New York.
- ICHANGI, D. W., (1983, MSC. NBI). The geochemistry of pyrite mineralisation of Bukura-Mbesa area, western Kenya.
- LEE, K. and WEIMER, R., (1975). Geologic interpretation of Skylab photographs: Remote Sensing report, 1975 - 1976, Colorado School of Mines, Golden Colorado, p. 77.
- LOE'VE, M., (1955). *Probability Theory*: D. van Norstrand Company, Princeton, N. J.
- LILLESAND, T. M., (1987). *Remote sensing and Image Interpretation*, Published by John Wiley and Sons.
- MELHORN, W. N. and SINNOCK, S., (1973). Recognition of surface, Lithologic and Topographic patterns in south - west Colorado with ADP Techniques, in *Proceedings of the Symposium on Significant Results obtained from ERTS - 1*, NASA SP - 237, Vol . 1 Sec. A, P. 473 - 481.
- MELTON, F. A., (1959). Aerial photographs and Structural Geology: *Journ. Geol.*, Vol. 67, No. 4 p. 351 - 370.
- MILLER, J. B., (1975). Landsat images as applied to petroleum exploration in Kenya NASA Earth Resources Survey Symposium, NASA TM X-58168VI-B pp 605-624.
- MILLER, J. M., (1954). *Geology of Cherangani Hills*. Report No. 35, Geol. Surv. Kenya.

- NATIONAL ATLAS OF KENYA, (1970). Pub. Survey of Kenya.
- NGECU, W. M., (1991, PH.D, NBI). The stratigraphy of the Kavirondiant rocks of western Kenya.
- O'LEARY, D. W., FRIEDMAN, J. D. and POHN, H. A., (1976). Lineaments, Linear, Lineations: Some proposed new standards for old terms: Geol. Soc. America, Bull. Vol. 87p. 1463-1469.
- ONYWERE, S. M., (1990, MSc., NBI). Application of Remote Sensing Techniques in geological mapping of Nairobi area (MSc. Thesis, University of Nairobi).
- OPIYO, A., (1988, PH.D, LEUCESTER). The geology and geochemistry of the late Greenstone Belt of the Maseno area, western Kenya.
- PODWYSOCKI, M. H., GUNTHER, F. and BLODGETT, A., (1977). Discrimination of rock and soil types by digital analysis of Landsat data NASA - Goddard Space Flight center Document X - 923 - 77 - 17, p. 37.
- POHN, H. A., (1970). Remote sensor application studies progress report, 1968 - 1969: Analysis of Images and Photographs by a Ronah Grating: U.S. Geological Survey report PB 197-101, p.9.
- RICH, J. L., (1951). Geomorphology as a tool for Interpretation and mapping: Geol. Soc. Amer. Prof. paper 373, p. 230.
- ROWAN, L. C., (1975). Application of Satellite to Geologic exploration; Amer. Scient., Vol. 63, No. 4, p. 393 - 403.
- ROWAN, L. C., GOETZ, A. F. H. and AHLEY, R. P., (1969). Discrimination of hydrothermally altered and unaltered rocks in the visible and near-infrared: Geophysics, Vol. 42, p. 522-535.

- SABINS, F. F. JR., (1987). Remote Sensing Principles and Interpretation. 425 p. W.H. Freeman and Co. San Francisco.
- SANDERS, L. D., (1963). Geology of the Eldoret area. Report No. 64, Geol. Surv. Kenya.
- SANDERS, L. D., (1965). Geology of the contact between the Nyanzian Shield and the Mozambique Belt in western Kenya. Bull. No. 7, Geol. Surv. Kenya. (A revised geology of the Broderick Falls area, Degree sheet 33, N.E. Quarter).
- SMEDES, H. W., PIERCAE, H. W., TANGUAY, M. G. and HOFFER, R. M., (1969). "Digital Processing of multispectral scanner (MSS) imagery" in Environmental Remote Sensing; Applications and achievements, Barnett E.C. and Curtis, L.F. (eds.), Edward Arnold, London, pp 185-214.
- SWAIN, P. H. and DAVIES, S. M., (1978). Remote Sensing- The quantitative Approach: McGraw - Hill Book Co., New York.
- THORNBURY, W. D., (1969). Principles of Geomorphology, 2nd Ed.: New York, Wiley, p. 594.
- VILJOEN, M. J., GROOTENBOER, J. and LONGSHAW, T. J., (1975). ERTS - 1 Imagery: An appraisal of application in Geology and Mineral exploration: Mineral Scie. Eng., Vol. 7, No. 2, p.132 - 168.

Appendix one

Wave-Surface interaction mechanism

When the electromagnetic wave interacts with a solid material, several mechanisms affect the properties of the resulting wave. Some of the mechanisms operate over a narrow band of the spectral region, while others are wide bands and thus affect the entire spectrum from 0.3 - 2.5 micrometres. The narrow band interactions are associated with "resonant molecular and electronic processes". These mechanisms are affected by the crystalline structure leading to the splitting, displacement and broadening of the spectral lines into separate bands. The wide band mechanisms are associated with non-resonant electronic processes which affect the material index of refraction (Elachi, 1987).

When the interface of a material is very smooth relative to the incident wavelength (wavelength \gg interface roughness), the reflected energy is in the secular direction and the reflectivity is given by Snell's law (fig. 9). The reflection co-efficient is a function of the complex index of refraction n and the incidence angle A . The expression of the reflection co-efficient is given by:

$$[R_h]^2 = \sin^2(A-A_t) / \sin^2(A+A_t)$$

for horizontally polarised incident wave and

$$[R_v]^2 = \tan^2(A-A_t) / \tan^2(A+A_t)$$

for vertically polarised incidence wave. A_t is the transmission angle and is given by

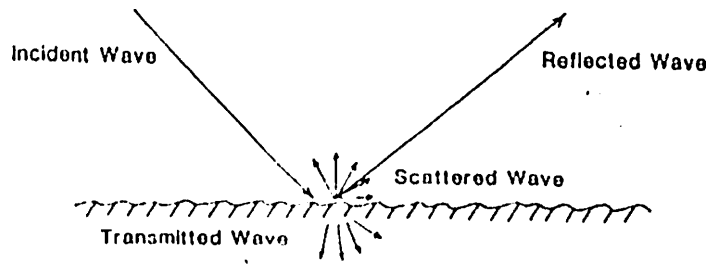


Figure 9 - Wave interaction with an interface.
(Based on Etochi, 1987).

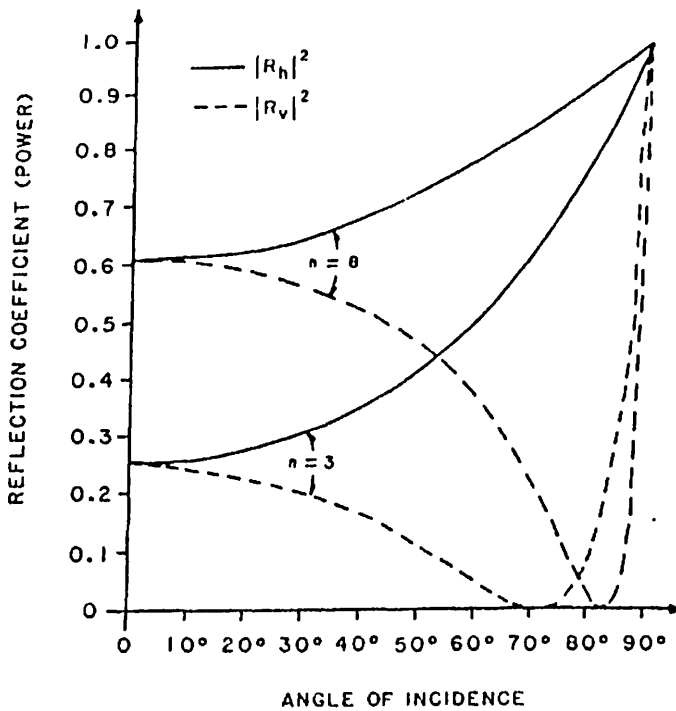


Figure 10: Reflection coefficient of a half-space with two indices of refraction ($n = 3$ and $n = 8$) as a function of incidence angle. The continuous curve corresponds to horizontal polarization. The dashed curve corresponds to vertical polarization. (Based on Etochi, 1987).

$$\sin A = n \sin A_t$$

The behaviour of the reflection co-efficient as a function of the incidence angle is illustrated in figure 10. One special aspect of the vertically polarised configuration is the presence of a null (no reflection) at an angle which is given by

$$\tan A = n$$

and which corresponds to $R_v = 0$. This is called the Brewster angle. In the case of normal coincidence, the reflection co-efficient is

$$\begin{aligned} R_h = R_v = R &= (n - 1) / (n + 1) \\ &= (N_r + iN_i - 1) / (N_r + iN_i + 1) \end{aligned}$$

and

$$[R]^2 = \{(N_r - 1)^2 + N_i^2\} / \{(N_r + 1)^2 + N_i^2\}$$

where N_r and N_i are the real and imaginary parts of n respectively. In the spectral regions away from any strong absorption bands, $N_i \ll N_r$ and

$$[R]^2 = \{(N_r - 1) / (N_r + 1)\}^2$$

However in the strong absorption bands

$N_i \gg N_r$ and

$[R]^2$ is approximately equal to 1

If a wide spectrum light is incident on a polished surface, the reflected light will contain a relatively large portion of spectral energy around the absorption bands of the surface material. This is called "Restrahlen".

Most natural surfaces are rough relative to the wavelength and usually consist of particulates. The spectral signature is determined by scattering and the particulates' size. The mechanism of the latter can be understood by a rigorous solution of the Maxwell's equation. This includes multiple scattering. If Raleigh's law applies, the scattering cross-section is a fourth power of the ratio $a/\text{wavelength}$. This means scattering is approximately $(a/\text{wavelength})^4$ in which a is the particle size. This explains the colour of the sky. When molecules and fine dust scatter blue light about four times more than red, the sky appears blue. In the case of a particulate surface, the incident wave is multiple scattered and some of the energy which is reflected toward the incident medium penetrates some of the particles. Thus if the material has an absorption band, the reflected energy is depleted in that band. As the particles get larger, the absorption feature becomes more pronounced even though the total reflected energy is decreased.

In the general case of natural surfaces, the reflectivity is modelled by empirical expressions. One such expression is the Minnaert law (Minnaert, 1941) which gives

$$B_{\text{cos}A_s} = B_0 (\text{cos}A_i \text{cos}A_s)^k$$

Where B is the apparent surface brightness of an ideal reflector at the observation wavelength, k as a

parameter that describes darkening at zero phase angle and the A_i , A_s are the incident and scattering (or emergency) angles, respectively. For a Lambertian surface, $k=1$ and

$B = B_0 \cos A_i$ which is the commonly used darkening law.

In some special cases, diffraction grating is encountered in nature. For instance, opal consists of closely packed spheres of silicon dioxide and a little water embedded in a transparent matrix that has similar composition but slightly different index of refraction. The spheres have a diameter of about 0.25 micrometre. Dispersion of white light by three dimensional diffraction grating gives rise to spectrally pure colours that glint from within an opal.

The reflection of visible and near infrared waves from natural surfaces occurs within the top few microns. Thus, surface cover plays an important role. For example, the iron oxide in desert varnish can quench or even completely mask the spectrum of underlying rocks. Fundamental vibrations for water and carbondioxide are shown in figure 11 while signature diagram of a variety of geologic materials according to Hunt (1977), is represented in fig. 12.

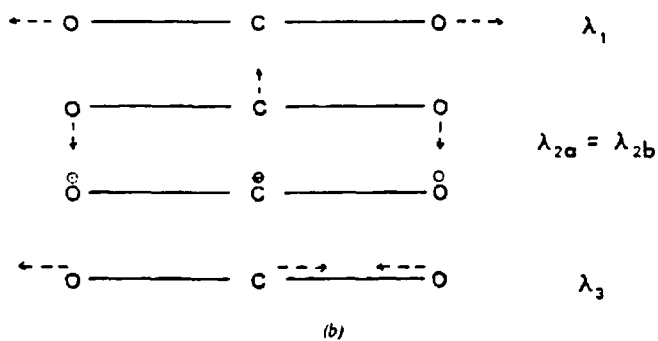
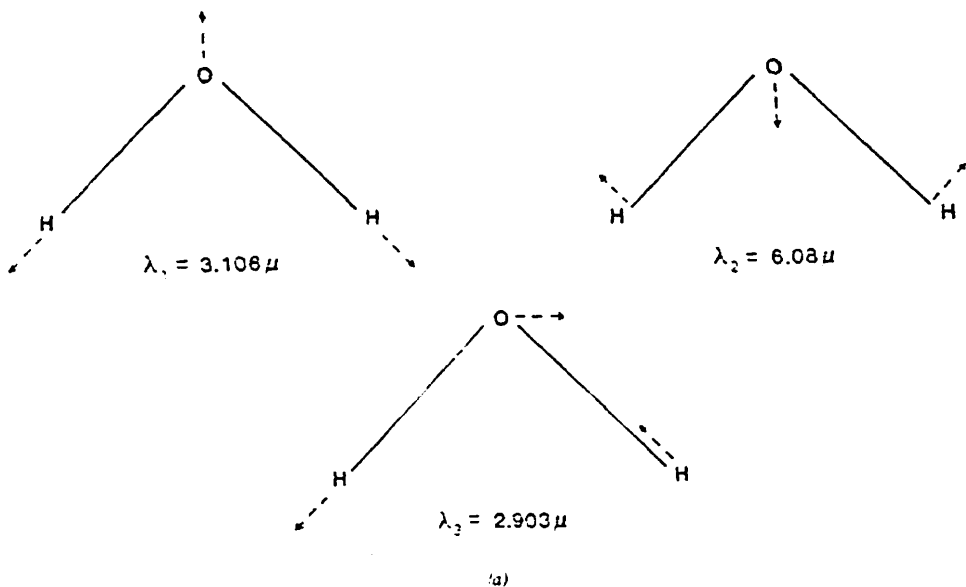


Figure 11 : (a) H_2O molecule fundamental vibrational modes. (b) CO_2 molecule (linear) fundamental vibrational modes. —(Based on Elachi, 1987).

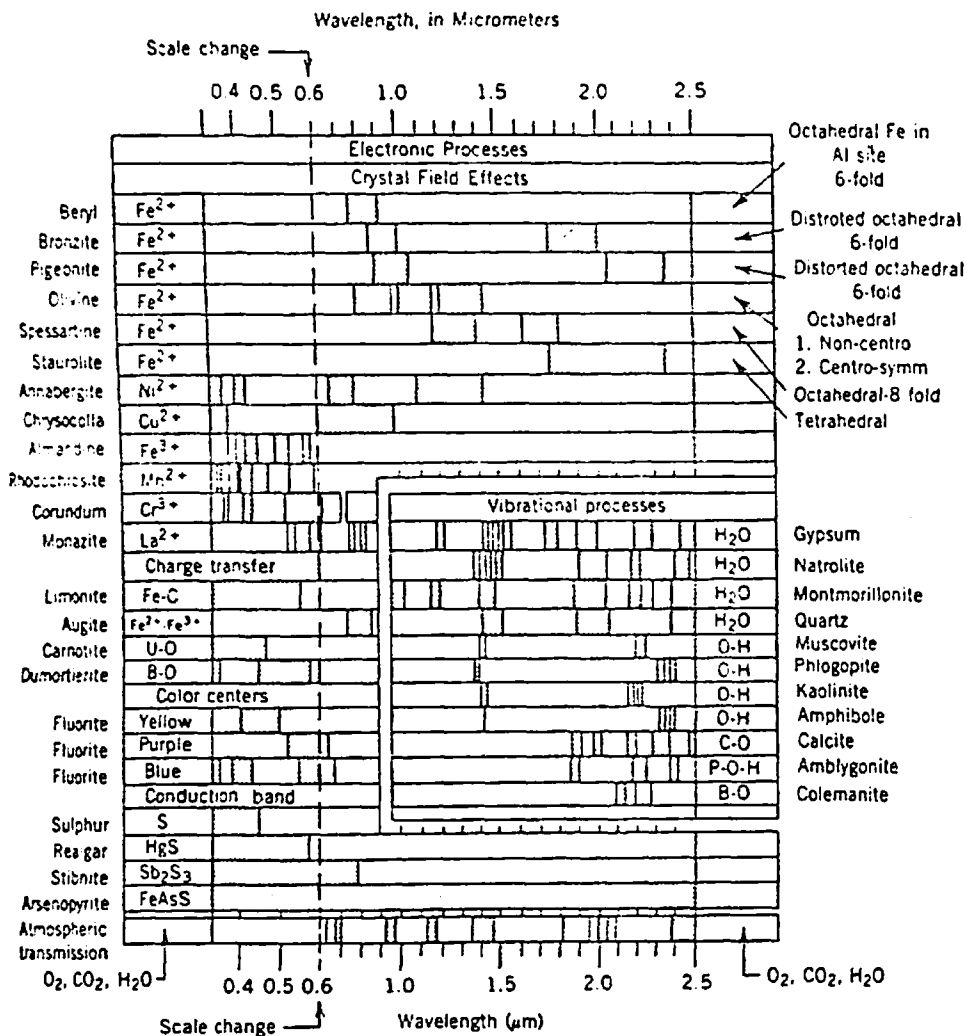


Figure 12 : Spectral signature diagram of a variety of geologic materials. (Based on Hunt, 1977.)

Appendix two

Landsat Sensor Characteristics

Sensor System	Characteristics
---------------	-----------------

"Multispectral scanner (MSS)"	
-------------------------------	--

This is a cross-track sensing system.

It scans 185 km wide at 11.56 degrees (Landsats 1, 2 and 3, shown in figure 13).

At 705 km altitude, the scan angle is 11.49 degrees (Landsats 4 and 5) and swathes at 185km.

At 918 km altitude, the 0.087 mrad IFOVS produces a ground resolution cell of 79 by 79 metres.

It has four spectral bands whose mirror sweep is determined by six scan lines.

The spectral bands are in the 0.5-1.1 micrometre wavelength region and the spectral characteristics and colour signatures for MSS are comparable to those of IR colour aerial photographs. Bands include:

4, 0.5-0.6 micrometer, green colour

Blue - IR composite image colour

5, 0.6-0.7 micrometer, red colour

Green - IR composite image colour

6, 0.7-0.8 micrometer, reflected IR

Red - IR composite image colour

7, 0.8-1.1 micrometer, reflected IR
Red - Composite image colour

"Thematic
mapper
scanner (TM)"

Deployed on Landsats 4 and 5, TM records both east and west bound sweeps thereby reducing dwell time (fig. 14).

A cross-track scanner similar to MSS and has a spatial resolution cell of 30 metres with an extended spectral range in the visible and reflected IR regions.

It has an additional blue spectral data in band 1 which enables production of normal colour composite images and a thermal IR band with an improved detector sensitivity and radiometric resolution.

It has 6 bands in the 0.45-2.35 micrometer wavelength region and one band in the 10.40-12.50 micrometer wavelength region while each band has an array of 16 detectors.

The bands include:

- 1, 0.45-0.52 micrometer, blue-green, for discriminating soil and vegetation
- 2, 0.52-0.60 micrometer, green, for assessing plant vigour
- 3, 0.60-0.69 micrometer, for discriminating vegetation

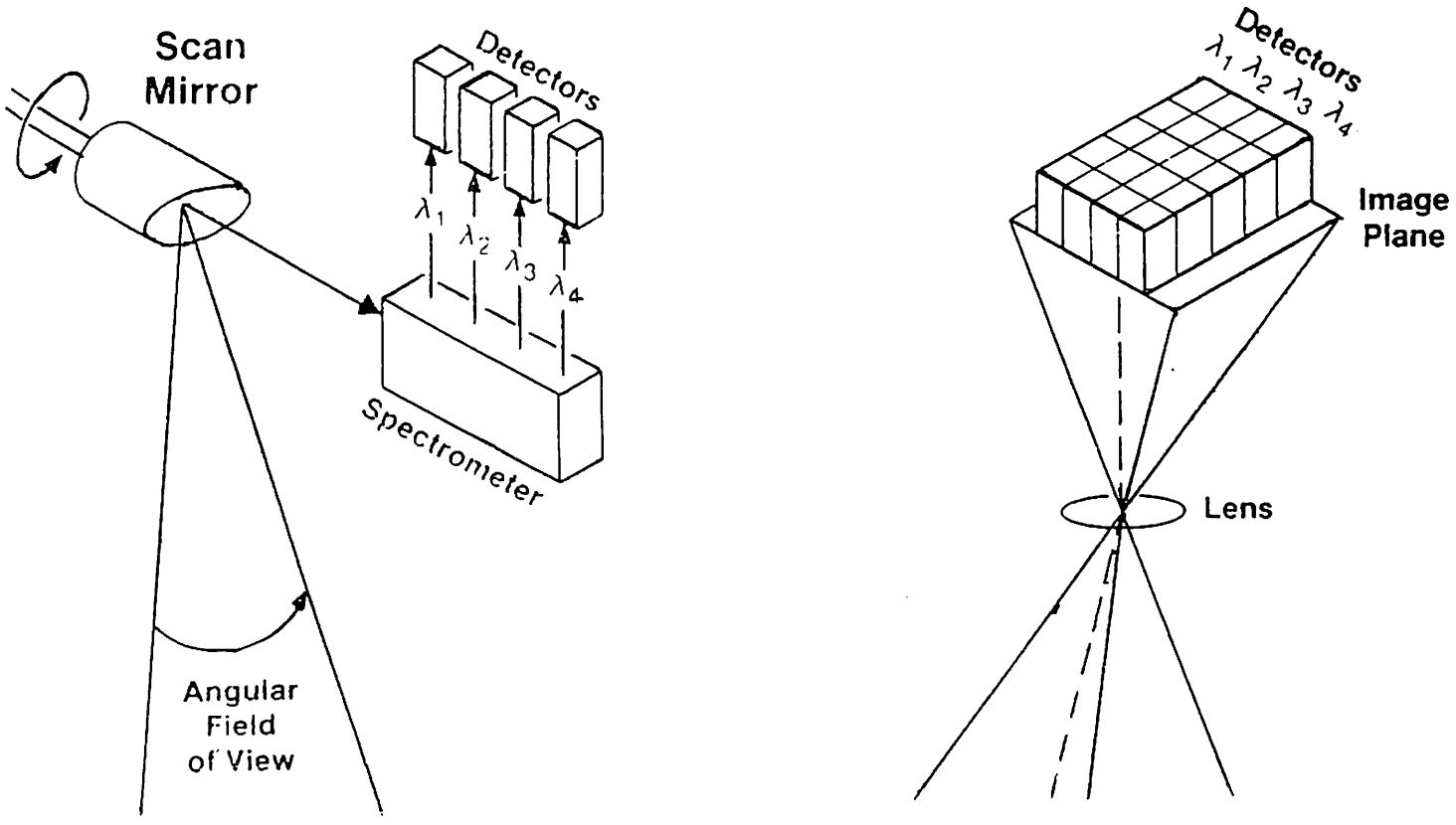


Figure 13 - Multispectral scanner systems. - by NASA

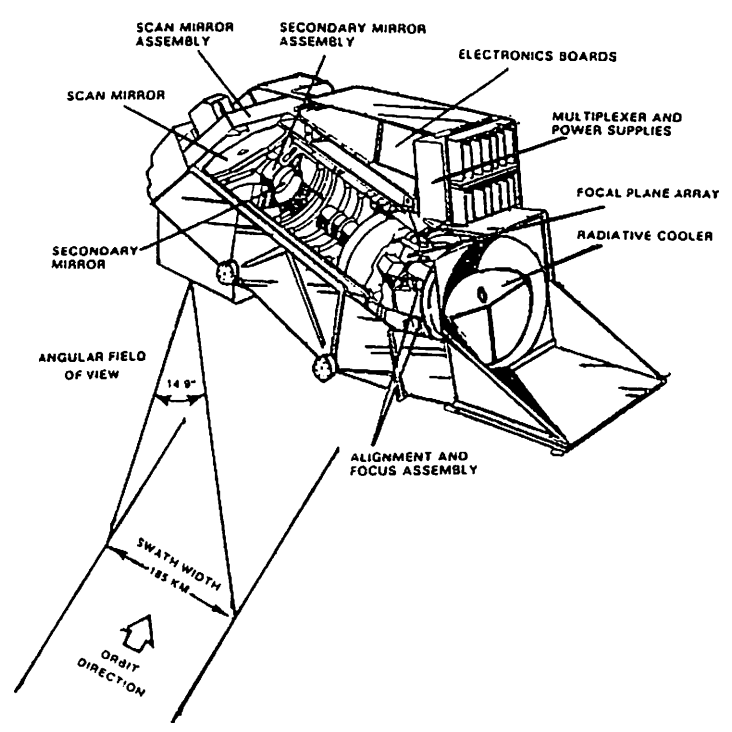


Figure 14 - Thematic mapper system. - by NASA

- 4, 0.76-0.90 micrometer, reflected IR, determining biomass content on shores
- 5, 1.55-1.75 micrometer, reflected IR, indicates moisture content for soil and vegetation
- 6, 10.40-12.50 micrometer, thermal IR, useful for soil and thermal mapping moisture
- 7, 2.08-2.35 micrometer, reflected IR, coincides with absorption band caused by hydroxyl ions in minerals, ratios of bands 5 and 7 are useful for mapping hydrothermally altered rocks

"SPOT"

It employs a high resolution visible (HRV) imaging system that has a long-track scanner. The later has an increased dwell time. The IFOVS of each detector sweeps a ground resolution cell along the train parallel with the flight-track direction using "Pushbroom Scanners" This is shown in figure 15.

It has three bands:

Green, 0.50-0.59 and 0.51-0.73 micrometer

(multispectral and panchromatic modes respectively)

Red, 0.61-0.68 micrometer, multispectral mode

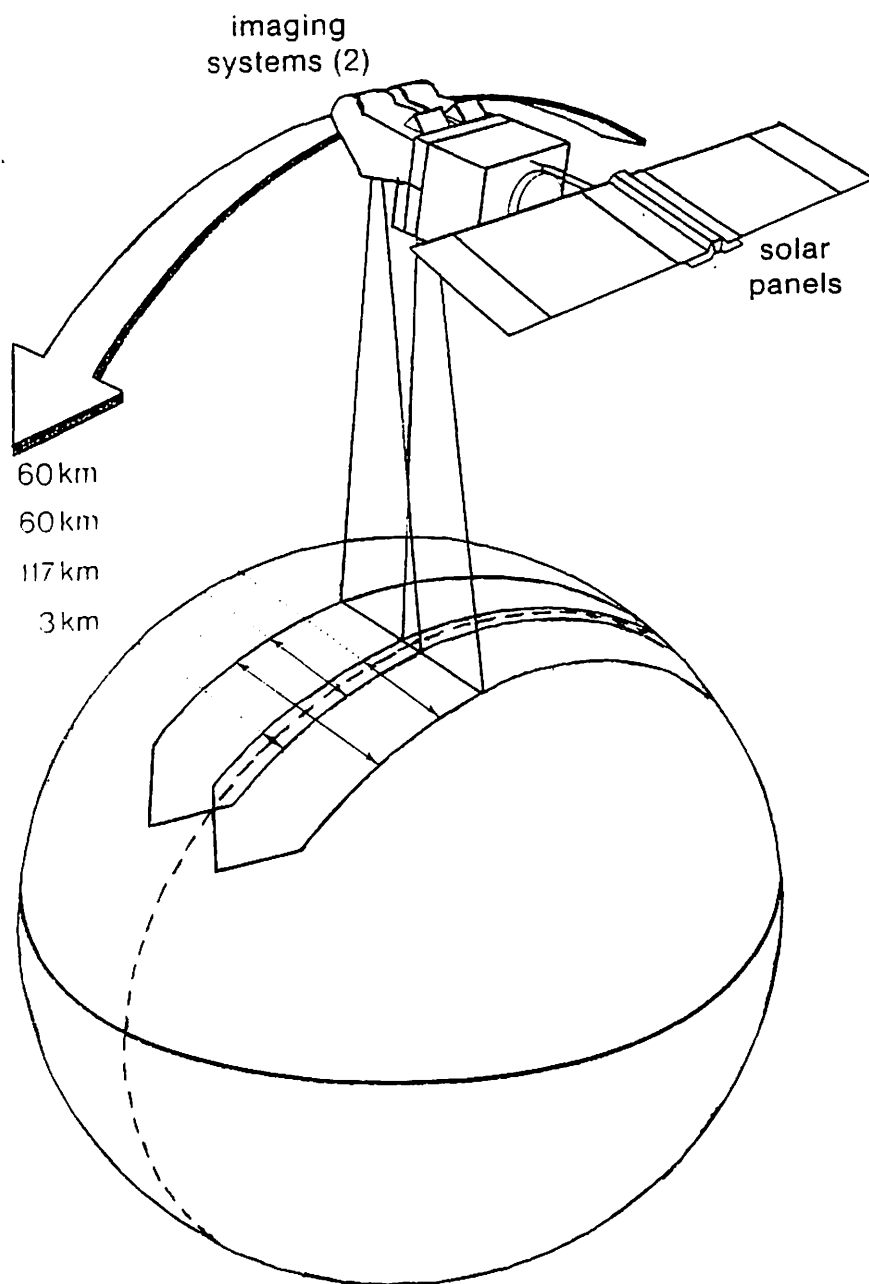


Figure 15 - SPOT satellite platform and image swaths acquired in the nadir-viewing mode. - by G. Weill, SPOT Image

Reflected IR, 0.79-0.89 micrometer,
multispectral mode

There is a linear array of charge coupled detectors (CCD) which receives focused images from tiltable mirrors.

The HRV system operates in either Multispectral mode or High Resolution Panchromatic mode.

The multispectral mode records green, red and reflected IR images in three arrays with a ground resolution cell of 20 by 20 metres, The high resolution mode has a 10 by 10 metre resolution cell and records a single panchromatic image in the 0.51-0.73 micrometer spectral band.

Both modes have a 60 km wide swath and operate in the " nadir and off-nadir" positions. They record images in three bands of green, red and reflected IR. The off-nadir positions provide images of stereo viewing. The capability of SPOT to revisit localities and its off-nadir viewing are schematically expressed in figures 16 and 17.

UNIVERSITY OF NAIROBI LIBRARY

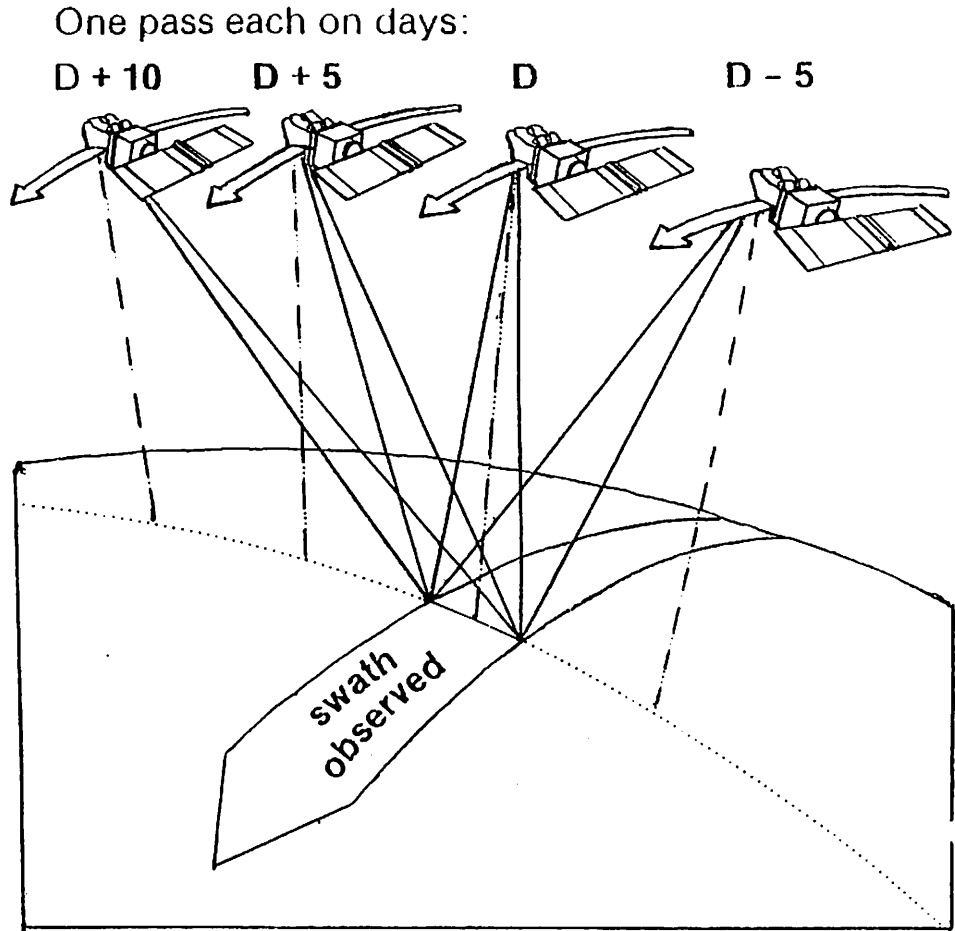


Figure 16 : Capability of SPOT to revisit localities during a 26-day cycle. Localities at this equator can be observed seven times; localities at latitude 45° can be observed 11 times. — by G. Weill, SPOT Image Corporation.

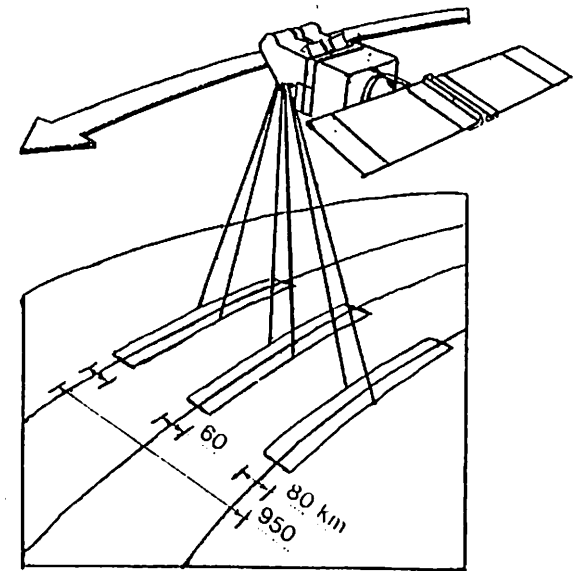
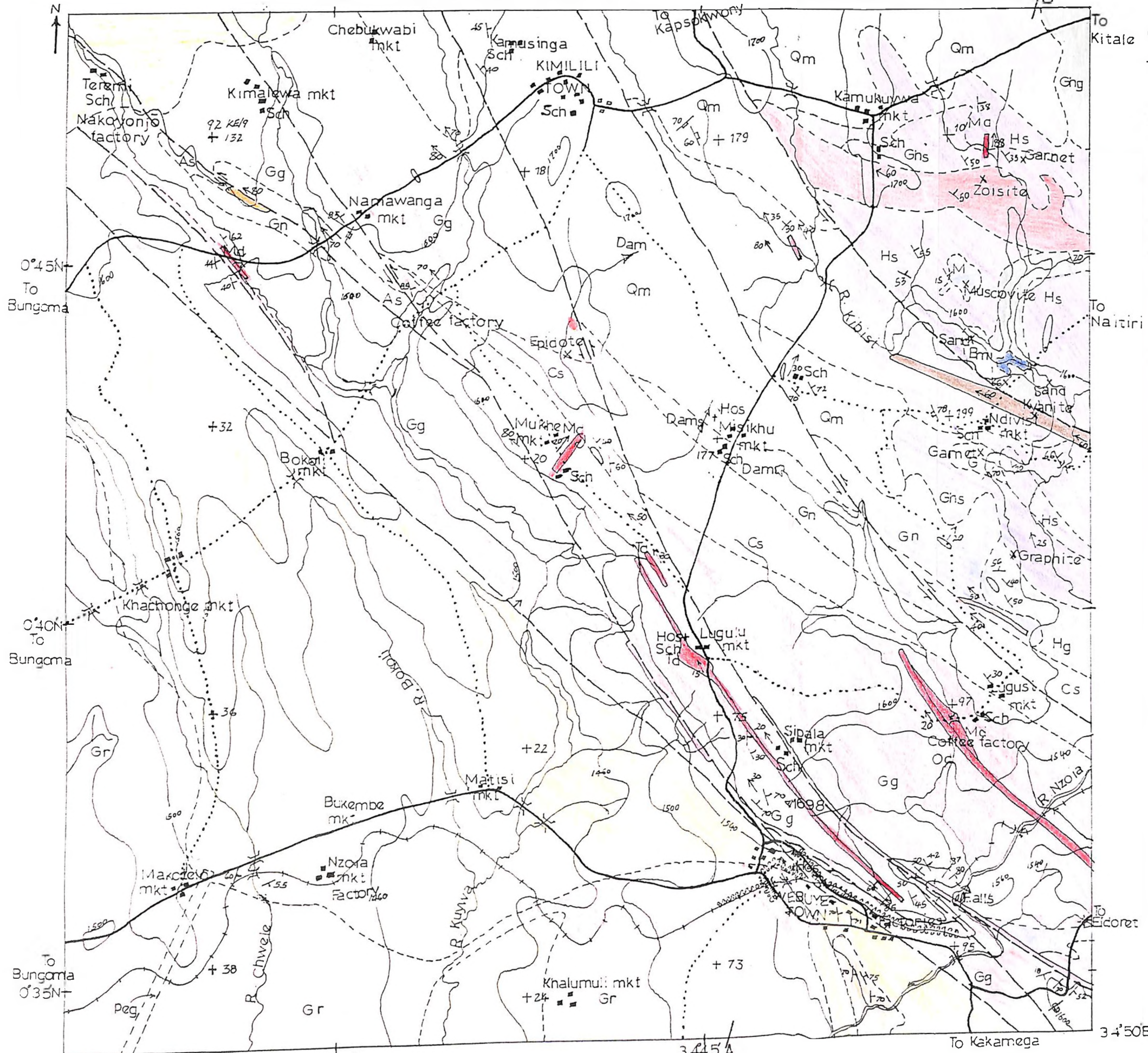


Figure 17 : Off-nadir viewing capability of SPOT using tiltable mirror. — by G. Weill, SPOT Image Corporation.

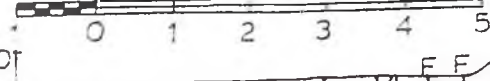
THE GEOLOGICAL MAP OF THE WEBUYE - BUNGOMA AREA (KENYA) B

LEGEND



- Q/nary Ironstone
- MOUNT ELGON SERIES
- Tertiary Nephelinite
- TUROKA GROUP
 - Muscovite quartzite
 - Qtz-muscovite schist (Qm), Gneiss (Gn)
 - Muscovite schist (Ms), Garnet schist (G)
 - Biotite-muscovite schist (Bm)
 - Hornblende gneiss (Hg)
 - Garnet-hornblende gneiss (Ghg)
 - Hornblende schist (Hs)
 - Garnet-hornblende schist (Ghs)
- Lower Palaeozoic & Upper Pre-Cambrian
 - Migmatitic granodiorite
 - Crust granite
- ARCHAIC
 - KAVIRONDIAN GROUP
 - Grits & Phyllites
 - Mudstone
 - NYANZIAN GROUP
 - Actinolite schist (As)
 - Chlorite schist (Cs)
 - Banded ironstone
- INTRUSIVES
 - Granodiorite (Gr)
 - Gneissose granodiorite (Gg)-m. morphosed
 - Olivine dolerite (Od), Meta-dolerite (Mc)
 - Tholeiitic dolerite (Td)
 - Quartz-monzonite
- Geological boundaries:
 - observed
 - approximate
 - Dip of foliation
 - Vertical foliation
 - Strike foliation
 - Joints inclined
 - Joints vertical
 - Wrench faults
 - Thrust zone with dip foliation
 - Mylonite zones
 - Giant quartz vein
 - Pegmatite (peg)
 - Falls
 - Railway line
 - Roads
 - main
 - secondary
 - Trigonometrical stations:
 - primary
 - secondary
 - Air photo principal point with sortie number
 - Rivers
 - Contours
 - Buildings

Scale 1:100,000



Cross Section A-B

